Technische Universität Berlin

The Techno-economic Transformation towards a Renewable Energy System

Developing and Applying Bottom-up Planning Models

vorgelegt von
M. Sc.
Leonard Göke
ORCID: 0000-0002-3219-7587

an der Fakultät VII – Wirtschaft und Management
der Technischen Universität Berlin
zur Erlangung des akademischen Grades

Doktor der Ingenieurwissenschaften
— Dr.-Ing. —

genehmigte Dissertation

Promotionsausschuss:

Vorsitzender:	Prof. Dr. Georg Meran (TU Berlin)
Gutachter:	Prof. Dr. Christian von Hirschhausen (TU Berlin)
Gutachter:	Prof. Dr. Tom Brown (TU Berlin)
Gutachterin:	Prof. Dr. Frauke Wiese (Europa-Universität Flensburg)

Tag der wissenschaftlichen Aussprache: 23. September 2021

Berlin 2021

Zusammenfassung

Das Thema der Dissertation ist die Entwicklung und Anwendung numerischer Modellierungsmethoden, um die Transformation vom fossil-fissilen zum erneuerbaren Energiesystem abzubilden. Der Fokus liegt dabei speziell auf techno-ökonomischen Planungsmodellen basierend auf linearer Optimierung.

Das erste Kapitel hinterfragt die Funktion von Planungsmodellen und beschreibt sie als Instrumente im fachöffentlichen Diskurs über die Zukunft des Energiesystems. Aus dieser Einordnung werden Empfehlungen für Modellentwicklung und -anwendung abgeleitet.

Das folgende Kapitel analysiert, ob die Verwendung reduzierter Zeitreihen eine adäquate Strategie zur Reduktion von Modellkomplexität bleibt, wenn Energiesysteme zunehmend durch fluktuierende Erzeugung aus Wind und Solar charakterisiert sind. Zu diesem Zweck werden Kombinationen verschiedener Methoden zur Erzeugung und Modelleinbettung reduzierter Zeitreihen hinsichtlich ihres Effekts auf Endergebnisse verglichen. Ergebnisse zeigen, dass fluktuierende Erzeugung, aber auch die zunehmende Bedeutung saisonaler Speicher, die Aussagekraft reduzierter Zeitreihen stark einschränkt, wobei die genauen Effekte in erster Linie von der Modelleinbettung abhängen. Abschließend wird die Entwicklung alternativer Methoden zur Reduktion von Modellkomplexität empfohlen.

Darauf aufbauend stellt das dritte Kapitel einen auf Graphentheorie basierenden techno-ökonomischen Modellierungsansatz vor, der Mengen von Modellelementen, wie Zeitschritte oder Regionen, in hierarchischen Bäumen anordnet. Neben weiteren Neuerungen ist der Ansatz in der Lage, den zeitlichen und räumlichen Detailgrad innerhalb des Modells je nach Energieträger zu variieren. Damit erreicht der Ansatz einerseits eine erhebliche Komplexitätsreduktion und kann andererseits die inhärente Flexibilität von Infrastrukturen wie dem Gasnetz berücksichtigen.

Das vierte Kapitel dokumentiert AnyMOD.jl, ein Software-Framework, das die Formulierung von Planungsmodellen auf Grundlage des Graph-basierten Ansatzes automatisiert und so die ansonsten sehr komplexe Methode öffentlich und einfach zugänglich macht. Darüber hinaus implementiert das Framework weitere numerische Methoden zur Reduktion von Modellkomplexität.

Im letzten Kapitel der Dissertation werden die entwickelten Methoden angewandt, um die Substituierbarkeit von Netzausbau durch einen räumlich gezielten Zubau von Speichern und erneuerbaren Energien zu analysieren. Zu diesem Zweck wird ein optimales Szenario, das Ausbau von Netz, Speichern und erneuerbaren Energien gleichzeitig optimiert, mit einem sequenziellen Ansatz verglichen. Bei diesem Ansatz zuerst erneuerbare Energien sowie Speicher und erst danach der Netzausbau optimiert, um das aktuelle Planungsverfahren abzubilden. Das angewandte Modell zeichnet sich durch einen breiten räumlichen und sektoralen Betrachtungsrahmen, aber gleichzeitig hohen zeitlichen Detailgrad aus, der durch den Graph-basierten Ansatz ermöglicht wird. Die Ergebnisse weisen darauf hin, dass bei Berücksichtigung der Flexibilität aus Sektorenkopplung der Ausbaubedarf des Stromnetzes durch den gezielten Einsatz saisonaler Speicher deutlich reduziert werden kann.

Schlüsselwörter: techno-ökonomische Planungsmodelle, Makroenergiesystem, Energiesystemmodellierung, Open-Source-Modellierung, erneuerbare Energie

Abstract

This dissertation develops and applies numerical methods to model the transformation from a fossil and fissile towards a renewable energy system. Its specific focus is on bottom-up planning models based on linear programming that analyze the system from a techno-economic perspective.

The first chapter reflects on the purpose of bottom-up planning models and describes how models are instruments in the expert and public discourse that shape the energy system's future. From this basis, implications for the development and application of bottom-up planning models are derived.

The next chapter assesses whether time-series reduction is still an adequate strategy to reduce the computational complexity when modeling renewable energy systems. To evaluate how reduction affects model results, the chapter combines different methods for deriving reduced time-series and for implementing them into bottom-up models. We find that intermittency of renewables and dependency on seasonal storage reduce the accuracy of time-series reduction, but effects are highly dependent on how reduced time-series are implemented. The chapter proposes investigation of alternative methods to reduce computational complexity.

Following up on this, the third chapter introduces a novel graph-based formulation for bottom-up planning models. The approach is based on organizing sets of elements in rooted trees and is, among other things, capable to vary temporal and spatial resolution by energy carrier within the same model. As a result, high resolutions can be limited to the power sector to achieve a substantial reduction of computational complexity and capture the inherent flexibility of large-scale infrastructures.

The fourth chapter introduces AnyMOD.jl, a modeling framework implementing the graph-based formulation and automating the creation of models applying it. The purpose of the tool is to make the method freely available and easily accessible. In addition, it introduces further technical features to reduce model complexity.

The final chapter of the dissertation applies the developed methods to evaluate the benefits of considering storage systems and different placement of renewables as substitutes for grid expansion. To analyze these benefits, a first-best scenario that simultaneously optimizes expansion of generation, storage, and the transmission grid is compared to several sequential scenarios. Due to its large scope and detailed representation of sector integration, the applied model can provide new insights and suggests that storage systems could greatly reduce the need for grid expansion, even if sector integration doubles the demand for electricity.

Keywords: bottom-up planning models, macro-energy system, energy system modeling, open-source modeling, renewable energy

Rechtliche Erklärung

Hiermit versichere ich, dass ich die vorliegende Dissertation selbstständig und ohne unzulässige Hilfsmittel verfasst habe. Die verwendeten Quellen sind vollständig im Literaturverzeichnis angegeben. Die Arbeit wurde noch keiner Prüfungsbehörde in gleicher oder ähnlicher Form vorgelegt.

Leonard Göke
Berlin, 23. Juli 2021

Table of Contents

List of Figures

List of Tables

List of Acronyms

CAES compressed air energy storage

CCGT combined-cycle gas turbine

CHP cogeneration of heat and power

IEA International Energy Agency

NGO non-governmental organizations

PV photovoltaic

TSO transmission system operators

TSR time-series reduction

WEO World Energy Outlook

1 Introduction

1.1 Motivation

Energy supply from renewable sources is a fascinating but not a novel idea. First visions for renewable energy systems surfaced in utopian literature authored in the early stages of industrialization (Armytage 1956). In 1865 William Stanley Jevons' *The Coal question* warned about the expected depletion of coal reserves sparking one of the first public debates on energy supply (Ergen 2015). In the following, the idea of renewable energy took deeper hold and in the late 19th century advances in solar and wind power attracted academic attention rendering them potential substitutes for steam engines (Kapoor 2019). In his main work *Women and Socialism* August Bebel predicted that after the depletion of coal, a shift to renewable energy is inevitable and will lead to a valuation of land based on renewable potential (Bebel 1900; cited by Abelshauser 2014). Later Émile Zola's novel *Travail* in 1901 or Archibald Williams' book *The Romance of Modern Invention* in 1910 introduced the idea of renewable energy to a popular audience (Zola 1901; cited by Febles 2008; Williams 1910; cited by Ergen 2015).

However, in spite of showing promise, renewable energy systems remained science fiction and the industrial shift from steam to electricity was, with the exception of hydro power, mainly fueled by coal and later oil. Insufficient technical maturity as a sole explanation for this falls short of how technical and societal development are intertwined. Building on Thomas Hughes (1993) historical studies on electricity supply, Ergen points out that early inventors were too focused on engineering and failed to convey a broader vision for renewable energy systems to governments and private investors. As a result, renewables did not receive long-term investment to achieve learning effects and reach maturity. As an additional reason for little support of renewable energies, Abelshauser (2014) cites that Jevons' expectations regarding the scarcity of fossil fuels turned out to be unfounded, especially due to the increasing exploitation of oil and gas.

Correspondingly, renewables re-gained momentum in the United States when awareness for the risk of depending on oil imports increased during the 1950s. Solar technology progressed at the same time and the presentation of a first photovoltaic cell in 1954 met great public reception being described by the New York Times as the eventual *"realization of one of mankind's most cherished dreams — the harnessing of the almost limitless energy of the sun for the uses of civilization"* ("Vast Power of the Sun Is Tapped by Battery Using Sand Ingredient" 1954; cited by Ergen 2015). However, photovoltaic was not yet market-ready and lacked government support that rather focused on advancing nuclear power, also due to synergies between its civil and military use (Ergen 2015; Clarke 2014).

In subsequent years growing opposition to nuclear power and oil dependency reinforced interest in renewable energy systems. In his article *Energy Strategy: The Road Not Taken?* Amory Lovins (1976) contrasted energy systems characterized by fossil-fissile fuels and large-scale infrastructure with an alternative path based on energy efficiency and small-scale renewables tailored to end-use. Krause, Bossel, and Müller-Reissmann (1980) substantiated these ideas for Germany and in 1980 introduced a comprehensive concept for a renewable energy system. About the same time, similar studies on technical feasibility and economic implications were also conducted for other countries like the United States, France, or Sweden (Martinot et al. 2007).[1] The common denominator in all these works is how they take a systematic perspective to propose serious visions and thus mark the point where renewables exited the realm of science fiction and entered public debate.

Since the 1980s, these visions were partly put into practice. With scientific consensus about climate change as an additional driver, renewable energy made significant progress quadrupling its global consumption of primary energy from 1980 to 2019. Due to rising consumption in emerging economies, global shares only rose from 6.7% to 11.4% but in industrialized countries the increase was more pronounced, for example from 1.4% to 17% in Germany (Ritchie and Roser 2020). Reinforced investments induced learning effects that diminished levelized costs of electrictiy from photovoltaic (PV) and wind in the last ten years by 89% and 70%, respectively (Roser 2020).

The trend towards renewables is reflected again by the visions that are projected into the future today. Studies on renewable energy systems are growing in number and detail (Hansen, Breyer, and Lund 2019; Jacobson et al. 2017; Hohmeyer and Bohm 2015; Oei et al. 2020). While in the 1980s many scholars expressed their skepticism or blunt rejection of the idea, consensus emerged that renewable energy will make a significant contribution to energy supply and controversy shifted to whether renewables can fully replace nuclear and fossil fuels (Hammond 1977; Schmitz and Voß 1980; T.W. Brown et al. 2018). Outside of academia, new visions for renewable futures, like the Green New Deal, are put forward and many stimulus packages in response to the COVID-19 pandemic are committed to a green recovery, eventually moving renewable energy into the center of public policy (Galvin and Healy 2020; Carbon Brief 2020).

The outlined (and non-exhaustive) history of renewable energy illustrates how evolution of energy systems is more than a deterministic process dictated by technology, but equally shaped by human expectations for the future and their ingenuity, when facing it. Against this background, the following section introduces Jens Beckert's concept of fictional expectations driving economic development and applies it to how planning of energy systems builds on scenarios (Beckert 2013). The subsequent section introduces bottom-up planning models, the key method for energy scenarios and focus of this dissertation. Section 1.4 links the two previous sections and applies the insights on energy scenarios and derives implications for developing and applying bottom-up planning models. Afterwards, the individual chapters of the dissertation are outlined with specific regard to how they address the identified and the last section concludes with the next steps proposed for future research.

1.2 Fictional expectations in energy scenarios

According to Beckert, economic behavior regarding the future is limited by unknowability. Unlike uncertainty, unknowability is not only non-deterministic, it also cannot be captured probabilistically to enable rational decisions. To remain capable of taking decisions, intentionally rational actors develop fictional expectations of the future in place of perfect information. These expectations extend empirical facts with assumptions that are narratively convincing and formed by calculation and imagination. As a result, fictional expectations are socially contingent and rest on conceptions "influenced by culture, history and power

1. The first corresponding study for Denmark was published even earlier in 1975 (Sørensen 1975).

relations" (Beckert 2016; cited by Jackson 2017). Although not inevitably accurate, fictional expectations are treated by actors *"as-if"* and, thus, decisively shape their actions (Beckert 2013). In application of his concept, Beckert revisits microeconomics to explain how fictional expectations open a creative moment for innovation and, more importantly, considers forecasts of economic or technological development as fictional expectations whose purpose is not to predict the future, but to coordinate economy activity (Beckert 2016).

The equivalent to forecasts in energy are scenarios. Originating from military planning, scenarios are strategic tools describing a hypothetical future and pathways from the present to this future (Nielsen and Karlsson 2007). Scenarios are often categorized as either predictive describing the most probable future, explorative investigating an imaginable future or normative outlining a desirable future (Nielsen and Karlsson 2007). Correspondingly, Beckert describes forecasts as *"coordinating, performative, inventive, and political"* (Beckert 2016, p. 217). Different energy scenarios reflect these properties to a varying degree depending on the author: Scenarios issued by governmental agencies are mostly predictive aiming to coordinate public policy and private investment, but to build credibility and acceptance they refrain from innovation and reflect political consensus. Scenarios from non-governmental organizations (NGO), consulting firms, or industrial companies seek to influence public policy and opinion in their respective favor. Therefore, they are more political, often normative and sometimes, when it is inevitable to achieve their objective, innovative. Scientific scenarios exhibit the greatest level of innovation and exploration, especially if addressed to an academic audience and not the general public. In addition, energy scenarios can greatly differ in scope and can range from comprehensive pathways for the entire world, like the IPCC report (Edenhofer et al. 2014), to explorative concepts for energy supply of single buildings (Knosala et al. 2021).

To examine how scenarios shape decisions and drive the development of energy systems, the following sections successively transfers the characteristics of forecasts identified by Beckert to energy scenarios. As a result, the section's structure loosely mirrors the chapter on forecasts in Beckert (2016).

1.2.1 Power of persuasion

To convince recipients and guide their decisions, forecasts must be convincing. Beckert identifies two instruments to achieve this, which are typically combined: quantitative model results and narrative elements. For example, economic forecasts consist of a computed growth rate and a story about economic development to support the rate. The purpose of quantitative results and the underlying mathematical method is to evoke precision and objectivity (Beckert 2016, p. 220). To reinforce this perception, method complexity is even increased if it does not benefit accuracy (Beckert 2016, p. 226). Narrative elements convince by suggesting causal relationships and tying forecasts to existing knowledge and convictions of the recipients (Beckert 2016, pp. 91, 221, 245). In *Narrative Economics* Robert Shiller (2019) provides a similar, but more comprehensive description of narratives as an overlooked factor driving markets and investment decisions.

Energy scenarios combine quantitative methods and narrative elements in a very similar way (Nielsen and Karlsson 2007). Elaboration of quantitative and narrative parts varies and scenarios targeting a professional audience typically emphasize quantitative elements; targeting a general audience emphasizes narratives.

Similar to economic forecasts, the purpose of complex methods in energy scenarios is to create legitimacy and credibility (Schmidt-Scheele 2020). This is for example reflected by critique of the IIASA energy scenarios in Keepin and Wynne (1984). They find that the applied model is needlessly complex and simple calculations using a few key assumptions are sufficient to largely reproduce its results (Keepin and Wynne 1984; Häfele et al. 1981). In addition, results are not robust to minor changes of these key assumptions. Based on this analysis, Wynne (1984) even goes as far as stating that energy models are *"symbolic vehicles for gaining authority"* only used to create an appearance of scientific objectivity.

The role of narrative elements in energy scenarios is equally acknowledged in the literature (Upham, Klapper, and Carney 2016; Moezzi, Janda, and Rotmann 2017). In contrast to purely technical descriptions, stories get people engaged and create awareness for the societal significance of energy scenarios, which is particular relevant for public policies (Miller et al. 2015; Janda and Topouzi 2015).

Analogously to forecasts, energy scenarios are deemed plausible, if narratives correspond to the knowledge and convictions of the recipient (Schmidt-Scheele 2020). Therefore, narratives for transformative scenarios often draw on similar events in the past like the industrial revolution or disruptions in other industries (Jänicke and Jacob 2009; Clark II and Li 2013).

For the same reason, energy scenarios are often associated with various political ideals. Although there are several studies questioning the objectivity and authority evoked by quantitative methods in energy scenarios, there is no research critically examining the association of normative ideals. This seems particularly intriguing, because associations are often conflicting and range from a broad political spectrum. For example, sovereignty is a reoccurring argument in favor of national resources, both conventional and renewable, and was first cited by Jevon regarding Britain's dependence on coal (Jevons 1865; Sica and Huber 2017). Economic growth and the creation of jobs is also equally used as an argument in favor of conventional and renewable energy (The White House 2021). At the same time, the idea of degrowth serves as an argument for renewables as well. Conventional energy is often promoted arguing it will induce economic growth to lift a significant share of the world's population out of poverty. On the other hand, ambitious mitigation scenarios are often motivated by pointing out how climate change has the most severe impact on people in poverty. Sometimes, this argument is also made specifically for women in poverty. Finally, renewable energy is argued to increase democratic participation through decentralization of energy supply (Krause, Bossel, and Müller-Reissmann 1980; Hirschhausen et al. 2018; Stephens 2019).

Beyond methods and storylines, persuasiveness of a scenario also depends on the authority of its author (Schmidt-Scheele 2020). Braunreiter and Blumer (2018) for instance observes that researchers refrained from citing a scenario by an environmental organization, not because its quality was questioned, but because it would not *"look serious"*.

1.2.2 Coordinating actors

Beckert points out that despite becoming increasingly sophisticated, economic forecasts are rarely accurate and have a long record of not foreseeing recessions (Beckert 2016, pp. 241-223). He ascribes this to flaws of the forecasting process itself, like incomplete data, inaccurate models, or inability to foresee major changes but also to unpredictable exogenous shocks to the economy, like political events or natural disasters (Beckert 2016, pp. 228-231). That from today's perspective also global pandemics must be added to this list, demonstrates how unpredictable exogenous shocks are. Nevertheless, considerable effort is dedicated to forecasting and forecasts are received with great reception, because their true purpose, according to Beckert, is to coordinate economic activity. Facing an unknown future, relying on forecasts enables actors to be seemingly rational and partly relieves them from responsibility, if decisions turn out to be poor (Beckert 2016, p. 236). Consequently, government, businesses, and consumers adapt their decisions to the same forecasts and as a result forecasts achieve consistent behavior across the whole economy. This implies that forecasts are performative meaning they do not just predict, but also shape economic activity (Beckert 2016, p. 237).[2]

Again, Beckert's characterization of forecasts can be transferred to energy scenarios. Overall, projections of energy scenarios are as inaccurate as economic forecasts, partly because they must build on economic forecasts (Paltsev 2017; Stern 2017; Trutnevyte 2016). To stay abreast even long-term scenarios 30 years into the future are outdated so quickly that they require

2. It does not necessarily imply that forecasts are self-fulfilling. For example, an optimistic forecast on the eve of an unexpected recession might in fact have the opposite effect and deepen the recession.

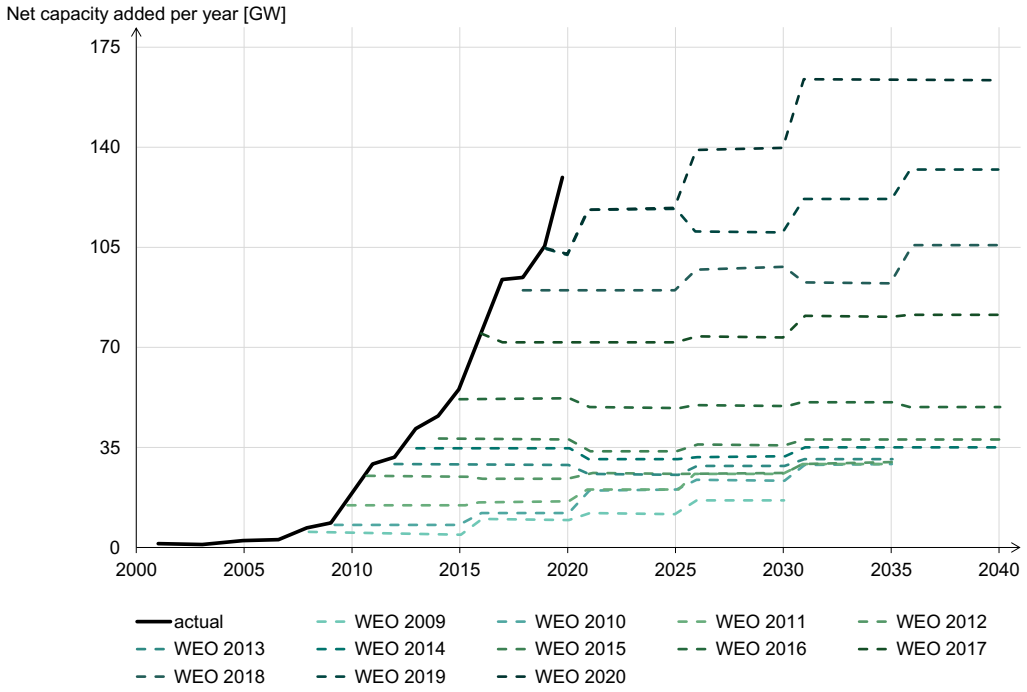

Figure 1.1: Comparing actual global additions of solar capacities to WEO, data from Carbon Brief (2021)

substantial revision every year, for instance the World Energy Outlook (WEO) is updated annually. Similar to forecasts, energy scenarios struggle to incorporate exogenous shocks affecting demand or fuel prices (Govorukha et al. 2020; Craig, Gadgil, and Koomey 2002). In addition, scenarios often neglect major changes and assume an overly conservative continuation of present trends. A prominent example of this bias is displayed in Fig. 1.1. It shows how the WEO continuously underestimated solar installations in the last ten years although estimates were continuously revised upwards (Metayer, Breyer, and Fell 2015).

Irrespective of accuracy, scenarios impact the development of the energy system, because they affect decisions of governments and investors (Schubert, Thuß, and Möst 2015). This applies in particular to predictive scenarios from established institutions, like the International Energy Agency (IEA), large companies, or governments. For example, higher solar projections in the WEO could have encouraged additional investments and further drive up renewable expansion (Carrington and Stephenson 2018). Similarly, Midttun and Baumgartner (1986) argue that expansion of French nuclear capacities in the 1970s anticipated increasing electricity demand based on prominent scenarios. These scenarios became self-fulfilling, when the added capacity lowered prices and induced additional demand.

The importance of credible scenarios for decision making conversely implies that diverging scenarios hinder planning and can stall the development of the energy system (Grunwald 2011). For example, the official governmental objective in Germany is to achieve a renewable share of 65% in power consumption by 2030, but currently implemented policies will only achieve around 55% (Agora Energiewende, Wattsight 2020; Oei et al. 2019). In addition, very heterogenous actors advocate for much higher shares up to 100% and projections for consumption these shares are based on diverge as well (Gierkink and Sprenger 2020; Kendziorski et al. 2021). Overall, the emerging uncertainty not only discourages investment into renewables, but into complementary technologies like storage, electric mobility, or electric heating as well.

Explorative scenarios, often from academia or NGOs, rarely have a direct impact on investments, but constitute an avant-garde and drive long-term innovation. If they become sufficiently convincing, their ideas are eventually established and included into predictive scenarios. For instance, first scenarios for renewable energy systems referenced in section 1.1

were rejected by the established experts at the time and did not encourage great investments (Schmitz and Voß 1980; Häfele and Rogner 1986). Also, they appear outdated from today's perspective including no PV, no electrification of heating, and an exclusive use of synthetic fuels in the transport sector. Nevertheless, these scenarios sparked public discussion and further academic research on renewables that finally resulted in significant progress and recognition of renewables by established scenarios. A similar case can be made for the use of hydrogen as an energy carrier, which was already described by Jules Vernes in his 1876 novel *The Mysterious Island* and debated among experts since the 1970s, but only included in governmental scenarios recently (Verne 1901; Bockris 2013; GOV.UK 2020; The White House 2021).

Finally, scenarios do not only influence governments and investors, but other scenarios as well. To increase the legitimacy of their own work, researchers frequently use assumptions or results from established scenarios as inputs to their own scenarios (Braunreiter and Blumer 2018). As a result, potential bias transfers to academic scenarios, which is especially critical in case of sensitive assumptions like final demand.

In notable difference to economic forecasts, energy scenarios have become more reflective about their epistemic value. According to Beckert, economic forecasts purport to predict the future, despite their long record of inaccuracy. The IEA, publisher of the WEO, on the other hand, acknowledges that *"there is no single story about the future of global energy and no long-term IEA forecast for the energy sector"* and similarly many academic publications stress the fictionality of energy scenarios (International Energy Agency 2021). However, this clarification is of no difference, because actors nonetheless treat them as predictions when making decisions. So, when the IEA states *"the course of the energy system might be affected by changing some of the key variables"* to underline the limitations of their work, they are modestly omitting that one variable are energy scenarios like the WEO (International Energy Agency 2021).

1.2.3 Competition for influence

Since convincing forecasts affect decision-making, their authors hold considerable influence over the future. Therefore, the competition for credibility between forecasters is also a competition for political influence and forecasting methods are assets in this competition (Beckert 2016, p. 80).

In energy, scenarios are key contributions to the debate about the system's future since they shape economic and political decision-making. To influence expectations according to their interests, different actors publish competing scenarios and create a *"battlefield"* of energy system planning (Nørgård 2000; cited by Nielsen and Karlsson 2007).

In this debate, the state holds a central role, because planning concerns infrastructure and the environment—both public goods (Midttun and Baumgartner 1986). Through research funding, subsidies, market design, and building permissions the government decisively shapes the energy system and examples like nuclear power or renewable energy demonstrate that government support is a necessary (but not sufficient) condition for new technologies to emerge (Ergen 2015). Therefore, scenarios by the government possess authority because they are likely to reflect the future course of public policy.

Other actors present in the debate and publishing energy scenarios include industry organizations, environmental NGOs, and academia (Kainiemi, Karhunmaa, and Eloneva 2020). It is commonly acknowledged that scenarios often reflect their publishers' interests, for example scenarios from industry organizations tend towards higher consumption, and scenarios from environmental NGOs towards lower consumption (Nielsen and Karlsson 2007). Drawing up scenarios must carefully balance between diverging from the consensus to promote own interests on the one hand but comply with the consensus to remain credible on the other. In addition to these professional organizations, also the general public increasingly engages in the debate, but unlike other groups, members of the general public do not typcially study energy scenarios

directly and instead learn about their content from media (Braunreiter, Stauffacher, and Blumer 2020).

The role of professional organizations and the authority of complex models restrict influence on the debate and consequently on the development of the energy system as well. In extreme cases, professional networks between universities, industry, and government form a *"cognitive monopoly"* characterized by a common perspective on the energy system (Midttun and Baumgartner 1986). Outsiders pointing out deficiencies of that perspective can be denounced as uninformed by pointing out their lack of recognized expertise or sophisticated methodology (Wynne 1984). Illustrating this, Midttun and Baumgartner (1986) describe how environmentalists in several European countries had to establish expertise and forecasting methods of their own to influence public policy according to their interests. At the time, established models and scenarios expected a strong growth in demand that suggested the expansion of nuclear power. In opposition to nuclear power, environmentalists rejected these scenarios and developed methods forecasting constant demand. After gaining recognition, these scenarios were included into planning of future polices and eventually proved much more accurate. Overall, the process added new perspectives to the debate about energy and created awareness of bias in models.

Finally, the previous description of how political debate shapes the energy system can be used to reject a popular but illusive concept of scientific policy advice. Decision-makers do not simply derive their actions from the scenarios presented by research, but decisions emerge out of the current state of debate instead (Grunwald 2011). Only scenarios contributing to this debate can have an actual, although indirect impact.

1.3 Bottom-up planning models

Bottom-up planning is the most frequently deployed quantitative method in the development of energy scenarios (Laes, Gorissen, and Nevens 2014). In the past, scenarios from models like MARKAL/TIMES or PRIMES had a considerable impact on energy policy (Taylor et al. 2014). *Bottom-up* modeling refers to representing physical flows in the energy system and is therefore also termed as the *"engineering approach"* (Ringkjøb, Haugan, and Solbrekke 2018). It is opposed to a top-down approach pursued by integrated assessment or computable general equilibrium models that build on economic and social abstraction. *Planning* implies investigating the optimal design of the system. Planning models are opposed to simulations performed by agent-based or mixed-complementarity models, that account for the individual objectives of different actors. Bottom-up planning models decide on the expansion and operation of technologies to satisfy demand and maximize social welfare. In case of perfectly in-elastic demand, a common assumption, maximizing social welfare is equivalent to minimizing system costs. To solve large and detailed models within reasonable time, bottom-up planning models are usually formulated as linear optimization problems.

Bottom-up planning models are also referred to as partial equilibrium or market models, since markets achieve a welfare maximum if perfect competition is assumed. However, these terms can be misleading, because several conditions of perfect competition do not apply to the energy system. First, unknowability of the future, illustrated by the inaccuracy of scenarios documented in the previous section, violates the assumption of perfect information. Second, the energy system is subject to significant externalities, like environmental damage or massive government intervention. Finally, perfect competition requires a long-term equilibrium, but the transformation of the energy system is a dynamic process. Note that violations of perfect competition apply particularly to the expansion of technologies, viz the planning part of models. For bottom-up models limited to the operation of predefined capacities the term *market model* can be considered more appropriate.

Thanks to their engineering focus, bottom-up planning models can identify technically feasible solutions to satisfy demand under certain constraints, for example an upper limit on

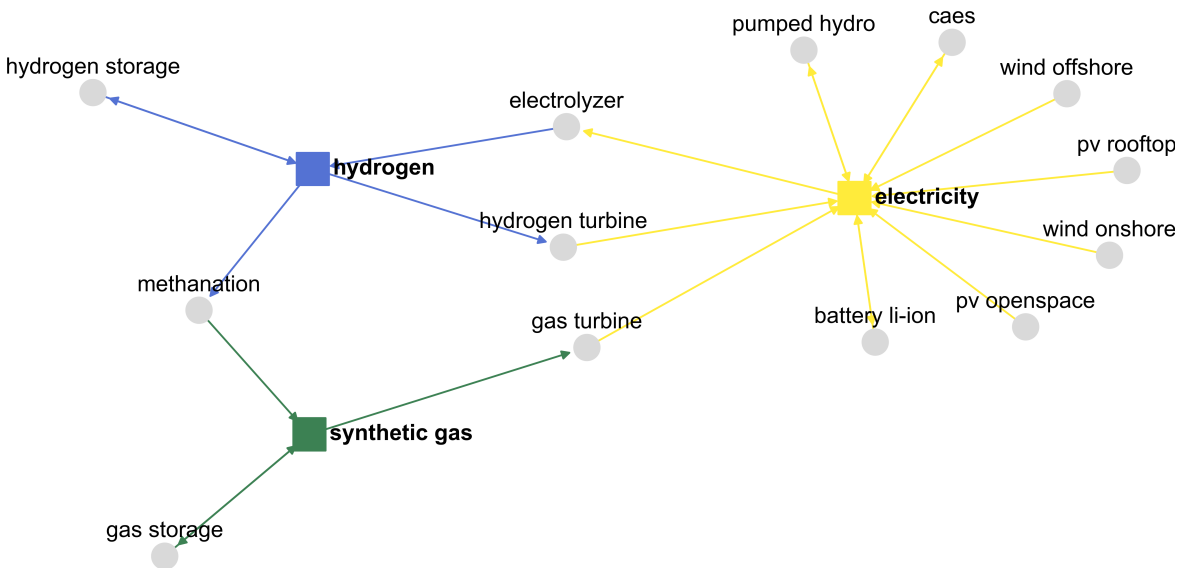

Figure 1.2: Graph representing exemplary bottom-up planning model

carbon emissions. By attributing costs to each decision on expansion and operation, models can also estimate the economic costs of solutions. These characteristics render bottom-up planning models suitable for techno-economic analyses of energy scenarios. Typical research includes: to investigate the trade-offs between different technologies, for example heating with electricity or hydrogen; to quantify the benefits of potential innovations, like further decreasing costs of renewables; and to foster a systematic understanding of how technologies interact, for example this dissertation finds that PV and batteries are typically complements, but power grids and batteries substitute each other. To analyze specific policies, like a political limit on wind power in certain areas, the effect of the policy must be translated into an appropriate boundary condition of the model, for instance a corresponding capacity limit.

Since bottom-up planning models take a system perspective, they do not consider the different agents in the system, like generators, consumers, or regulators and monetary flows between these agents, like subsidies, taxes, or market prices. Accordingly, computed costs are system costs, not the costs of individual agents, and computed prices are opportunity costs of meeting demand, not the market price of transactions between agents. Consequently, planning models are not suited to address strictly economic questions regarding individual profits, market design, or subsidy schemes, which are better addressed by simulative tools. In fact, this is not so much a shortcoming of optimization models, but rather reflects how identifying an optimal system precedes research on implementing the system practically. For example, if bottom-up planning models robustly find great benefits from expanding electricity storage, but investments are not profitable under current regulations, this is not a flaw of planning, but of the current policy framework.

The scope of bottom-up planning models ranges from single buildings over countries or continents to the entire world. Since comprehensive decarbonization scenarios have to consider more than one building, the term *macro-energy systems* has been termed to refer to larger systems (Levi et al. 2019). In addition, also the sectoral scope of models varies ranging from only one sector, like the power sector, to coverage of several sectors, like the power, heating, and transport sector, plus their interaction. The graph in figure 1.2 shows the structure of a stylized bottom-up planning model that is introduced in section 2 of chapter 2. In the graph, carriers are symbolized by colored and technologies by gray vertices. Entering edges of technologies refer to input carriers; outgoing edges refer to outputs. Accordingly, this model is focused on the power sector and additionally includes hydrogen and synthetic gas to represent technologies for long-term storage of electricity. Chapter 3 provides an exhaustive example for the mathematical formulation of bottom-up planning models.

1.4 Implications for bottom-up planning

This section applies insights on energy scenarios from section 1.2 to derive implications for the development and application of bottom-up planning models introduced in section 1.3.

1.4.1 Openness and accessibility

Since scenarios are important communication tools in the debate about energy futures, equal opportunity to participate in the debate implies equal access to the scenarios underlying modeling knowledge. The consequence here is twofold: First, methods and inputs of scenario must be transparent, so everybody in the debate has the knowledge to critically assess them. Second, modeling tools must be openly available and accessible, so everybody in the debate can contribute scenarios. In the academic literature the need for both transparent scenarios and open models has been widely acknowledged (Pfenniger et al. 2017; Weibezahn and Kendziorski 2019; Morrison 2018; Junne et al. 2019). Since Keepin's critique of the IIASA model that was only possible because he worked at IIASA himself, influential models like TIMES have been made publicly available and open-source has become the standard for new models (Wynne 1984; E4SMA 2021).

An essential but often overlooked factor in this context, especially beyond the scientific community, is accessibility. Many actors outside of academia do not have the resources in terms of working time or technical knowledge to familiarize themselves with complex data documentations or programming tools. Open modeling tools that require substantial programming skills, scenario data that is provided in a rare data format, or extensive documentations that are hard to understand all formally comply with openness, but do little to open up the debate.

1.4.2 Bias minimization

Analysis in section 1.2 revealed that quantitative models are not objective tools and inevitably biased, either by the pursued method, or the assumed parameters. Nevertheless, there are strategies to be transparent about potential bias and minimize it.

Methodologically, the engineering approach of bottom-up planning models leaves less room for bias than models based on economics or other social sciences. In contrast to economic laws, which can be highly ambiguous—Beckert describes for example how different macroeconomic models either assume a positive, a negative, or no effect of public spending on economic growth—natural laws are unambiguous (Beckert 2016, p. 229). However, bottom-up models are not exact representations of the physical energy system but must approximate certain laws and heavily aggregate the system to keep complexity reasonable. For instance, models usually approximate the physical power grid by neglecting distribution grids, aggregating the transmission grid into larger nodes, and applying some linear approximation of power flow equations (Leuthold, Weigt, and Hirschhausen 2012). On the upside, research frequently questions such simplifications and tests them against more accurate representations for validation (Neumann and Brown 2021; Frysztacki et al. 2021; Fattahi et al. 2021). In addition, an increasing number of studies compares different models to investigate differences and identify bias (H. Lund et al. 2007; Landis et al. 2019). To increase transparency about methodological bias, this research should be pursued further and in addition, scenario studies should openly discuss how their methods might bias results, especially if they diverge from standards.

The second source of bias in bottom-up planning models are quantitative assumptions. Similar to methods, the reasonable range for technical parameters is much smaller than for parameters that are related to economic or social questions. Calorific values of energy carriers are exactly defined, full-load hours of renewables are limited by empirical data, and Carnot's rule gives maximum efficiencies, but estimates of capital costs, investment costs, or the socially feasible potential of renewables can vary greatly. As described in the previous sections, some

assumptions also depend on results of the scenario itself, for example heavy expansion of a technology can induce learning effects and reduce investment costs. Here, one approach can be to include this mechanism, in this case learning rates, into the model, although this always comes at the risk of obscuring bias instead of reducing it, for instance, because a subjective cost estimate is just replaced with a subjective learning rate (Lopion et al. 2019). A similar example is to replace an exogenously fixed demand with an assumed demand elasticity.

In general, modelers should try to assess parameters critically and refrain from unquestioned adoption of parameters used in other scenarios, even if they hold high authority. All parameters should be documented transparently and key parameters with strong impact on results, like demand or renewable potential, should be compared to the range from other scenarios and ideally subjected to sensitivity analysis (Wynne 1984; Pfenniger et al. 2017).

1.4.3 Unknowability and probabilistic methods

Based on the concept of fictional expectations, Beckert draws conclusions about probabilistic methods in economics, which can be transferred to bottom-up planning models. He states that if future events are unknowable, and not uncertain, probabilistic methods are as inaccurate as deterministic methods (Beckert 2016, p. 43). But, because probabilistic methods add sophistication and probabilistic statements about the future are harder to refute, they are still being used.

Various studies recommend the implementation of probabilistic methods into bottom-up planning models to account for uncertainty and increase their accuracy (Pfenniger and Pickering 2018; Ringkjøb, Haugan, and Solbrekke 2018; Wiese et al. 2018). Given the limitations of probabilistic methods, this can only be recommended for parameters that are actually uncertain, not unknowable. In other words: Probabilistic implementation of a parameter requires a well-founded estimate of its distribution to add accuracy and not just complexity to a model. For example, historic weather data can quantify the distribution of renewable generation very well rendering its probabilistic implementation sensible. On the other hand, deriving a robust stochastic distribution for economic parameters, like capital or investment costs, appears much more difficult, so a probabilistic implementation should be considered carefully.

1.4.4 Influence on decision making

Above methods and parameters, the ability of scenarios to advance the debate on energy futures decisively depends on how they are deployed. The influence scenarios have on current debates and decisions—often referred to as *policy relevance*—can be used to draw two implications for modeling.

First, scenario scope, and therefore model scope must coincide with the decisions and questions under consideration. Accordingly, Hughes and Lipscy (2013) describe how long-term scenarios for decarbonization rarely have an effect on short-term decisions, because actors find their insights difficult to apply. Overall, scope in bottom-up planning models can be divided into temporal, regional, and sectoral scope, each having its significance. A temporal scope of multiple years is important to model the dynamics of decarbonization, a large regional scope to consider how energy carriers are exchanged between different regions, and a broad sectoral scope to reflect the utilization of electricity outside of the power sector. For example, analysis of the additional renewable capacity to achieve a certain renewable share by 2030 has to consider how much of the existing capacity is decommissioned by 2030, net exchange of electricity with neighboring countries, and the amount of added demand from the heat and transport sector. To cover a large scope while maintaining a sufficient technical detail is challenging for bottom-up planning models. Even if methods to reduce computational complexity are deployed, models cannot have all-encompassing scope or detail and must flexibly adapt to questions investigated in a specific scenario.

Second, energy scenarios should carefully consider technical feasibility to prevent severe path dependencies. To demonstrate the disruption, if widely shared fictional expectations, or scenarios, are realized to be infeasible too late, Beckert attributes the financial crisis of 2008 to expectations regarding housing prices and homeownership that suddenly proved false (Beckert 2016, p. 120). In energy scenarios, speculative assumptions on the availability of technologies, for example the maturity of technologies like carbon capture or the effective potential of specific renewables, could create similar effects (Braunger and Hauenstein 2020). If their availability is widely expected and anticipated by decisions, sudden unavailability will cause failure to achieve mitigation goals. Therefore, scenarios should focus on a risk-averse approach and deviating, more explorative, scenarios should be labelled as such and be aware of imposed path dependencies.

1.4.5 Socio-scientific questions

Bottom-up planning takes a technical perspective on energy systems, although section 1.2 shows how system development is equally a social process. Against this background, a growing number of studies suggests that bottom-up planning models increasingly address socio-scientific questions, too (Nikas et al. 2020; Senkpiel et al. 2020). Specific questions to be addressed include: adoption of consumer technologies, acceptance of industry-scale technologies, and, similar to past debates described in Midttun and Baumgartner (1986), behavioral change of end-users. Literature discusses two ways for bottom-up planning models to address these questions, either endogenously by integrating them into models or exogenously by adjusting inputs accordingly (Senkpiel et al. 2020).

Generally, incorporating socio-scientific questions regarding individual preferences and convictions into engineering-focused bottom-up models is not advised. Behavioral change or attitude towards technology call for simulative or qualitative methods, but since bottom-up planning models are based on optimization, any representation of social aspects within them is restricted to optimization, too. To address socio-scientific questions anyway, external costs that reflect social aspects can be added to the model and incorporated into the optimization problem, analogously to other cost components. For example, the perceived discomfort from wind turbines can be translated into monetary values and added to the objective function to account for social acceptance of technologies. But the choice of considered externalities and the quantification of their social costs is highly subjective. Estimates for specific technologies often vary by a factor of 100, while estimates for other uncertain parameters, like capital costs, investment costs, or renewable potential rarely vary by more than a factor of two (Stirling 1997; Kost et al. 2018; Bogdanov, Child, and Breyer 2019).[3] Therefore, models considering external costs will carry a huge potential bias imposed by the selection of external costs. Overall, the optimization-based approach of bottom-up planning models is not well suited for socio-scientific questions and, if used anyway, the great range of conceivable social costs is likely to introduce a bias.

Nevertheless, bottom-up planning models can sensibly address socio-scientific questions if their focus remains techno-economic and input assumptions reflect social aspects instead. For example, behavioral change of end-users can be simulated using independent models and then reflected by the exogenous inputs on demand to quantify its potential for climate mitigation. Similarly, the adoption of consumer technologies can be analyzed separately and translated into corresponding boundary constraints for optimization. Questions of public acceptance are already addressed in various studies using bottom-up planning models. Typically, these studies apply modeling for alternatives and quantify the additional cost arising if deployment of certain technologies is limited according to social preferences (Buchholz, Gamst, and Pisinger 2020; Neumann and Brown 2021; Pedersen et al. 2021).

3. See section 3 in chapter 5 for a comparison of renewable potential assumed in different studies.

In conclusion, striving for holistic planning models to address socio-scientific questions is elusive (Silvast et al. 2020). The strictly techno-economic perspective of bottom-up planning models is not a weakness but a strength, because it allows for robust results and small bias. Non-technical questions are best addressed by interdisciplinary research connecting different disciplines and their respective methods.

1.5 Outline and contributions of this dissertation

This dissertation advances bottom-up planning models to create techno-economic scenarios for the transformation towards a renewable energy system. It consists of four original research articles displayed in Fig. 1.3 starting with a revision of existing modeling approaches followed by the development of an own approach and a corresponding software tool to address identified shortcomings. Finally, this approach is applied in a scenario study on the planning of transmission infrastructure to demonstrate its capabilities. In addition, the method was used for several other research and policy papers not part of this dissertation, but listed in Table 1.1. An overview of the chapters including my own contribution and publication status is given in Table 1.2. Both tables are provided at the end of this section. All programming scripts, input data, and result files of the dissertation are openly available.

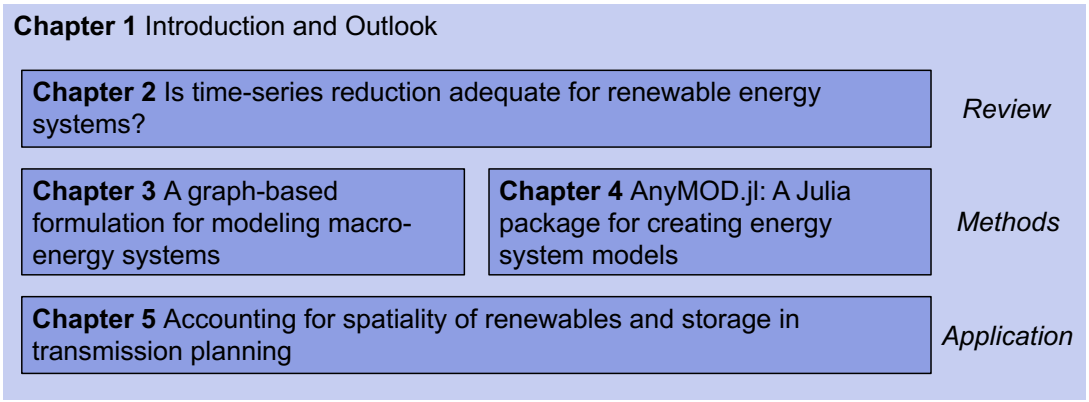

Figure 1.3: Outline of dissertation

Chapter 2 – Is time-series reduction adequate for renewable energy systems?

The chapter evaluates if time-series reduction (TSR) is adequate to use for bottom-up planning models of renewable energy systems. Due to their extensive temporal, spatial, and sectoral scope, macro-energy models commonly use a reduced time-series that is ought to preserve all key characteristics of the original time-series, but contains fewer elements, aiming for a favorable trade-off between complexity and accuracy (Hoffmann et al. 2020; Buchholz, Gamst, and Pisinger 2019).

The characteristics of energy systems with high shares of renewables put the use of reduced time-series into question. Unlike thermal generation, supply from wind and solar fluctuates and depends on energy storage to match generation with demand. Moderate shares of renewables only require small amounts of short-term storage, for example battery or pumped-hydro, but needs change substantially as shares further increase towards 100%. In this case, in addition to short-term storage, systems increasingly depend on long-term storage, for example based on synthetic hydrogen, to balance supply and demand across seasons (Zerrahn and Schill 2017; Schill 2020; Jenkins, Luke, and Thernstrom 2018). If reduced time-series cannot adequately capture fluctuations and storage requirements, computed scenarios will either be sub-optimal or cannot fully satisfy demand.

For the analysis, the paper combines different methods for deriving reduced time-series and for implementing them into bottom-up models. Considered implementation methods include grouped periods with an extension for seasonal storage introduced in Kotzur et al. (2018b) and chronological sequences. To evaluate different combinations of methods, a stylized bottom-up planning model is first solved with a reduced time-series and then run again with a full resolution, but capacities fixed to the values computed previously. Afterwards adequacy of the reduced time-series is measured based on the amount of lost load in the second step. The analysis deploys two external open-source tools, Calliope and TimeSeriesClustering.jl, and extends the latter with additional methods.

The results show that TSR should be applied with caution when modeling renewable energy systems, because intermittency of renewables and dependency on seasonal storage adversely affect its accuracy. As suggested by former research, we found the accuracy of TSR to increase with the length of the reduced time-series. Grouped periods did not consistently achieve small shares of lost load and showed no bias towards certain technologies. For implementation as chronological sequences, results highly depend on how the reduced time-series is scaled to achieve consistency with a full time-series. Depending on the scaling method, results are either biased towards short-term or long-term storage. The bias towards short-term storage causes considerable loss of load, but when scaling with a bias towards long-term storage, loss of load is small at the expense of overestimating system costs. Compared to chronological sequences, grouped periods require more time to solve for the same number of time-steps, because the approach requires additional variables and constraints. Therefore, the chapter proposes investigation of alternative methods to reduce computational complexity, specifically the use of different temporal resolutions within the same model and advanced solution algorithms.

Chapter 3 – A graph-based formulation for modeling macro-energy systems

Following up on the previous conclusions, this chapter introduces a novel graph-based formulation for bottom-up planning models of macro-energy systems. It aims at reducing computational complexity to mitigate dependence on TSR when modeling high shares of renewables. In addition, it enables a large temporal scope not limited to a single year, but capable of modeling pathways of multiple years under perfect foresight.

The formulation organizes sets of elements in rooted trees with multiple levels. For instance, the tree for time-steps will typically have years on the first and the subsequent time-steps within the year, likes days or hours, on the consecutive levels. Other sets organized in the same fashion include regions, energy carriers, and technologies.

Specific models are created by defining these sets and relationships between them, like assigning input and output energy carriers to technologies. Similarly, energy carriers are assigned to time-steps and regions on a specific level to define the temporal and spatial resolution they are modeled at. As a result, temporal and spatial resolution can be varied per energy carrier, for instance modeling electricity hourly, but balancing supply and demand of gas daily. This achieves the temporal detail to capture fluctuations of wind and solar, but reduces the effort dedicated to other carriers and captures the inherent flexibility of large-scale infrastructures, like the gas grid. To account for the substitution of energy carriers, a carrier can substitute each of its ancestors on the preceding levels of the rooted tree. For example, if a technology uses the carrier *methane* as an input and *methane* has the descendants *natural gas* and *synthetic gas*, both can equally be used as an input fuel. The concept applies analogously to demand, storage, and transport of energy carriers.

In addition, the formulation introduces several new features to model expansion and operation of technologies. For expansion, these features aim to model the transformation of the system more accurately and include uniform capacity expansion across several years, endogenous decommissioning of capacities, and accounting for technological advances, like increasing efficiencies of electrolyzers. For operation, features aim for a better representation of flexibility. This includes different operational models for technologies, like cogeneration

plants adjusting their heat-to-power ratio, and the combination of generation and storage technologies, like home batteries paired with PV panels.

To demonstrate feasibility of the presented formulation, an example model is created and solved at different temporal resolutions. Results show that limiting an hourly resolution to electricity and modeling other carriers daily or in four-hour blocks reduces computation time by about 70% but has negligible effects on system costs and installed capacities.

Chapter 4 – AnyMOD.jl: A Julia package for creating energy system models

The graph-based formulation introduced in the previous chapter holds great benefits but is complex to implement. Against this background, the chapter introduces AnyMOD.jl, a modeling framework implementing the graph-based formulation and automating the creation of models applying it.

Following the ideas proposed in section 1.4.1, AnyMOD.jl promotes openness and accessibility. Accordingly, it is implemented in the open programming language Julia deploying the packages JuMP.jl as a backend for linear optimization and DataFrames.jl for efficient SQL-style data processing. In addition, it is compatible with any open or commercial solver implemented in Julia. Besides the open-access publication of this chapter, a comprehensive online documentation and the commented code of the tool are publicly hosted on GitHub.[4]

To facilitate access, AnyMOD.jl follows an easy-to-use principle and creates individual models solely from CSV files and a few lines of standard code. As a result, analyzing inputs, running an existing model, or performing sensitivity analysis requires very little knowledge about the framework or programming. A deeper understanding of the framework enables users to create new models themselves and familiarity with the Julia language allows to add own features to a model. Since models are defined from CSV files and short code scripts, the framework supports version-controlled model development to promote collaboration and transparency.

The read-in of parameter data exploits the tree-structure sets are organized in and enables highly specific control over inputs but avoids redundance at the same time. Since parameter data can be freely structured and distributed across input files, new models can be modularly constructed from existing files.

To enable modeling at large scope and detail, AnyMOD.jl makes several efforts to increase the performance of creating and solving models. To increase the performance of interior-point-solvers, a scaling algorithm automatically moves coefficients of the model's underlying optimization problem into a desired range. In addition, model creation heavily deploys multithreading and prevents creation of unnecessary model elements, like variables and capacity constraints for PV generation during the night. As a result of these efforts, the model deployed in chapter 2 is solved 80% faster when created with AnyMOD.jl compared to Calliope but will provide the exact same results.

Finally, the chapter displays an application of the framework that was part of a policy paper on the stimulus packages of the European Union in response to the COVID-19 pandemic. Additional research and policy papers deploying the tool are listed in Table 1.1. The section also introduces the framework's capabilities to visualize model structure and results.

Chapter 5 – Accounting for spatiality of renewables and storage in transmission planning

The final chapter of the dissertation applies the developed methods to evaluate the benefits of considering storage systems and different placement of renewables as substitutes for grid expansion. To analyze these benefits, a first-best scenario that simultaneously optimizes expansion of generation, storage, and the transmission grid is compared to several sequential

4. Link to the repository: https://github.com/leonardgoeke/AnyMOD.jl

scenarios. These scenarios determine generation capacities in the first step assuming a copperplate and then address grid expansion in a consecutive second step with fixed generation capacities and a relaxed copper-plate assumption. Variations of the sequential scenarios additionally allow the expansion of short- or long-term storage in the second step.

Analysis is focused on a renewable German power system but takes detailed account of sector integration and exchange with other countries. The applied model is based on the graph-based formulation for bottom-up planning models and the AnyMOD.jl framework. In the model, capacity expansion is limited to technologies generating or storing either electricity, hydrogen, or synthetic gas. Final demand for all carriers is set exogenously and accounts for decarbonization of the heating, transport, and industry sector. The model applies an hourly resolution for electricity while hydrogen and synthetic gas are balanced daily. Assuming flexible charging, battery electric vehicles must cover their electricity demand across one day. Residential and process heat apply a four-hour resolution to account for the thermal inertia of buildings and load shifting potentials in the industry.

The spatial scope of the model includes 29 European countries and 38 NUTS-2 regions for Germany, the focus of the study. Other European countries are included to account for the flexibility im- and export of electricity and hydrogen provides, but to avoid a distortion of results, capacities in these countries are fixed to the same value for all scenarios. Due to its long lifetime, the current transmission infrastructure for electricity and gas is included in the model and aggregated according to the covered regions. Apart from that, the model takes a greenfield approach and is limited to a single year.

Results show that consideration of long-term storage as a substitute greatly decreases grid expansion and thus also system costs, regardless of whether it is available in the fist-best or one of the sequential scenarios. At a 4.5 percent increase of system costs, storage can substitute grid expansion entirely. On the other hand, only small effects on grid expansion and system costs arise from short-term storage or placing renewables differently. The latter is partly explained by modest assumptions on renewable potential that is almost fully exploited to satisfy demand and leaves little room to optimize placement.

In conclusion, the model achieves a great spatial and sectoral scope, high temporal detail and a flexible representation of sector integration and provides results suggesting that modifications to the current policy framework could greatly reduce the need for grid expansion, even if sector integration doubles the demand for electricity. However, the chapter concludes that additional research with a different perspective is necessary to ensure the robustness of these findings, in particular more detailed models of grid operation.

Table 1.1: Additional applications of the graph-based formulation and AnyMOD.jl

Publication details
European Green Deal: Using Ambitious Climate Targets and Renewable Energy to Climb Out of the Economic Crisis (Hainsch et al. 2020) Policy paper on the stimulus packages of the European Union in response to the COVID-19 pandemic. AnyMOD.jl was used to re-iterate results of the energy system model GENeSYSMOD at higher detail.
100% Renewable Energy Scenarios for North America—Spatial Distribution and Network Constraints (Zozmann et al. 2021) Research paper on a renewable North American electricity system with a focus on the trade-off between transmission and local generation.
100 Prozent erneuerbare Energien für Deutschland: Koordinierte Ausbauplanung notwendig (Kendziorski et al. 2021) Policy paper on options for a fully renewable Germany energy system highlighting the need for a coordinated expansion of different infrastructures.
The potential of sufficiency measures to achieve a fully renewable energy system - A case study for Germany (Blaumann et al., forthcoming) Research paper on sufficiency measures in the industry, heat, and transport sector and their effect on the energy system.

Table 1.2: Chapter origins and own contribution

Chapter	Pre-publications & Own Contribution
2	**Is time-series reduction adequate for renewable energy systems?**
	This chapter is based on: Göke, L., and M. Kendziorski. 2021. "The adequacy of time-series reduction for renewable energy systems." *Energy* 238:121701. doi: 10.1016/j.energy.2021.121701
	Joint work with Mario Kendziorski. L.G. and M.K. both developed the model and methodology and curated the data. L.G. wrote the paper and managed the review and editing process.
3	**A graph-based formulation for modeling macro-energy systems**
	This chapter is based on: Göke, L. 2021a. "A graph-based formulation for modeling macro-energy systems." *Applied Energy* 301:117377. doi: 10.1016/j.apenergy.2021.117377
	Single-author original research article.
4	**AnyMOD.jl: A Julia package for creating energy system models**
	This chapter is based on: Göke, L. 2021b. "AnyMOD.jl: A Julia package for creating energy system models." *SoftwareX* 16:100871. doi: 10.1016/j.softx.2021.100871
	Single-author original research article.
5	**Accounting for spatiality of renewables and storage in transmission planning**
	This chapter is based on: "Accounting for spatiality of renewables and storage in transmission planning", Under review in *Energy Economics*
	Joint work with Mario Kendziorski, Claudia Kemfert, and Christian von Hirschhausen. L.G. and M.K. both developed the model and methodology and curated the data. L.G. wrote the paper and managed the review and editing process. C.K. and C.v.H. initiated the research and provided critical feedback.

1.6 Research outlook

Irrespective of their exact design, future energy systems will be increasingly shaped by electricity generation from wind and solar and its consumption outside of the power sector. To create techno-economic scenarios of this transformation, the dissertation advances and applies bottom-up planning models of macro-energy systems. It provides several starting points for further research that can be grouped into methodological refinements and scenario applications.

1.6.1 Methodological refinement

As discussed in the previous section, the purpose of varying the temporal resolution within a model is not only to reduce its size, but also to achieve a more accurate representation of the system's flexibility. Modeling carriers like hydrogen or gas at a daily resolution is well justified, after all gas is traded daily and gas sector models typically have a daily resolution, too, but the appropriate resolution applied to electric mobility or heating is debatable. The best way to validate these assumptions is to explicitly represent their demand-side management potential using existing formulations and compare results against different temporal resolutions (Zerrahn and Schill 2015). Investigating this topic further also appears promising from a policy perspective, because studying how different assumptions on demand-side flexibility impact system costs is important to assess whether implementation of smart meters or bidirectional charging is worth the effort.

Despite the considerable progress, computational complexity still limits the scope and detail of bottom-up planning models. One approach to further reduce computation that has not yet been exhaustively addressed is the solution algorithm deployed to solve a model. At the moment, bottom-up planning models are best solved with off-the-shelf interior-point algorithms that cannot exploit the specific problem structure and hardly benefit from parallelization on high-performance computers.

Therefore, one promising strategy appears to decompose models into smaller parts and then apply parallelized solution methods to solve them. First approaches of this kind have already been published: Sepulveda (2020) introduces a solution algorithm combining various decomposition methods and Rehfeldt et al. (2021) apply a specialized interior-point solver. In addition, comparable approaches have been developed for models of small-scale systems that unlike macro models include integer constraints (Bahl et al. 2018; Baumgärtner et al. 2020). Advanced solution algorithms are particular necessary when bottom-up planning models extend their scope to consider multiple climatic years within the same model, which several recent studies recommend (Pfenninger 2017; A. P. Hilbers, D. J. Brayshaw, and Gandy 2021; Ohlendorf and Schill 2020). From an application perspective, algorithms should intitally focus on model feasibility at high temporal resolution rather than finding a guaranteed optimal solution.

1.6.2 Scenario applications

The methodological improvements introduced in this dissertation open up several opportunities for new research on decarbonization and renewable-based systems from a technical and non-technical perspective.

On the technical side, the graph-based formulation can be applied to study how sector integration impacts storage requirements of renewable energy systems, similar to the way chapter 5 addresses grid expansion. Sector integration provides numerous options to provide flexibility like flexible charging of electric vehicles, demand-side management, or heat storage, but existing research does not account for all of them and often omits other options, like reginal balancing, too. As a result, storage requirements could be overestimated, in particular for short-term storage like batteries. Addressing this question would benefit from validating

temporal resolutions as discussed in the previous section and from modeling the heat and transport sector more explicitly.

Modeling pathways instead of single years is a feature of the formulation that has hardly been used so far but offers insightful applications as well. Specifically, an analysis of the consistency between short-term scenarios from transmission system operators (TSO), like the Ten-Year Network Development Plan, and long-term scenarios for decarbonization appears interesting (ENTSO-E 2020). For example, long investment cycles in the industry imply that facilities built in the near future will still operate when the energy system should be fully decarbonized, and switching these facilities to hydrogen requires the timely expansion of infrastructure in the power sector to supply electricity for electrolyzers. If the power sector cannot supply enough electricity, switching to hydrogen in time is impossible and will lead to stranded assets or failure to achieve mitigation goals later.

The modular structure of AnyMOD.jl also facilitates the creation of new applications from existing models for regions other than Europe or Germany. For example, one model is currently developed for Round 37 of the *Energy Modeling Forum*[5] on *High Electrification Scenarios for North America*.

On the non-technical side, future work should concentrate on the impact that changes in energy consumption can have on decarbonization pathways. As outlined in section 1.4.5, this is not exclusively a task for bottom-up planning models but requires to connect input assumptions on demand in planning models with independent analyses of consumption and its sensitivity to behavioral change. A first analysis of this kind using the methods presented in this dissertation is conducted in Blaumann et al. (forthcoming).

Finally, further research should compare how the system perspective of planning models compares with how agents actually decide. One conceivable approach is to assess the profitability of investments made by bottom-up models under the current policy framework and use results as a starting point to evaluate the potential of specific policies to incentivize investment.

5. The Energy Modeling Forum (https://emf.stanford.edu/) is an international group for collaborative work on energy system modeling to inform decision-making.

2

Is time-series reduction adequate for renewable energy systems?

This chapter is based on a revised submission of Göke, L., and M. Kendziorski. 2021. "The adequacy of time-series reduction for renewable energy systems." *Energy* 238:121701. doi: 10.1016/j.energy.2021.121701.

2.1 Introduction

Mitigation of climate change and the consequential decarbonization of energy systems relies on quantitative modeling. In particular long-term planning models investigate how large-scale expansion of renewable energy, especially wind and solar, can replace fossil fuels. As result, such models are characterized by an extensive temporal, spatial, and sectoral scope and require special methods to keep their computational complexity manageable (Levi et al. 2019). The most common approach is to use a reduced time-series, that is ought to preserve all key characteristics of the original time-series, but contains fewer elements, aiming for a favorable trade-off between complexity and accuracy (Hoffmann et al. 2020; Buchholz, Gamst, and Pisinger 2019).

The characteristics of energy systems with high shares of renewables put the use of reduced time-series into question. Unlike thermal generation, supply from wind and solar fluctuates and requires energy storage to match generation with demand. While moderate shares of renewables only require comparatively small amounts of short-term storage, e.g. battery or pumped-hydro, needs change substantially as shares further increase towards 100%. In this case, in addition to short-term storage, systems increasingly depend on long-term storage, for example based on synthetic hydrogen, to balance supply and demand across seasons (Zerrahn and Schill 2017; Schill 2020; Jenkins, Luke, and Thernstrom 2018). If reduced time-series cannot adequately capture fluctuations and storage requirements, models will determine results, like installed capacities, that are sub-optimal or cannot fully satisfy demand.

Although is often used to determine capacity scenarios with high shares of renewables, evaluations of its accuracy for such systems are rare. When novel methods of TSR are introduced, their accuracy is typically only tested for existing systems with moderate shares of renewables (Teichgraeber and Brandt 2019; Nahmmacher et al. 2016; Almaimouni et al. 2018; Poncelet et al. 2016b).

The highest renewable share evaluated in the existing literature is 90% (Pfenninger 2017). The analysis compares resulting capacities and system costs for a hourly resolution of 8,760 time-steps to various reduced time-series with 168 to 2,920 time-steps derived by down-sampling, heuristics, k-means and hierarchical clustering. Results show that the accuracy of TSR greatly depends on the reduction method and length of the reduced time-series, but generally decreases at higher shares of renewables. In addition, the inclusion of short-term storage is found to increase accuracy of TSR, whereas the impact of seasonal storage is not investigated.

Mallapragada et al. (2018) analyze the impact of TSR on capacity expansion models up to a renewable share of 70% and without any storage. For this purpose, 16 steps grouped into independent slices are compared to a chronological sequence with 288 steps, both computed using k-means clustering. When testing results with a detailed dispatch model, capacities computed using grouped periods cannot meet between 0.15% and 0.5 % of demand. For the chronological sequence unmet demand never exceeds 0.1% and strongly increases with the renewable share. For both methods, low temporal resolution is found to overestimate solar investments while underestimating wind and gas power plants.

Similarly, Reichenberg, Siddiqui, and Wogrin (2018) test TSR at a renewable share of 50% omitting any storage technologies. With k-means clustering times-series of up to 200 steps are derived and implemented into a capacity expansion model, either using an "integral" method with limited suitability for more complex applications or, analogously to Mallapragada et al., grouped periods. Again, a low resolution is found to overestimate solar at the expense of wind and gas.

Instead of enforcing a specific renewable share, Merrick (2016) analyze how adding wind and solar to a stylized model impacts the accuracy of TSR. For this purpose, the paper adopts a heuristic reduction algorithm and find that the reduced time-series needs to be extended from 10 to 1,000 steps for the model to remain accurate when wind and solar are added.

In addition to the literature cited above, two other types of studies on TSR can be identified. First, there are several studies investigating high shares of renewables and even include storage, but are limited to operation of pre-set capacities (Scott et al. 2019; Raventós and Bartels 2020). At high shares of renewables, operational costs are negligible compared to investment, which renders the studies inapplicable for comparison in the context of this paper. A second group of studies considers TSR and capacity expansion, but does not analyze large-scale systems, which also hinders comparison. Instead the focus is on models of small-scale systems, like residential homes or industrial sites, with very different characteristics, for example the option of flexible supply from the grid or integer constraints (Fahy et al. 2019; Schütz et al. 2018).

In summary, previous work finds that increasing shares of wind and solar reduce the accuracy of TSR in large-scale capacity expansion models, though adequate reduction methods and increased temporal resolution mitigate this effect. So far evaluations are limited to renewable shares up to 90 % and consequently also neglect the need for seasonal storage arising if shares increase further. Therefore, this paper evaluates the adequacy of TSR in capacity expansion models of fully renewable macro-energy systems. For this purpose, capacities computed with a reduced time-series are tested with regard to system costs and generation adequacy using a full time-series again. Here, "full" refers to hourly data, which is the standard generally considered adequate for large-scale models. Since these models cover extensive geographical regions, any sub-hourly fluctuations are assumed to be balance out within each region (T.W. Brown et al. 2018).

Our analysis of TSR makes a strict distinction between how reduced time-series are implemented into models and how they are derived from a full time-series. Section 2.2 and 2.3 respectively introduce the different methods considered for implementation and derivation of reduced time-series. Section 2.4 briefly introduces the capacity expansion model used to evaluate the reduced time-series followed by section 2.5 that discusses the impact on model results and solve time. The paper is closed of by a summary of key findings and their implications for future modeling work.

2.2 Implementation of reduced time-series

Since literature shows that the way models implement reduced time-series greatly affects results, this paper evaluates TSR for different implementation methods. We strictly separate implementation of reduced time-series from their derivation that is discussed in the following section. This section introduces two fundamentally different approaches to implement reduced time-series and discusses their capabilities to account for storage.

2.2.1 Grouped periods

The first method groups the elements of the reduced time-series into periods and then considers each of these periods separately. In this paper, we will refer to this method as "grouped periods". Historically, this method originates from long-established models for planning energy systems like TIMES or MARKAL (Loulou et al. 2016; Kannan 2011).

There are various terms for "grouped periods" in literature, that we've decided not to fall back on, because their use is highly inconsistent and ambiguous. For example, Reichenberg, Siddiqui, and Wogrin use the term "representative days" for this implementation method, while Mallapragada et al. use the same term in a literal sense referring to days representative for a whole year regardless of how they are implemented. On the other hand, Mallapragada et al. refer to grouped periods as "time-slices", but Pfenninger uses the same term to describe a method for deriving reduced time-series, not for their implementation into models.

Fig. 2.1 illustrates the method: A reduced time-series is grouped into several independent periods each containing a chronological sequence of time-steps. The length of these sequences is arbitrary, although most commonly each period is set to represent one day. Since time-steps

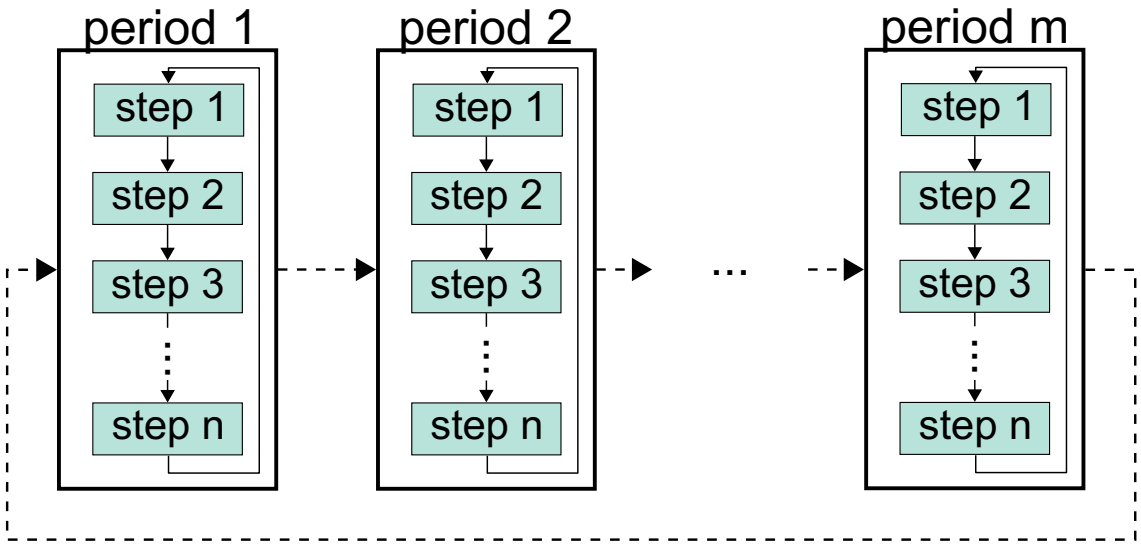

Figure 2.1: Concept of grouped periods

from different periods are considered independently, computational effort is reduced, and periods can be weighted to reflect characteristics of the original time-series more closely.

However, the use of independent periods faces limitations when modeling storage. As indicated by the arrows in Fig. 2.1, cyclic conditions connecting the storage levels of consecutive time-steps can only be enforced within each period. This prevents the exchange of energy across periods, for example charging in period 1 and discharging in period 2. While this simplification can argued to be reasonable for short-term storage, it cannot model seasonal storage—a key component of renewable energy systems as described in section 2.1 (Zerrahn and Schill 2017; Schill 2020; Jenkins, Luke, and Thernstrom 2018). Several studies identified and addressed this drawback by extending the original approach that is limited to short-term storage to include season storage as well (Kotzur et al. 2018a; Tejada-Arango et al. 2018).

For our test on the accuracy of TSR in renewable energy systems, we will apply the method introduced in Kotzur et al. (2018b), because it is most widely used for large-scale capacity expansion problems. Instead of enforcing an independent cyclic condition for each period, Kotzur et al. introduce a new variable for the storage levels across periods, which is illustrated by the dotted line in Fig. 2.1. This intra-period variable is subject to a yearly cyclic condition replacing cyclic conditions in each grouped period. Its value is computed from the net-balances of charging and discharging within each, formerly independent, period of the reduced time-series. For example, consider a grouped period from the reduced time-series, that that was selected to represent 12 periods of the original time-series and consequently has a weight of 12. If charging and discharging of a storage technology in the grouped period nets to 5 GWh, 5 times 12 GWh will consecutively be added to the intra-period storage level. In addition, the capacity limits on each inter-period storage level are replaced with limits on the sum of the intra-period variable and net-charging at each time-step. In summary, instead of enforcing the same storage levels for each grouped period, the approach enforces charging and discharging, the first derivative of the storage level, to be the same for each grouped period.

2.2.2 Chronological sequence

Alternatively to grouping periods, a reduced time-series can be implemented as one chronological sequence. This method, illustrated by Fig. 2.2, simply puts the time-steps of the reduced time-series into chronological order and connects the first and last step with a cyclic condition for storage, which is analogous to how models represent time-series data that has not been reduced. In contrast to grouped periods, chronological sequences prohibit to assign individual weights to the steps of the reduced time-series. Most commonly, this method is applied by

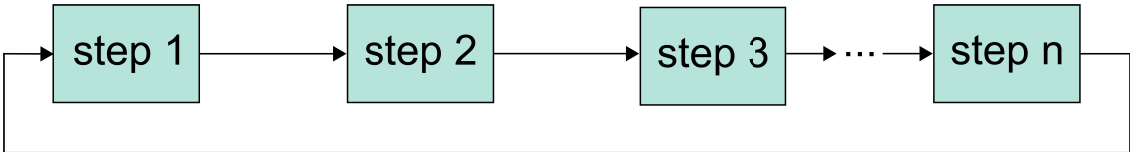

Figure 2.2: Concept of chronological sequence

capacity expansion models focused on the power sector (Tröndle et al. 2020; Neumann and Brown 2021).

When implementing a reduced time series as a chronological sequence, there are two ways to achieve consistency with a full time-series and still represent an entire year: First, the size of each time-step can be increased, 2-hour instead of hourly steps for instance will reduce a time-series from 8,760 to 4,380 steps. Second, step-size can be kept constant and instead the year compressed to a smaller number of hours. This means, that, for example, 3,380 hourly time-steps now represent an entire year. Finally, both approaches can be combined, for example, compressing the year to 2,190 hourly time-steps and then applying a 2-hour resolution finally resulting in 1,095 time-steps.

Both approaches have not yet been formalized or discussed with regard to their impact on model results, but are frequently deployed in the literature. Often implementation is closely tied to the method for deriving reduced time-series. For example, down-sampling, a common method for TSR, uses a reduced time-series derived by summing successive hours into new times-steps, which increases step-size but keeps the length of the year constant (Hoffmann et al. 2020). In contrast, Gerbaulet and Lorenz (2017) derive a reduced time-series by selecting every n-th hour of the full time-series and implement the selected hours without adjusting their size, effectively compressing the year. However, it is conceivable in both examples to combine the methods for deriving and implementing reduced time-series differently. Down-sampling could average instead of sum successive hours to keep step-size constant and compress the year instead. On the other hand, hours selected by the method from Gerbaulet and Lorenz could be scaled up and represent an entire year.

To demonstrate how implementation affects model variables and final results, consider the capacity expansion problem in Eqs. 2.1a to 2.1h. To differentiate them, variables are written in capital and parameters in lower-case letters. According to the energy balance in Eq. 2.1b, the sum of generation Gen_t, storage input St_t^{in} and storage output St_t^{out} has to match demand given by the parameter dem_t at each time-step t. The following storage balance connects storage in- and output with the storage level St_t^{size} at each time-step t. Eqs. 2.1d to 2.1f enforce capacity constraints on storage in- and output, storage levels and generation ensuring production does not exceed the capacity $Capa_i$. For generation, capacity constraints include a capacity factor cf_t that specifies the share of capacity available for generation at time-step t. Finally, the objective function Eq. 2.1a is composed of total investment costs $InvC$ computed from capacities $Capa_i$ and specific investment costs $invC_i$ in Eq. 2.1g and total variable costs $VarC$ computed from generation Gen_t and specific variable costs $varC$ in Eq. 2.1h.

In the example, time-series data includes the capacity factor cf_t and demand dem_t. Demand is given in power units and is scaled according to the respective step-size by the parameter α. At a step-size of 2 hours for instance, α has a value of 2 scaling a demand of 40 GW to 80 GWh. As a result, scaling changes the level of generation and storage variables requiring to scale capacity variables accordingly. Note that the energy capacity of storage is not scaled, because it is already denoted in energy units.

If the year is compressed by TSR, energy demand covered in the energy balance does not correspond to actual demand. For example, if the reduced time-series consists of 4,380 hourly steps, all generation variables will only sum to 50% of actual demand. To correct this, the parameter β scales-up all other occurrences of the generation, storage input, or storage output

variable outside of the energy balance, storage balance or the capacity constraints. In the stylized example this only affects the computation of variable costs in Eq. 2.1h.

$$\begin{aligned}
\min\ & InvC + VarC && && && \text{(2.1a)}\\
\text{s.t. } & Gen_t + St_t^{out} - St_t^{in} && = && dem_t \cdot \alpha && \forall t \in T && \text{(2.1b)}\\
& St_{t-1}^{size} - St_t^{out} + St_t^{in} && = && St_t^{size} && \forall t \in T && \text{(2.1c)}\\
& cf_t \cdot Capa_{gen} \cdot \alpha && \geq && Gen_t && \forall t \in T && \text{(2.1d)}\\
& Capa_{st} \cdot \alpha && \geq && St_t^{out} + St_t^{in} && \forall t \in T && \text{(2.1e)}\\
& Capa_{size} && \geq && St_t^{size} && \forall t \in T && \text{(2.1f)}\\
& \sum_{\forall i \in I} Capa_i \cdot invC_i && = && InvC && && \text{(2.1g)}\\
& \sum_{\forall t \in T} Gen_t \cdot \beta \cdot varC && = && VarC && && \text{(2.1h)}
\end{aligned}$$

Since β compensates any artificial shortening of the year induced by a compressed time-series, the parameter can be defined as the inverse to the share of demand covered by the summed generation variables. This share can again be expressed as the number of time-steps m times the step-size α relative to the total number of hours, which translates into the relation displayed in Eq. 2.2.

$$\beta = \left(\frac{m \cdot \alpha}{8760}\right)^{-1} = \frac{8760}{m \cdot \alpha} \tag{2.2}$$

Applied this relation shows that, if a reduced time-series of 384 time-steps is implemented with an hourly step-size implying an α of 1, β equals $\frac{8760}{384}$. If conversely the time-series should be implemented uncompressed, β takes a value of 1 and instead the step-size α increases to $\frac{8760}{384}$. In addition, infinite valid combinations of α and β in between these two points exist. The graph in Fig. 2.3 plots these combinations for different lengths of the reduced time-series m and shows how scaling factors decrease, when temporal resolution increases until α and β ultimately converge to one for an hourly resolution.

At first glance, our formalization of implementation methods may appear captious. After all, model results should not change, regardless of whether generation takes a smaller value in the energy balance, but is re-scaled in other places, or takes a larger value in the first place. However, this only holds true in the absence of any inter-temporal effects, like energy storage. If models include storage, scaling step-size or compressing the year imposes a bias—each in a different way. If step-size is increased, demand that is spread across a longer time span is allocated to a single time-step. Therefore, any fluctuations and mismatches of supply and demand within that time-step are neglected and investment into short-term storage to address them is underestimated. On the other hand, only compressing the TSR, but leaving step-size unchanged, neglects seasonal fluctuations. To illustrate this, consider a reduced time-series of 384 steps. Since these steps were chosen to be representative for the entire year, average demand complies with average demand of the full time-series, but total demand is smaller by a factor of $\frac{8760}{384}$. As a result, short-term storage systems with small energy capacities are capable to shift energy from beginning and middle to the time-series, representing spring and autumn, and effectively operate as seasonal storage.

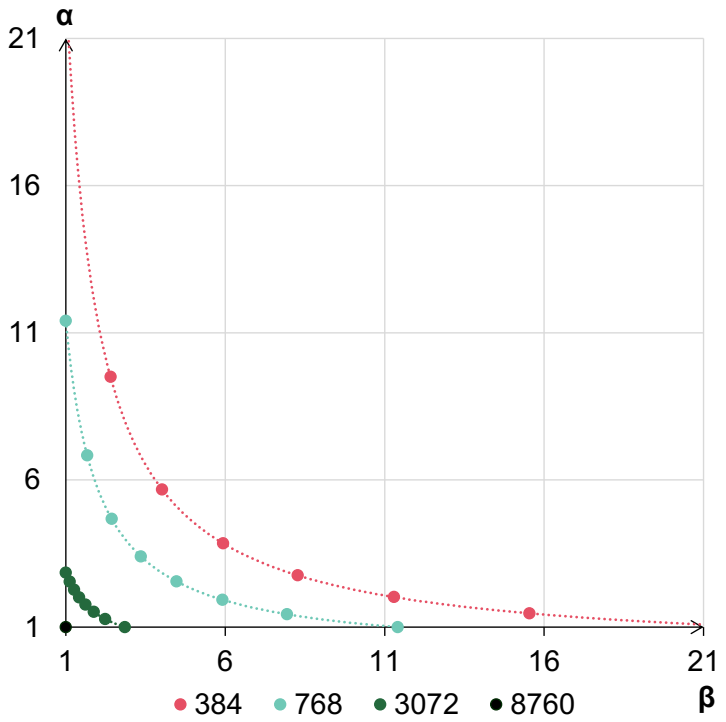

Figure 2.3: Curves of valid scaling factors

2.3 Derivation of reduced time-series

The other important characteristic of TSR is how to derive the reduced from the full time-series. Depending on whether a derivation method requires or prevents weighting of time-steps, it can only be implemented as grouped periods or as a chronological sequence. If weighting is optional, a method can be used with both.

Table 2.1 gives an overview of which derivation methods are applied for which implementation method in this paper. The methods were chosen so that a broad range is covered, and the most common approaches are included. The first column specifies the method itself, while the second columns list all included variations. Input to all clustering methods are demand and capacity factors for wind and solar for the six different regions according to the model description in section 2.4. All time-series were normalized to be equally weighted by the respective reduction algorithms.

In the following, each of the considered reduction methods is briefly introduced. A comprehensive documentation of each method can be found in the cited publications. When deriving reduced time-series grouped into periods, each of these periods represents one day and different lengths are achieved by selecting a different number of days, as it is the norm.

- **k-Means**: The method belongs to the group of partitional clustering algorithms that minimize the Euclidean distance between the center of each cluster and its members (Teichgraeber and Brandt 2019). In the centroid case, the center is the mean across all members of the cluster. Whereas in the medoid case the center corresponds to the median, the member of the cluster most similar to all others. The number of clusters is pre-set and corresponds to the number of grouped periods meaning in our case the algorithm clusters days based on their respective time-series. The individual weights for each period then correspond to the number of days assigned to each cluster. This weighting prevents implementation as a chronological sequence but facilitates representation of periods that are rare and extreme.

		Grouped periods	Chronological sequence
k-Means	centroid	X	
	(medoid)	X	
Hierarchical	centroid	X	
	(medoid)	X	
Poncelet	10 bins	X	X
	20 bins	X	X
	(40 bins)	X	X
Gerbaulet			X
Re-Sampling			X

Table 2.1: Combinations of methods considered for TSR

- **hierarchical**: The used agglomerative hierarchical clustering algorithm consecutively merges the closest points into clusters until the desired number of clusters is reached. This process is again based on the Euclidean distance and either the centroid or medoid of the existing clusters (Teichgraeber and Brandt 2019). Apart from that, the way clusters translate into grouped periods is analogous to the k-Means algorithm.
- **Poncelet**: This method aims to match the duration curves of the reduced and the full time-series (Poncelet et al. 2016a; Poncelet et al. 2016b). For this purpose, each duration curve is stepwise linearized with the number of steps named bins. Afterwards, days for the reduced time-series are selected minimizing the difference between the linearized duration curve of the reduced and full time-series. Originally, the method includes different weightings for each selected day. For this paper it was extended with uniform weighting, so results can not only be implemented as grouped periods, but as a chronological sequence as well. Since periods are solely selected and weighted to match the duration curve of the full time-series, representation of extreme periods is limited.
- **Gerbaulet**: The method referred to as "Gerbaulet" in this paper combines heuristic and optimization in a 3-step process (Gerbaulet and Lorenz 2017). In the first step, every 25th (or 49th and so forth) of the full time-series is selected. Afterwards, the resulting time-series is smoothed with a moving average to prevent sharp jumps in the time-series. Finally, the resulting time-series is scaled using a non-linear optimization to match minima, maxima and full-load hours of the reduced time-series with the full time-series. As a result, the method preserves the extrema of each time-series, but not how they are correlated, e.g. time-steps with high demand and low capacity factors.
- **Re-Sampling**: In case of re-sampling adjacent time-steps of the full time-series are joined together into a single step. Typically, two-, four- or six-hour blocks are used for this purpose and characteristics of the new time-steps are obtained by averaging the original values.

In case of the Poncelet method, for the "40 bins" variation final results did not significantly differ from results for the "20 bins" variation, which is they were omitted from the subsequent analysis. The same applies for "medoid" and "centroid" clustering. To apply the k-means and hierarchical clustering methods their implementation in the TimeSeriesClustering.jl package

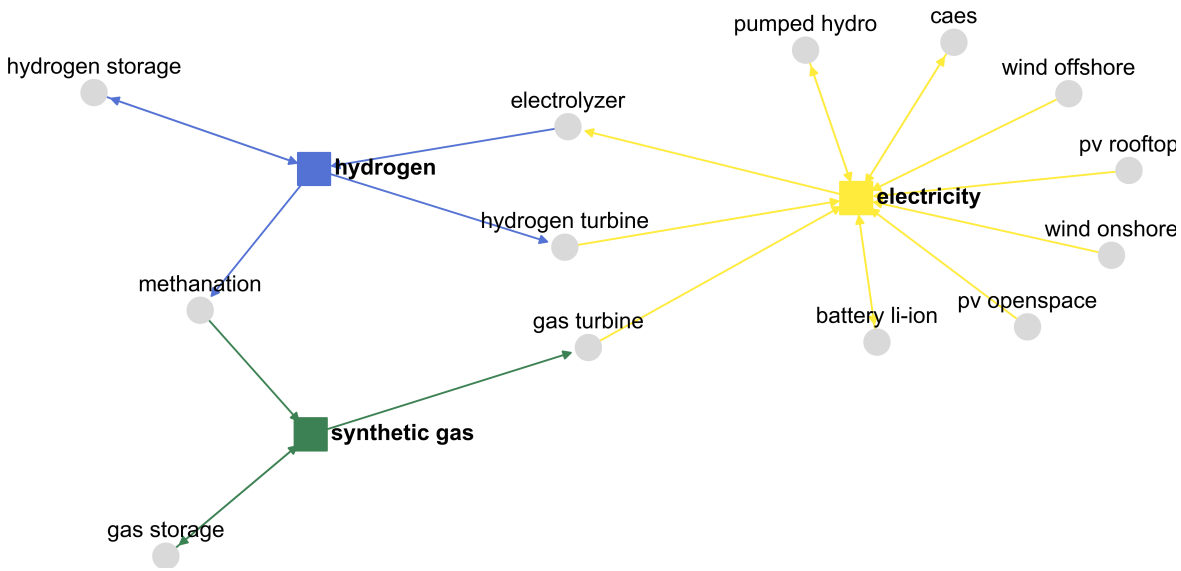

Figure 2.4: Graph of considered energy carriers and technologies

was used (Teichgraeber, Kuepper, and Brandt 2019). In addition, the package was extended with the Poncelet method for the purpose of this paper. For details see the supplementary material.

2.4 Test case for time-series reduction

The various methods for TSR are evaluated based on a stylized capacity expansion model. The model is focused on the power sector due to its high relevance for future energy systems with fully renewable generation. The spatial scope of the model is limited to a single node, resulting in a so-called "island" system. Renewable potential and demand for that node corresponds to data for Germany. Like most large-scale capacity expansion problems, the model is formulated as a linear optimization problem without binary or integer variables.

Demand for electricity includes electricity demand from the heating, industry, and transport sector, based on a scenario where these sectors are fully decarbonized (Hainsch et al. 2020).[1] Accordingly, demand totals 956 TWh with conventional applications only accounting for 299 TWh and instead 456 TWh for industrial heating, 91 TWh for residential heating, and 109 TWh for the mobility sector. The applied load profiles also reflect the change in composition of electricity demand. Since decarbonizing other sectors is found to exhaust the available energy potential of biomass, power generation from biomass is excluded. The model does however include the option of shedding load at a cost of 11,000 €/MWh (Growitsch et al. 2013). Since estimates of load shedding costs greatly differ across sources, we also tested the model with costs reduced by a factor of 10 to ensure robustness (Praktiknjo, Hähnel, and Erdmann 2011; Leahy and Tol 2011).

Figure 2.4 provides an overview of the technologies and energy carriers considered in the model. In the graph, carriers are symbolized by colored and technologies by gray vertices. Entering edges of technologies refer to input carriers; outgoing edges refer to outputs.

In accordance with the research question, the model only includes renewable generation technologies like wind, PV, and run-of-river. Capacity limits and factors for these technologies are differentiated according to the six regions displayed in Fig. 2.5. Overall, potential for openspace and rooftop PV amounts to 198 GW and 707 GW, respectively, for onshore wind a potential of 297 GW is assumed, for offshore wind 84 GW. These limits are based on assumptions used in the H2020 project openEntrance, the time-series of capacity factors are

1. In the respective study full decarbonization is achieved by 2040.

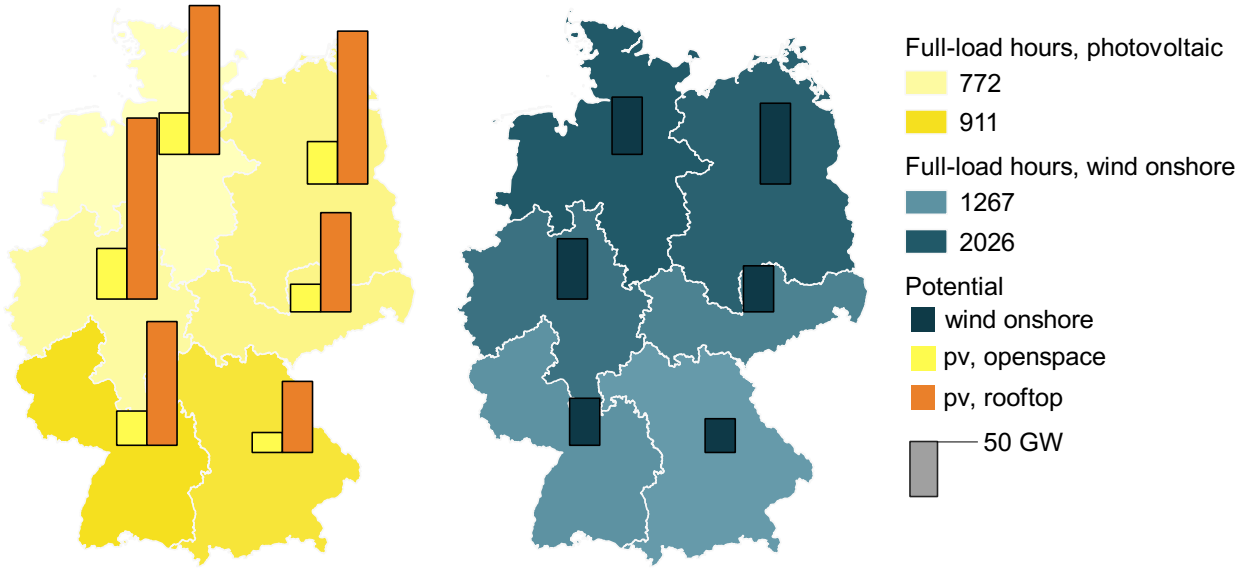

Figure 2.5: Full-load hours and potential of renewables by region

taken from Kunz et al. (2017). The analysis separately considers the climatic years 2015 and 2017. In 2015 full-load hours of PV and wind are close to the long-term average; in 2017 full-load hours are above average for PV and below for wind.

The included technologies for short-term storage include lithium-ion batteries, pumped-hydro, and compressed air energy storage (CAES). Capacities for pumped-hydro are subject to an upper limit of 7 GW for power capacity and 35 GWh for energy capacity, which matches the capacities installed today. For CAES, power and energy capacity is limited to 6 GW and 24 GWh, respectively (Elsner and Sauer 2015). For lithium-ion batteries only the ratio of energy to power capacity is restricted and cannot exceed 10. The modeling of seasonal storage is more elaborate and distinguishes the technologies for creation, storage, and re-conversion of synthetic fuels. These include hydrogen created through electrolysis and used by hydrogen turbines as well as synthetic gas created through methanation and used by conventional gas turbines.

The energy flows that result from solving the model with a full time-series are provided by the Sankey diagram in Fig. 2.6. Although the entire potential for CAES and pumped-hydro is exploited, short-term storage is still dominated by lithium-ion batteries. Seasonal storage of electricity is achieved by hydrogen, while synthetic methane does not play a role. Load shedding is not used, even in runs with the value of lost load reduced by a factor of 10. Total system costs amount to 61 billion of which 85% relate to PV and wind, 9% to long-term and 6% to short-term storage.

For the subsequent analysis of TSR, the model will first be solved with a reduced time-series. In a second step, the model is run again, but with a 8,760 hourly time-steps and capacities fixed to the values computed using TSR to evaluate, if demand can be satisfied. Evaluation includes all the combinations of implementation and derivation methods listed in Table 2.1 and various lengths of the reduced time-series ranging from 24 to 7,680 time-steps.

All model runs implementing reduced time-series as grouped periods were carried of with the Calliope framework, which includes the aforementioned extension for seasonal storage by Kotzur et al. (Pfenniger and Pickering 2018). Since Calliope does not support the different scaling methods for chronological sequences outlined in section 2.2.2, evaluation of chronological sequences was instead performed with the AnyMOD.jl framework (Göke 2021b, 2021a). To guarantee that observed differences result from the underlying methods and not from the use of different frameworks, we ensured Calliope and AnyMOD.jl return the exact same results

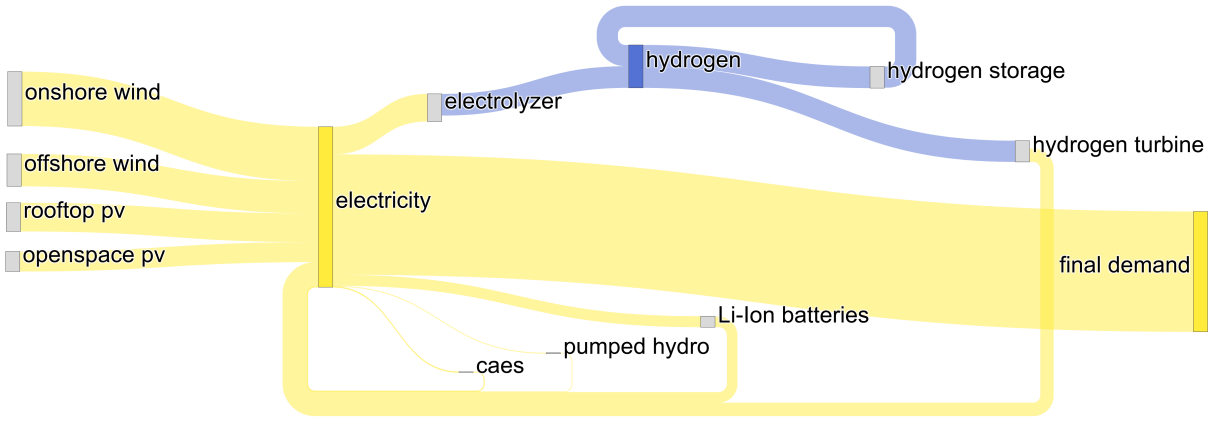

Figure 2.6: Energy flows when solving with full time-series

when run with a full hourly time-series. The supplementary material provides additional documentation of input data and used modeling tools.

2.5 Results

The results section focuses on how TSR impacts the capability to answer key question of modeling, what are feasible designs for renewable energy systems and what are their respective costs? Consequently, the section is centered on two metrics: First, the share of unmet demand, or loss of load, when running the model at full temporal resolution, but with the capacities obtained using TSR. Second, the deviation of system costs when using a reduced time-series compared to the reference case with full temporal resolution.

System costs when running at full temporal resolution, but with the capacities obtained using TSR, are not compared, because they are neither informative nor robust results. The only difference to system costs computed with TSR are costs associated with loss of load, that already amount to 80% percent of total system costs at 1% of lost load. As a result, system costs when running at full temporal resolution, but with the capacities obtained using TSR, are highly correlated with the loss of load and sensitive to the assumed value of lost load, that greatly differs across sources.

Based on the outlined test case, the first two section analyze TSR implemented as grouped periods or chronological sequences. Subsequently, two sensitivities of the test case are investigated and effects on solve time are discussed.

2.5.1 Implementation as grouped periods

For all reduction methods implemented as grouped periods, Fig. 2.7 provides the loss of load on the left and deviation of system costs on the right, both depending on the length of the reduced time-series. Results in the first row relate to 2015; results in the second to 2017. If the reduced time-series is short, all methods exhibit significant lost load of up to 15 %, that declines as length of the reduced time-series increases. This process is non-monotonic and subject to strong outliers, since the selection procedure of each reduction method introduces some randomness. None of the different methods for creating reduced time-series consistently performs better than the others. Overall, loss of load is much smaller for 2015, the year with average full-load hours, compared to 2017, which has above average full-load hours for PV.

Deviation of system costs shows a close and negative correlation with the share of lost load, which is plausible considering additional investments can prevent loss of load but increase system costs. When the reduced time-series is comparatively short, a small loss of load is only

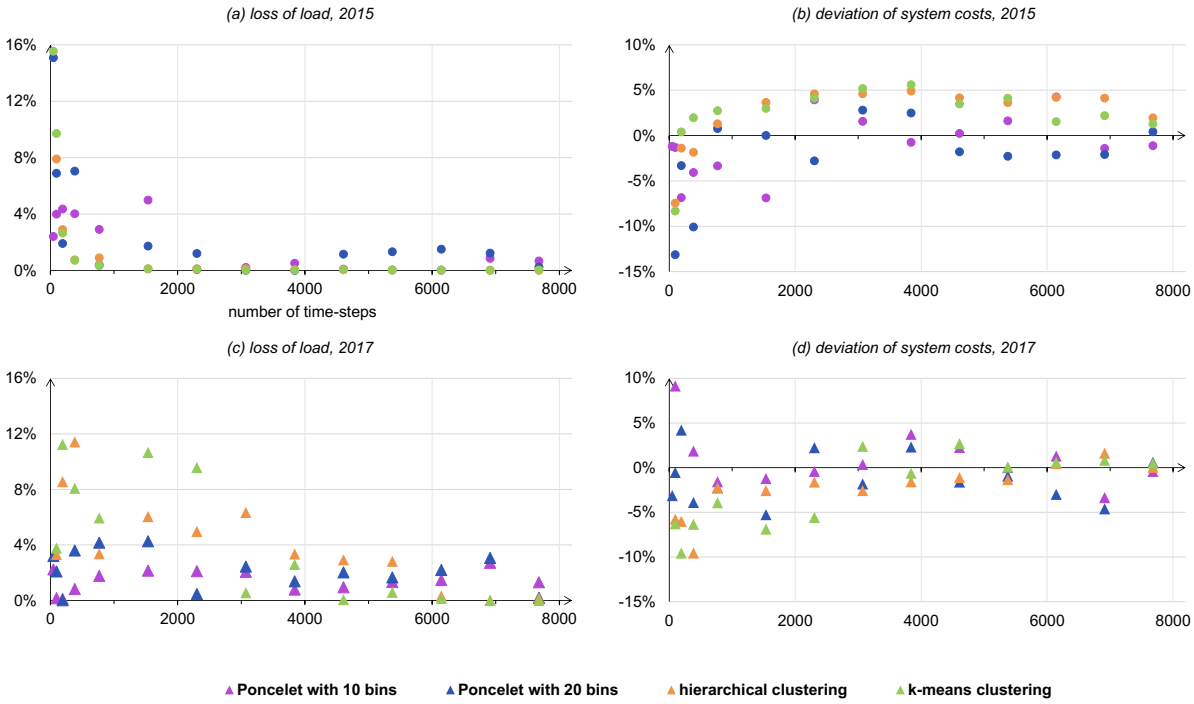

Figure 2.7: Loss of load and deviations of systems costs for TSR using grouped periods

achieved at the expense of overestimating system costs substantially. Increasing the length of the reduced time-series mitigates this trade-off and has capacities converging towards the optimal design of the system.

Fig. 2.8 compares installed power and energy capacities obtained with full resolution against a reduced time-series of 768 time-steps derived using the Poncelet method with 20 bins or hierarchical clustering for the climatic year 2015. Openspace PV, pumped-hydro and CAES are not included, because their technical potential is fully utilized in each case. Other technologies, like methanation or gas turbines, are omitted, because they are not invested in at all. In this example, Poncelet results in 0.8 % of lost load with unmet demand occurring in 107 hours of the year, compared to 0.9 % and 331 hours for hierarchical clustering. Poncelet overestimates system costs by 0.7%; hierarchical clustering by 1.2%.

The comparison shows that compared to a full time-series and Poncelet, hierarchical clustering finds much greater capacities for rooftop PV. Since generation from PV peaks in summer, technologies for seasonal storage, like electrolyzers, hydrogen turbines, and hydrogen storage, serve as a complement to shift generation from summer to winter and are consequently overestimated by hierarchical clustering as well. This relation among errors can be observed in other cases as well, but does not appear more frequently with a certain derivation method. Overall, results revealed no fundamental bias on installed capacities from the respective derivation method.

2.5.2 Implementation as a chronological sequence

Analogously to Fig. 2.7 for grouped periods, Fig. 2.9 provides the loss of load and deviation of system costs for chronological sequences in 2015; Fig. 2.10 provides the same results for 2017. Section 2.2.2 introduced two options for implementing chronological sequences, either compressing or or re-scaling the reduced time-series. Results when reduced time-series are compressed are provided in the first row of Fig. 2.9. In the following rows the method successively shifts until the forth row finally shows results if time-steps are strictly re-scaled. Since results do not substantially differ for 2017, Fig. 2.10 only shows results for strictly compressing or re-scaling.

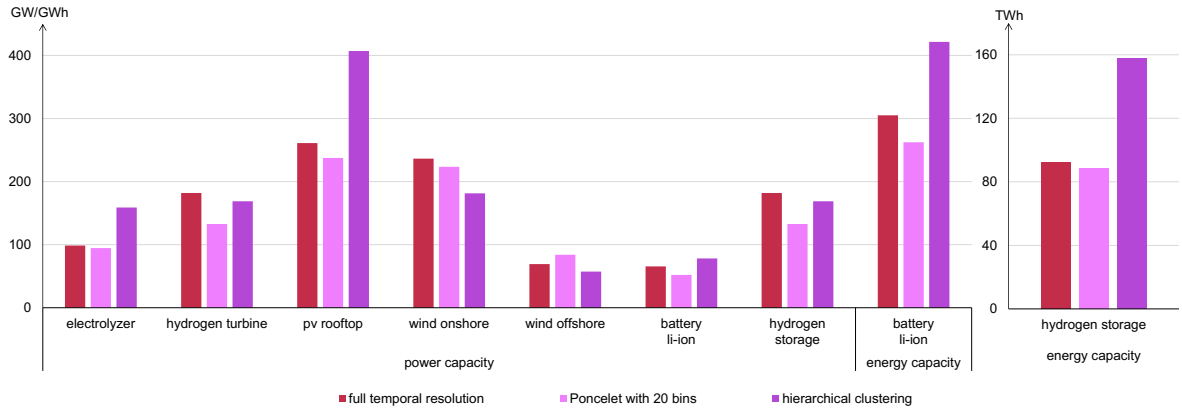

Figure 2.8: Comparison of installed capacities for different reduction methods

The left column shows the share of lost load when capacities computed with a reduced time-series are tested with a full time-series. Loss of load decreases with increasing length of the reduced time-series, in particular when the time-series is still comparatively short, since more time-steps can capture characteristics of the full time-series more accurately. As observed for grouped periods, the loss of load is substantially smaller for the climatic year 2015 than for 2017. Of all reduction methods, "Poncelet" consistently achieves the smallest loss of load, regardless of how many bins are considered, followed by "Gerbaulet" and lastly Re-Sampling.

However, the most significant impact on loss of load is not how the full time-series was reduced, but how the chronological sequence was implemented. Loss of load is highest if the reduced time-series is compressed. As implementation shifts towards demand, loss of load strictly decreases and for 2015 ultimately drops below 4% in all cases but one. System costs are again closely correlated with the share of lost load. High shares imply insufficient investment and a consequential underestimation of system costs. Higher investments in other cases decrease loss of load, but also drive up system costs, eventually even overestimating them.

Implementation also has significant impact on installed power and energy capacities, which are compared in Fig. 2.11 for the Poncelet method with 20 bins and a reduced time-series of 768 time-steps. Analogously to Fig. 2.8, technologies with the same investment across all cases are omitted. The graph confirms the bias of scaling proposed in section 2.2.2.

Compressing the reduced time-series overestimates investment into batteries, a technology for short-term storage, but underestimates investment into hydrogen turbines and storage, both technologies for seasonal storage. The effect of scaling on renewable generators depends on how they interact with storage. Since generation from PV peaks in summer, but demand peaks in winter, at one point additional PV generation can only be used, if it is stored seasonally. As detailed in section 2.2.2, compressing overstates the ability of short-term storage like batteries to provide seasonal storage and consequently overestimates investment into PV as well.

Results shift into the opposite direction when implementation shifts from compressing to re-scaling. Now the model accurately reflects the storage technologies' capability of seasonal storage, but neglects short-term fluctuations on a hourly or daily scale. Correspondingly, compressing greatly underestimates investment into battery storage, but approximates capacities for seasonal storage very well. Since seasonal storage is reflected well, investment into renewables also shifts from PV peaking in summer to wind with a more even seasonal profile.

The bias compressing imposes on short-term storage even remains significant if the reduced time-series is comparatively long and loss of load becomes negligible. When a full-time series is re-sampled into blocks of 4-hours, resulting in a reduced time-series of 91 days, for batteries power capacity is still underestimated by 73% and energy capacity by 23%. If sampled into 2-hour blocks, these values decrease to 12% and 6%, respectively.

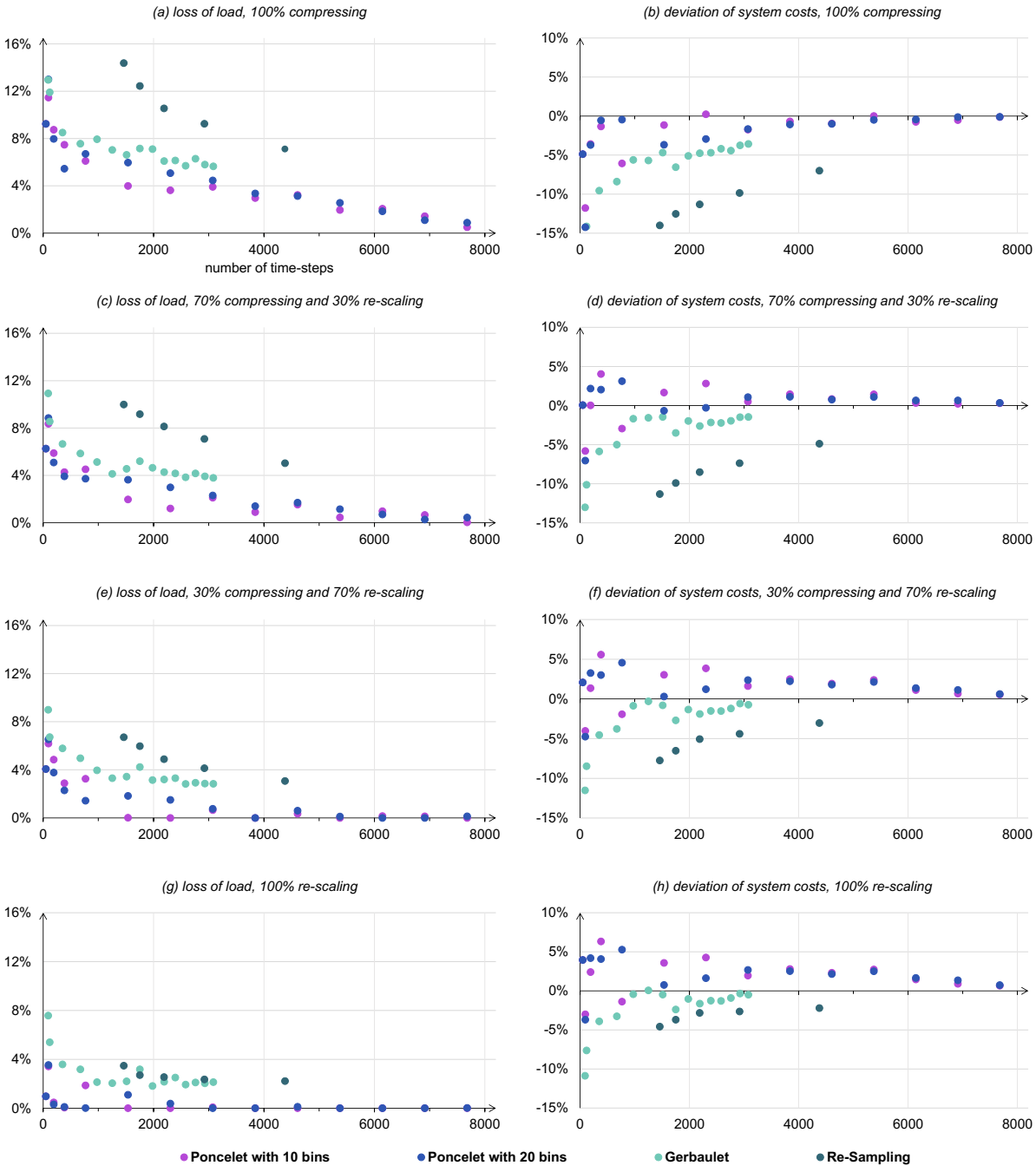

Figure 2.9: Loss of load and deviations of systems costs for TSR using a chronological sequences and climatic year 2015

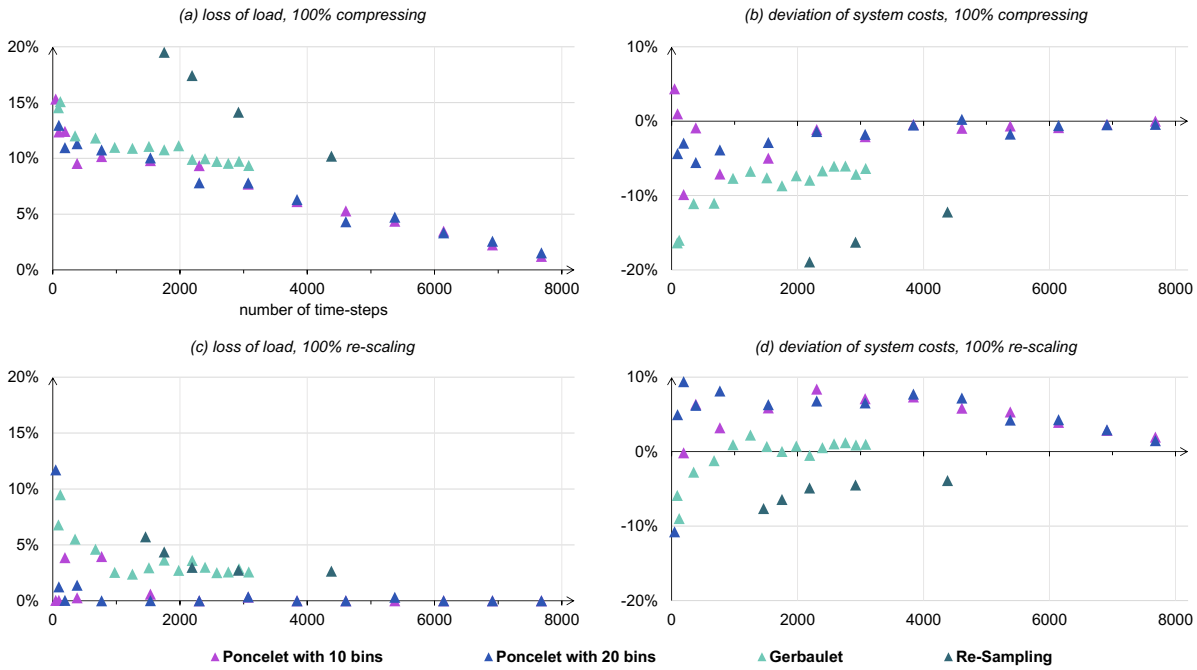

Figure 2.10: Loss of load and deviations of systems costs for TSR using time-steps and climatic year 2017

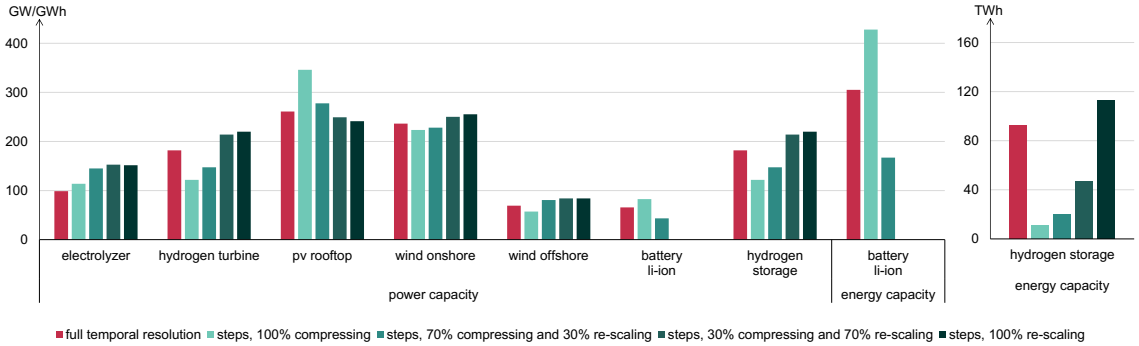

Figure 2.11: Comparison of installed capacities for different scaling methods

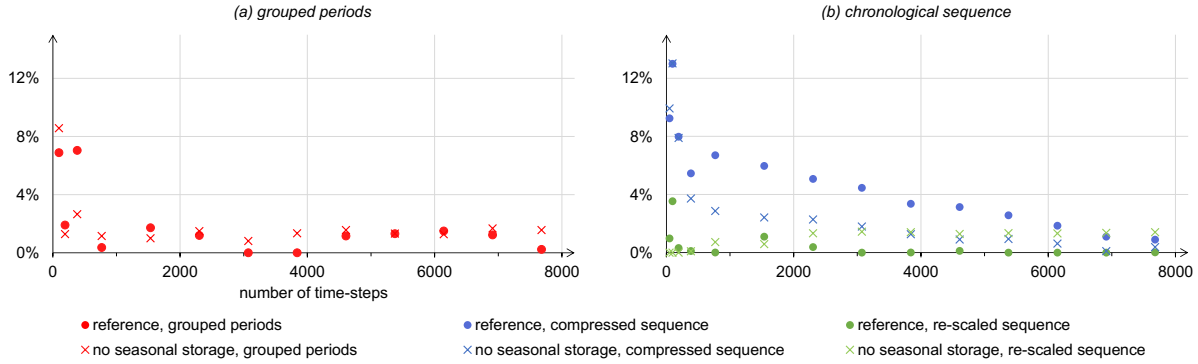

Figure 2.12: Loss of load sensitivity for seasonal storage

The discussed results on installed capacities, in particular for storage, also explain the effect scaling has on loss of load. Since compressing overstates batteries' capability of seasonal storage, investment into actual seasonal storage is insufficient and a significant amount of demand cannot be met, mostly during the winter months. Accordingly, if re-scaling is fully applied, in the example 6.6% of demand are unmet and loss of load occurs in 1126 hours, all of them in first or fourth quarter of the year. The implications of neglecting hourly and daily fluctuations in case of re-scaling are not as severe. Since the installed capacities for seasonal storage are technically also capable to balance short-term fluctuations, lost load is much smaller and only occurs in nine hours totaling 0.001‰ of demand.

2.5.3 Sensitivities for seasonal storage and sector integration

The test case introduced in section 2.4 differs from today's system in many ways. Not only does the test case exclusively include renewable generation technologies but is also distinguished by the role of seasonal storage and change of demand. Besides sector integration doubling total demand, new applications for electricity, in particular electric heating, greatly affect the profile of demand, seasonality becomes more pronounced and peak loads increase. These differences raise the question if the preceding results are only caused by intermittent renewables or also must be attributed to storage and demand.

Fig. 2.12 shows how loss of load for the reference case and climatic year 2015 compares against a sensitivity without any technologies for seasonal storage. In the figure, length of the reduced time-series and implementation method vary, but all cases apply the Poncelet method with 20 bins. Note that excluding seasonal storage only serves the purpose of analysis and is not a practical scenario since system costs double and battery capacity increase by a factor of eight.

Again results exhibit a strong random variation, but at least for compressed chronological sequences the share of lost load decreases, if seasonal storage is omitted from consideration. This indicates that for this method the error from TSR is not only caused by the intermittency of renewables, but also by difficulties to represent the operation of seasonal storage, which is plausible considering the method's characteristics.

Analogously to Fig. 2.12, Fig. 2.13 compares the reference case against a sensitivity on demand, that does not account for sector integration and uses conventional demand data from Germany in 2015 instead. In this case, results do not significantly improve or worsen for any of the implementation methods suggesting that how sector integration changes demand does not affect TSR.

2.5.4 Impact on computation time

Since the original motivation for TSR is to facilitate solving large models, Fig. 2.14 analyses the impact the implementation method and the number of time-steps have on solve time. All

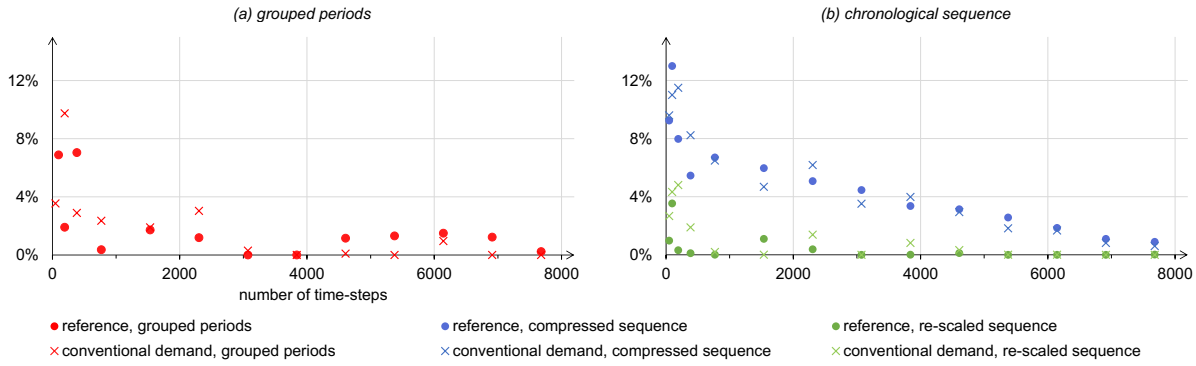

Figure 2.13: Loss of load sensitivity for demand

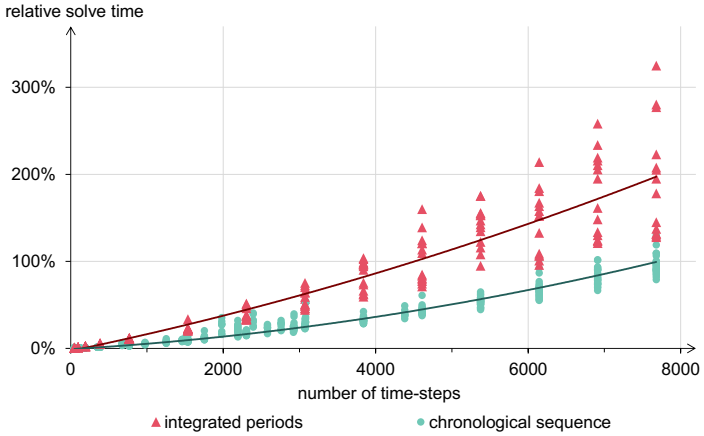

Figure 2.14: Solve time relative to full temporal resolution

solve times are denoted relative to the solve time of the model at full temporal resolution to adjust for the effect of the respective modeling framework.[2] The reported times only include optimizer time. All models were solved on the same cluster with Gurobi using the Barrier method and 2 threads.[3] Since solve times are subject to random variations, quadratic regression curves were added to the figure to visualize the general trend.

As expected, the reduction of solve time strongly depends on the number of time-steps used. At numbers around 3,000 that were found earlier to considerably reduce loss of load, TSR still reduces solve-time significantly. For chronological sequences, solve times converge towards the solve time with full temporal resolution, which is plausible considering chronological sequences are implemented analogously to a full time-series. Solve time for grouped periods increases faster and can even exceed the solve time with full temporal resolution. This effect is explained by the inter-period variables and constraints added to the model increasing its complexity.

2.6 Conclusion and outlook

The results show that TSR should be applied with caution when modeling renewable energy systems. Besides intermittency of renewables, dependency on seasonal storage adversely affects the accuracy of TSR. As suggested by former research, we found the accuracy of TSR to increase with the length of the reduced time-series.

Implementation of reduced time-series as grouped periods did not consistently achieve small shares of lost load. Furthermore, no generally advantageous method for creating reduced

2. AnyMOD.jl solved the full model in 65 seconds; Calliope in 330 seconds, both producing the exact same results.

3. The Gurobi parameters BarOrder and NumericFocus were set to 1 and 2, respectively.

time-series nor any fundamental bias on installed capacities was identified. Compared to chronological sequences, grouped periods required more time so solve for the same number of time-steps, presumably due to variables and constraints added to implement seasonal storage.

For implementation as chronological sequences, results highly depend on how reduced time-series are adjusted to achieve consistency with the full time-series. If the reduced time-series is not re-scaled, results show a bias towards short-term storage and considerable loss of load. If the reduced time-series is re-scaled on the other hand, results are instead biased towards long-term storage overestimating system costs but achieving small shares of lost load. These results are likely to differ for regions with less pronounced seasonal and greater short-term fluctuations. Regarding the creation of reduced time-series, the Poncelet method performed favorable with chronological sequences.

Our benchmark for TSR in this paper is a single climatic year at an hourly resolution, which is not exhaustive. The impact the respective climatic year had on our results, which is consistent with other studies, suggests to extend the scope of planning to multiple climatic years (Bloomfield et al. 2016; A. Hilbers, D. Brayshaw, and A. Gandy 2019). In addition, adequacy of hourly resolutions can be called into question, since it is based on assuming sub-hourly fluctuations balance out across sufficiently large areas (Deane, Drayton, and Ó Gallachóir 2014; T.W. Brown et al. 2018). This is in particular questionable, if models further increase spatial resolution to represent renewables more accurately, as frequently proposed (Frysztacki et al. 2021; Martínez-Gordón et al. 2021). Lastly, spatial and temporal detail must be weighed against methodological simplifications to reduce complexity and keep models linear. For instance, the capacity expansion model applied in this paper assumes that time-series are perfectly predictable and neglects unit commitment or operational constraints of thermal power plants (Seljom and Tomasgarda 2015). So, in conclusion, necessary detail beyond out test case adds to the deficiencies of TSR identified in this paper and suggests further efforts to reduce complexity of large-scale capacity expansion models.

On the one hand, existing methods for TSR can be further improved. One approach is to identify extreme situations in the full time-series where adequacy is threatened and add them to the reduced time-series. However, identifying such situations with low supply and high demand over a prolonged period of time is non-trivial, because both supply and demand again depend on investment decisions by the model. Against this background, Teichgraeber et al. (2020) introduce a method that iteratively adjusts the extreme periods in the reduced time-series by performing a feasibility check with the full time-series. Although their work is focused on small-scale systems, similar approaches could be adopted for macro-energy systems as well. Another approach is to vary temporal resolution within the model and only apply high detail where it is necessary. Renaldi and Friedrich (2017) introduce such a method for small-scale systems; Göke (2021b) develops a similar approach for macro-energy systems.

On the other hand, complexity can be reduced by partitioning problems into smaller parts. Therefore, one approach is to couple models with different scopes and resolutions instead of using one comprehensive but highly complex model to get a broader picture of the energy system. In this case, typically results of long-term planning models are evaluated with more detailed operational models (Antenucci et al. 2019; Collins et al. 2017; Pavičevića et al. 2020). A downside of this approach is the limited capability to feed information from the operational model, like hours with unmet demand, back to the planning model. Alternatively to coupling different models, complex models can be decomposed into smaller parts, typically relating to planning or operation as well, and then solved faster with advanced solution methods. With the exception of Sepulveda (2020), such methods have not yet been adopted for macro-energy systems and are focused on small-scale applications (Yokoyama et al. 2015; Bahl et al. 2018; Baumgärtner et al. 2020).

3

A graph-based formulation for modeling macro-energy systems

This chapter is based on the accepted manuscript for Göke, L. 2021a. "A graph-based formulation for modeling macro-energy systems." *Applied Energy* 301:117377. doi: 10.1016/j.apenergy.2021.117377.

3.1 Introduction

Averting the impending harms of climate change requires to cut carbon emissions from current record highs to zero by at least 2050. Fossil fuels account for the three quarters of all emissions and consequently need to be replaced by renewable energies (Edenhofer et al. 2014). Especially wind and solar have to take a predominant role, since their unexploited potential greatly exceeds hydro or biomass.

This transformation has profound implications for the entire energy system: On the supply side, the fluctuating nature of wind and solar requires additional flexibility to be reliable. On the demand side, the source of primary energy must shift towards electricity from wind and solar, either by direct electrification or synthetic fuels. To provide flexibility and shift primary energy to renewable electricity, the different sectors of the energy system have to be closely integrated. Charging electric vehicles for instance depends on supply from the power sector, but can also contribute to balancing fluctuating supply with demand (Doucette and McCulloch 2011). Similarly, many industrial processes require renewable electricity for decarbonization, but are capable of adding flexibility too (Burre et al. 2020).

Overall, these profound changes of the energy system result in new demands on models analyzing and planning energy systems. To address these demands, Levi et al. (2019) propose the discipline of "macro-energy systems" that is characterized by a large scope, covering several years, different sectors, and a large region and, as a consequence, a high level of complexity, that necessitates great abstraction. Following up on this idea, DeCarolis et al. (2020) argue that the challenges in modelling marco-energy system can best be overcome by collaborative development of open-source tools. The call for openness is also prominent in other publications and is a consequence of the impact models can have on energy and climate policy, since they allow assessing alternative designs of the system in terms of costs and emissions (Pfenniger et al. 2017; Weibezahn and Kendziorski 2019).

This paper introduces a novel graph-based formulation for modelling macro-energy systems. This novel formulation specifically addresses the challenges that the transformation towards a system with high levels of renewables and sector integration imposes. The following literature review provides a detailed overview of these challenges and how existing modelling frameworks meet them. Afterwards, section 3.3 presents the graph-based formulation and its distinctive features by listing the sets and equations constituting the model's underlying optimization problem. In section 3.4 the formulation is applied to create an example model and demonstrate the benefits of the introduced formulation. For this purpose, the open-source modelling framework AnyMOD.jl that implements the graph-based formulation is used. Finally, section 3.5 concludes.

3.2 Literature review

Subsection 3.2.1 summarizes the technical challenges in modelling future energy systems that previous research identified. The following subsection discusses how existing modelling frameworks address these challenges.

3.2.1 Challenges in macro-energy system modeling

A key requirement when modeling energy systems with large shares of renewables is high temporal granularity (Pfenninger, Hawkes, and Keirstead 2014). Former research shows that the number of representative time-steps an entire year can be reduced to strongly depends on the share of weather-dependant generation. At low resolutions utilization of wind and solar is overestimated, since fluctuations of supply cannot be captured adequately (Poncelet et al. 2016a; Nahmmacher et al. 2016; Haydt et al. 2011). Reinforced sector integration may cause a similar effect on electricity demand, if heat supply is increasingly electrified by

electrical heat pumps (Bloess 2019). Since all these temporal fluctuations are weather related and thus subject to uncertainty, high temporal granularity is ideally combined with a stochastic approach (Ringkjøb, Haugan, and Solbrekke 2018).

At the same time, spatial aspects gain in relevance too, when modeling high levels of renewables, since their *"economic potential and generation costs depend greatly on their location"* (Pfenninger, Hawkes, and Keirstead 2014). In addition, in a renewable system the capacity of individual generation units is about a magnitude smaller than in a system characterized by thermal plants. This creates the opportunity to match demand with local supply as an alternative to transporting energy carriers over long distances (Bauknecht, Funcke, and Vogel 2020). However, modeling such solutions does not only require a consistent representation of relevant technologies, for instance solar home systems with batteries, but a high spatial granularity as well.

The need for temporal and spatial granularity when modeling high levels of intermittent renewables and sector integration is directly related to the concept of flexibility. Flexibility can be defined as an energy system's capability to cope with variability and uncertainty in demand and generation (Heggarty et al. 2019). The arising need for flexibility and how it can be satisfied is widely recognized as a key question for future energy systems (Kondziella and Bruckner 2016; P. Lund et al. 2015). To fully account for these flexibility needs within models means to fully capture weather-driven fluctuations and consequently requires high temporal and spatial granularity.

On the other hand, including all options to provide flexibility into models calls for a detailed representation of sector integration. Many potential sources of flexibility involve complex interaction of technologies and energy carriers to build synergies between sectors (Orths et al. 2019). To give but one example, synthetic gas can be generated from electricity via electrolysis and methanation, when supply from wind or solar exceeds demand, stored and then used to provide heat or electricity at times of low intermittent supply. Models that omit these cross-sectoral sources of flexibility might fail to identify cost-efficient solutions and excessively invest into other storage and transport capacities instead (T. Brown et al. 2018).

Besides these challenges concerning granularity and detail, the way models are practically applied creates additional challenges that concern their temporal and spatial scope. Ideally, models can analyze how today's energy system can be transformed to comply with the climate objectives set for a certain year (Oberle and Elsland 2019). Therefore, their temporal scope should include multiple subsequent periods that are simultaneously optimized, also referred to as perfect foresight. If models are limited to single years, computing pathways has to rely on consecutively solving each year separately. This approach has been termed myopic foresight and found to cause suboptimal results due to stranded investments (Löffler et al. 2019; Gerbaulet et al. 2019). A large spatial scope is valuable, because energy systems of different regions are increasingly interlinked, be it through a common energy policy or interconnected markets and networks, as for example in the European gas and electricity sector. The latter is again relevant from a flexibility perspective as well: Especially exchange of electric between regions, can even out local fluctuations of wind and solar generation (Thellufsen and Lund 2017).

3.2.2 How challenges are addressed

Former research already proposed several formulations for modelling energy systems. Typically, these formulations are embedded into a corresponding software tool, also referred to as modelling framework, that is used to generate specific models (Groissböck 2019; Wiese et al. 2018). In the following, two modelling frameworks, OSeMOSYS and Calliope, are evaluated with regard to the challenges outlined in section 3.2.1 (Howells et al. 2011; Pfenniger and Pickering 2018; Pfenninger et al. 2020). The choice fell on these, because both are representative for a larger group of frameworks and models. OSeMOSYS is closely related to many long-established tools for energy system planning like PRIMES, MESSAGE or MARKAL. The Calliope framework

draws parallels to more novel tools like Balmorel, PyPSA and DIETER that are more focused on the power sector and high accuracy regarding intermittent renewables (Lopion et al. 2018; Groissböck 2019).

These different contexts are reflected in the way OSeMOSYS and Calliope treat time, which again affects temporal granularity. OSeMOSYS pursues an approach that aggregates an entire year into a few representative periods, also referred to as time-slices (e.g. a summer evening). Modeling these periods instead of the full year greatly decreases computational effort, but also limits temporal granularity and thus the capability to capture fluctuations of intermittent renewables. To avoid this, Calliope does not rely on representative periods, but rather uses unaltered continuous time series.[1] This comes at the cost of a steep increase in size and solve time, if not only the electricity sector, but the entire energy system is modeled (Lopion et al. 2018). Neither of the two frameworks can account for uncertainty of supply and demand.

The use of representative periods within OSeMOSYS also implies a loss of chronology, and thus restricts the modeling of storage, especially seasonal storage. If a time span, for example the entire summer, is reduced to one representative period, say a week, storage patterns determined for that period apply to the entire time span. Accordingly, storage levels would show the same pattern for each summer week and could not continuously increase over the course of the summer (Welsch et al. 2012). Since energy systems with high shares of variable renewables can be expected to heavily rely on storage, without major adjustments the approach is ill-suited to describe these systems (Kotzur et al. 2018b).

The temporal scope of OSeMOSYS may include multiple subsequent periods of capacity expansion to compute long-term pathways for transforming the energy system. However, properties of technologies cannot depend on their respective period of construction. As a result, technological advances, like increasing efficiency of power-to-gas technologies for instance, cannot be accounted for adequately. Calliope is limited to a single period of capacity expansion.

Besides these differences regarding temporal detail, both frameworks can achieve high spatial granularity and a large regional scope, since the number of regions can be chosen freely. In addition, Calliope also provides an option for discrete expansion and dispatch of technologies, which renders it appropriate for applications as detailed as the building level.

To extend the representation of technologies, OSeMOSYS supports different modes of operation, like either operating a cogeneration of heat and power (CHP) plant at a higher fuel utilization rate, but a smaller CHP coefficient or the other way round. Calliope provides a functionality to include technologies that can store a carrier for later use within a conversion, for example concentrated solar power plants that store heat for later conversion into electricity.

3.3 Model formulation

The graph-based formulation introduced in this paper relies on continuous time series instead of representative periods to achieve the temporal detail necessary for high shares of variable renewables. To model the long-term transformation of the energy system, it supports multiple periods of capacity expansion accounting for technological advance and endogenous decommissioning of capacities. In addition, it extends Calliope's functionality for technologies that first store and later use a carrier by also allowing for technologies that first generate and then store a carrier. This enables modeling decentralized storage systems, like a home battery paired with a PV panel, within large-scale system models. Furthermore, different operational modes for technologies are supported.

Beside these gradual improvements, the proposed formulation introduces two novel features to facilitate modelling high levels of renewables and sector integration:

1. Using representative periods is possible as well but is not the default option.

1. The level of temporal and spatial granularity can be varied by energy carrier. For instance, electricity can be modeled with hourly resolution, while supply and demand of gas is balanced daily. This achieves the temporal granularity required to capture fluctuations in renewable electricity generation but avoids applying it to all other carriers as well. Within spatially aggregated models, for many carriers, like gas for instance, a less detailed resolution will better reflect physical properties and avoid inflating the model. In Renaldi and Friedrich (2017), a similar method from process system engineering is used to optimize a solar district heating system. However, the method is only applied to the temporal granularity only and to technologies instead of carriers.
2. Substitution of energy carriers can be modeled in dependence of the respective context: conversion, storage, transport or demand. For example, heat from residential heat pumps and district heating plants might both satisfy heat demand, but only district heat can be stored within large-scale storage systems.

Since the proposed formulation is specifically aimed at macro-energy systems, it does not support discrete expansion and dispatch of technologies and therefore is not suited to be applied at the urban or building level.

3.3.1 Sets and mappings

This section discusses the sets defined within the modelling framework, in particular time-steps, regions, energy carriers, technologies, and modes, and how they are mapped to each other. To facilitate comprehension, the whole introduction of the framework revolves around an example model. Since the primary interest of that model is not its specific results, but its general method, the choice of energy carriers and technologies considered is not exhaustive. For the same reason, some modeling assumptions that could be argued to require an in-depth technical discussion, are only treated briefly.

Since the framework organizes all sets within rooted trees, first some concepts of graph theory and basic notations used throughout the paper have to be introduced. Any graph G is defined by its vertices V and edges E. A tree can be defined as a graph, where any two vertices are linked by a unique path along its vertices and edges. Distinguishing one vertex as the graph's root rt_G creates a rooted tree. The length of a path from a vertex v to the root is termed depth and provided by function $d\colon V \to \mathbb{N}_0$. Consequently, the depth of the root is always zero, which means that $d(rt_G) = 0$. All vertices on the path between a vertex v and the root are its ancestors and defined as set α_v. The descendants of a vertex v, henceforth given as δ_v, can be understood recursively: If a vertex u is an ancestor to v, v is a descendant to u. To indicate the vertex v itself should be included in a set of ancestors or descendants, we write α_v^+ or δ_v^+, respectively. The set of all ancestors or descendants of vertex v with depth z is denoted as α_v^z and δ_v^z. A subgraph of a tree that only contains the vertex v and all its descendants, is referred to as the subtree G_v. Lastly, all vertices without any descendants are called leaves. For all leaves, which are descendants of vertex v, we write λ_v. (Diestel 2000; Bondy and Murty 2008)

3.3.1.1 Regions

Fig. 3.1 shows the rooted tree R organizing all regions considered within the example problem. r be an arbitrary vertex of the tree representing a region. Exemplifying the definitions and notations introduced above, the descendants of vertex *'East'* are the vertices *'East South'* and *'East North'* or $\delta_{East} = \{$*'East South'*, *'East North'*$\}$. Since both *'East South'* and *'East North'* do not have any descendants, they are leaves and $\lambda_{East} = \delta_{East}$ applies. Also, the ancestor of vertex *'West North'* at depth 1 is the vertex *'West'*, which means $\alpha^1_{WestNorth} = \{$*'West'*$\}$. The subtree at vertex *'West'* would include the vertices *'West'*, *'West North'* and *'West South'* or $V(T_{West}) = \{$*'West'*, *'West North'*, *'West South'*$\}$.

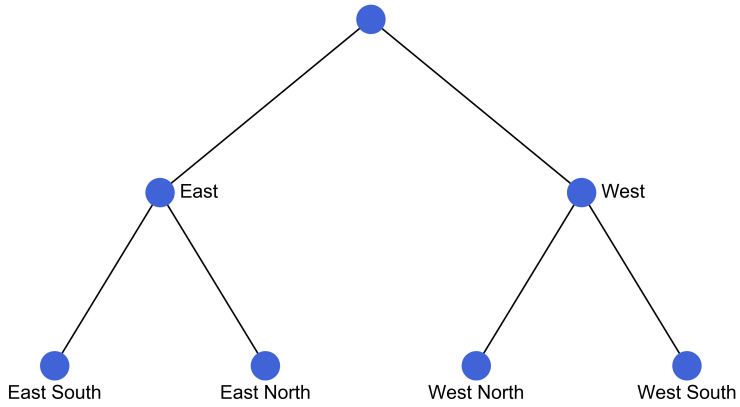

Figure 3.1: Rooted tree of regions in the example model

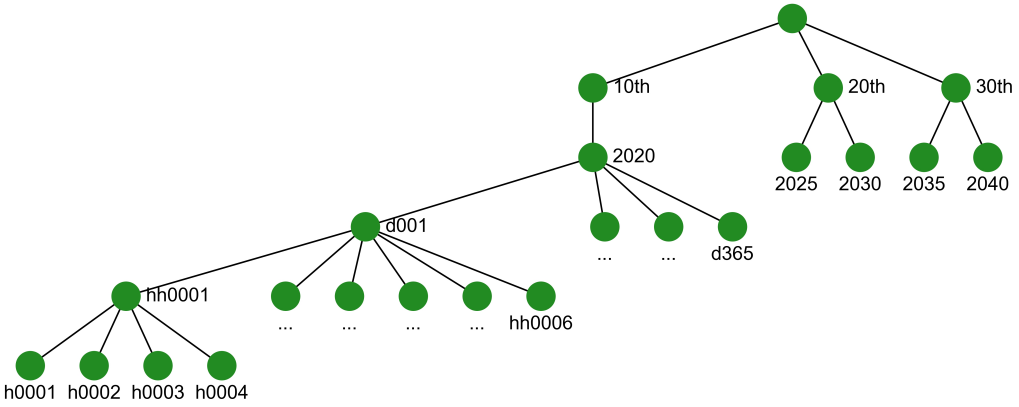

Figure 3.2: Rooted tree of time-steps in the example model

3.3.1.2 Time-steps

Analogously to regions, time-steps are organized in the rooted tree T with t representing an arbitrary vertex. In a reduced form, for the example model this tree is drawn in Fig. 3.2. Vertices with depth one each represent a decade, vertices with depth two correspond to all years considered within the respective decade and each year is then further dissected into daily, four-hour, and finally hourly steps.

3.3.1.3 Carriers

Fig. 3.3 displays the rooted tree C of all energy carriers defined within the model. While the vertices *'coal'* and *'electricity'* do not have any descendants, *'heat'*, which only refers to low-temperature heat, has one descendant *'district heat'* and gases are subdivided into *'hydrogen'* and *'natural gas'*, which again is split into *'synthetic gas'* and *'fossil gas'*. This arrangement is motivated by the fact that having carriers share a common ancestor is required for modeling them as substitutes in a certain context, as we will elaborate in section 3.3.2.

To specify the temporal and spatial granularities carriers are modeled at, each are assigned depths within the rooted trees of time-steps and regions. This is done separately for dispatch and expansion and summarized for the example model in Tab. 3.1.

Consequently, a depth of five for temporal dispatch of *'electricity'* means dispatch of the carrier is modeled for every time-step with depth five, which, going back to Fig. 3.2, corresponds to an hourly granularity. Likewise, *'heat'* and *'district heat'* are modeled at four-hour steps and all gases are balanced daily. Lastly, *'coal'* is only accounted for per year. Deciding on the temporal granularity of dispatch for a carrier is a crucial assumption on its

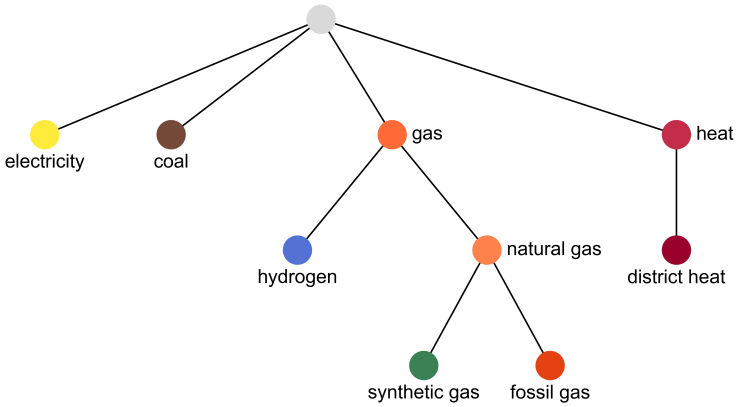

Figure 3.3: Rooted tree of energy carriers in the example model

Table 3.1: Depths assigned to energy carriers in the example model

carrier with depth 1	carrier with depth 2	carrier with depth 3	temporal		spatial	
			dispatch	expansion	dispatch	expansion
electricity			5	2	1	1
heat	district heat		4	2	2	2
gas	natural gas	synthetic gas	3	2	1	1
gas	natural gas	fossil gas	3	2	1	1
gas	hydrogen		3	2	1	1
coal			2	2	1	1

inherent flexibility. For electricity an hourly resolution is often considered adequate when using spatially aggregated models (T.W. Brown et al. 2018). As a result of its physical properties, gas, in contrast to electricity, is traded daily. In accordance with dedicated literature, a daily resolution is also applied here (Hauser 2019; Petrovic et al. 2017). For heat, a four-hour resolution was assumed to account for the thermal inertia of buildings.

The uniform depth of two for all carriers' temporal expansion granularity means decisions on capacity expansion are made for each year. If the depth were set to one instead, a decision on expansion would apply for an entire decade. Such a setup would be suited to mimic typical polices for the expansion of wind and solar capacities.

Spatial dispatch and expansion granularity for all carriers corresponds to the regions with depth 1, namely *'West'* and *'East'*, except for *'heat'* and *'district heat'*. Here a more detailed resolution was chosen, since heat, unlike electricity or gas, cannot be transported over greater distances to offset local imbalances between supply and demand.

Certain conditions can be defined that ensure the temporal and spatial granularities assigned to each carrier are suited to create a logical consistent energy system model. AnyMOD specifically checks compliance of these conditions and throws an error, if any of them is violated. To formulate these rules, the depths mapped to a specific carrier c will be termed dep_c.

First, a carrier may not be modeled at a dispatch granularity more detailed than any of its descendants, regardless if temporal or spatial. This means, the depth assigned to a specific carrier cannot exceed the smallest depth assigned to any of its descendants, as denoted in Eqs.

3.1a and 3.1b.[2]

$$dep_c^{dis,tp} \leq \min_{\hat{c} \in \delta_c} dep_{\hat{c}}^{dis,tp} \qquad \forall c \in V(C) \tag{3.1a}$$

$$dep_c^{dis,sp} \leq \min_{\hat{c} \in \delta_c} dep_{\hat{c}}^{dis,sp} \qquad \forall c \in V(C) \tag{3.1b}$$

The conditions originate from the way the framework models substitution of energy carriers. As section 3.3.2 will explain in detail, this is achieved by aggregating variables of descendant carriers with the ancestral carrier. However, such an aggregation is impossible, if for example the ancestral carrier has an hourly resolution, but one of its descendants is modeled daily.

The second group of conditions addresses the relation between dispatch and expansion granularity. As stated in Eq. 3.2, the spatial granularity of expansion may not be less detailed than the spatial granularity of dispatch for any carrier or, in terms of depths, the depth of dispatch cannot exceed the depth of expansion.

$$dep_c^{exp,sp} \geq dep_c^{dis,sp} \qquad \forall c \in V(C) \tag{3.2}$$

This condition is necessary to ensure each dispatch variable in the model can be mapped to a corresponding capacity. If, for instance, expansion is modeled at the country level, but dispatch considered separately for each state within the country, assigning a capacity to each of these states would not be possible. The opposite case with dispatch on the country level but regional expansion is supported and leads to an aggregation of regional capacities by country.

For the same reason a similar condition on temporal granularities is required. This condition states that for any carrier the temporal granularity of expansion may not be more detailed than the temporal granularity of dispatch. As formulated in Eq. 3.3, this implies the depth assigned for expansion cannot exceed the depth of dispatch.

$$dep_c^{exp,tp} \leq dep_c^{dis,tp} \qquad \forall c \in V(C) \tag{3.3}$$

If, in violation of Eq. 3.3, capacity expansion had an daily resolution, but dispatch were only modeled yearly, again a sensible assignment of capacity to dispatch variables would not be possible.

Modeling several periods of capacity expansion requires to define superordinate dispatch time-steps. Dispatch within each of these steps is self-contained, meaning dispatch decisions within the period do not affect any of the other periods. For instance, cyclic conditions for storage will enforce the same storage levels at the beginning and end of each of those periods. This also implies that capacities cannot vary within these periods. Most existing models take a yearly resolution for this purpose, but other granularities are conceivable as well.[3] Since these periods connect expansion and dispatch, their depth, denoted as dep^{sup}, must be within the interval from the most detailed expansion resolution to the least detailed dispatch resolution. This is expressed by Eq. 3.4:

$$dep^{sup} \in [\max_{c \in V(C)} dep_c^{exp,tp}, \min_{c \in V(C)} dep_c^{dis,tp}] \tag{3.4}$$

Φ is defined as the set of all superordinate dispatch time-steps. Each subordinate dispatch time-step t has exactly one ancestor within Φ, which is referred to as α_t^{sup}. In the example model dep^{sup} is two and consequently Φ corresponds to all years. For any hour or day t, α_t^{sup} assigns the year the respective day or hour is in.

2. The hat operator is used throughout the paper to indicate a vertex is a descendant to another vertex within the same equation.

3. Even varying this resolution within the model is theoretically possible, but does not appear practical and was not implemented.

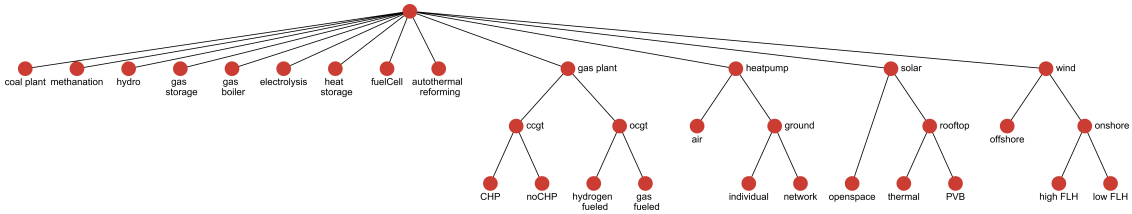

Figure 3.4: Rooted tree of technologies in the example model

3.3.1.4 Technologies

Technologies are organized in the rooted tree E, which is shown in Fig. 3.4 for the example model. Only leaves of this tree correspond to actual technologies, while all other vertices serve the sole purpose of organizing them. For instance, to reflect how PV and solar thermal rooftop systems compete for a limited amount of rooftop area, their shared ancestor *'rooftop'* can be used to enforce an upper limit on the sum of their capacities.

The function $g(e)$ maps technologies to one of three groups: *stock*, *mature* and *emerging*. Stock technologies cannot be expended and are limited to pre-existing capacities. Emerging technologies differ from mature technologies in the sense that their capacities are differentiated by time-step of construction. In the case of electrolyzers for example, substantial increases in efficiency are expected by 2050. To account for such improvements, capacities build in different years have to be considered separately. For mature technologies, no substantial advances are expected, and such differentiation would only cause an unnecessary increase in model size.

Generated and used carriers are mapped to technologies by the sets γ_e^{gen} and γ_e^{use}, respectively. Any used carrier c cannot be a descendant to another used carrier c'. The condition applies to generated carriers analogously and both conditions are formalized by Eqs. 3.5a and 3.5b.

$$c \notin \delta_{c'} \quad \forall e \in V(E), (c, c') \in \{\gamma_e^{use} \times \gamma_e^{use} \,|\, c \neq c'\} \tag{3.5a}$$

$$c \notin \delta_{c'} \quad \forall e \in V(E), (c, c') \in \{\gamma_e^{gen} \times \gamma_e^{gen} \,|\, c \neq c'\} \tag{3.5b}$$

Considering the combined-cycle gas turbine (CCGT) with CHP from the example, *'natural gas'* is converted to *'district heat'* and *'electricity'*, hence $\gamma_{CHP}^{use} = \{$*'natural gas'*$\}$ and $\gamma_{CHP}^{gen} = \{$*'district heat'*, *'electricity'*$\}$. Additionally assigning *'fossil gas'* as a used carrier would pose a logical contradiction since *'natural gas'* implicitly already includes its descendant *'fossil gas'* and consequently violate Eq. 3.5a.

Charged carriers are denoted as γ_e^{stI}; discharged carriers are referred to as γ_e^{stO}. By default, only carriers, which are leaves, can be explicitly stored. If a technology is defined to store a non-leaf carrier c, actually stored are only its leaves λ_c. For instance, in the example *gas storage* is defined to store *gas* which means the technology can equally store *hydrogen*, *synthetic gas* and *fossil gas*. Deviating from this approach gives rise to unintended effects.[4] To elucidate this, assume *gas storage* would directly store the carrier *gas* instead. Since descendants are included in the ancestors energy balance, *hydrogen* could still be charged. However, it would be discharged as *gas* and could not be used wherever *hydrogen* is specifically required.

The representation of storage is not limited to charging and discharging carriers from external sources but can also account for carriers generated or used by the same technology. To clarify this, we assume a carrier c is an element of γ_e^{stO}, but not within γ_e^{stI}. This implies it can be discharged, but not charged from an external source. However, if c is also an element of γ_e^{gen}, it can be charged by the technologies own generation instead. For instance, the PV battery system (PVB) in the example represents a PV panel combined with a home battery. In line with other research, we assume home batteries cannot be charged from the grid, but can

4. It can be explicitly enforced though, but this a special case not discussed within the paper.

provide electricity to the grid (Schopfer, Tiefenbeck, and Staake 2018). Therefore, *'electricity'* is an element of γ_{PVB}^{gen} and γ_{PVB}^{stO}, but γ_{PVB}^{stI} is empty. Nevertheless, the battery can still be charged by the system's own generation from the PV panel. Correspondingly, a charged carrier can be discharged internally if within γ_e^{use}. In this case, an industrial furnace provided with gas by an on-site gas storage could serve as an example. If carriers are charged or discharged internally, also non-leaf carriers can be stored.

Applying this, 3.6 and 3.7 define sets of stored carriers for a technology e. All carriers charged and discharged externally are provided by γ_e^{stEx}. This set is unified with all carriers charged externally and discharged internally as well as the other way around, to obtain all carriers stored γ_e^{st}.

$$\gamma_e^{stEx} \coloneqq \overbrace{\{\lambda_c : c \in \gamma_e^{stO} \cup \gamma_e^{stI}\}}^{\text{external charging or discharging}} \tag{3.6}$$

$$\gamma_e^{st} \coloneqq \gamma_e^{stEx} \cup \underbrace{(\gamma_e^{gen} \cup \gamma_e^{stO})}_{\text{internal charging}} \cap \underbrace{(\gamma_e^{use} \cap \gamma_e^{stI})}_{\text{internal discharging}} \tag{3.7}$$

The sets γ_e^{in} and γ_e^{out} collect all external in- and output carriers of a technology e:

$$\gamma_e^{in} \coloneqq \gamma_e^{use} \cup \gamma_e^{stEx} \tag{3.8a}$$

$$\gamma_e^{out} \coloneqq \gamma_e^{gen} \cup \gamma_e^{stEx} \tag{3.8b}$$

In addition, all technologies any conversion or storage carrier was assigned to are collected within the respective sets Γ^{cv} and Γ^{st}, which are defined by the following equations:

$$\Gamma^{cv} \coloneqq \{V(E) \,|\, \gamma_e^{gen} \cup \gamma_e^{use} \neq \emptyset\} \tag{3.9a}$$

$$\Gamma^{st} \coloneqq \{V(E) \,|\, \gamma_e^{st} \neq \emptyset\} \tag{3.9b}$$

The directed graph in Fig. 3.5 summarizes how in- and output carriers are mapped to technologies in the example model. In the graph all technologies are symbolized by grey vertices. Their entering edges relate to inputs γ_e^{in}; outgoing edges to outputs γ_e^{out}. Carriers are symbolized by colored vertices that have outgoing edges directed towards their ancestors. The graph demonstrates, how organizing carriers in rooted trees supports modeling the manifold ways energy carriers can be substituted and interact with technologies in an integrated energy system: Synthetic gas must be created from hydrogen, which again requires the use of electricity via electrolysis, while natural gas cannot be created from other carriers. However, both energy carriers can equally fuel gas boilers and power plants or be used for auto thermal reforming, a gas-based process to create hydrogen. Also, any of these carriers can be stored in a gas storage system, since *gas* is an ancestor to all of them.

Although the example model focuses on the interplay of gas-based fuels to demonstrate the capabilities of the presented method, it can be applied beyond: For instance, processes in the energy-intensive industry often require high-temperature heat at different levels, which makes decarbonization challenging (Bataille et al. 2018). However, providing a process with heat on a temperature level that exceeds its requirements is possible. Also, excess heat from one process can serve as an input to another. The qualitative energy flow diagram in Fig. 3.6 outlines how these aspects could be accounted for within energy system models by the introduced method. Since the carrier *'heat, above 500°C'* is a descendant of *'heat, 100 to 500°C'* and *'heat, below 100°C'*, in contrast to the other technologies *'gas furnace'* is able to satisfy demand on all levels. Also, a process that requires heat at the highest temperature level and provides excess heat again at a lower level, can be modeled.

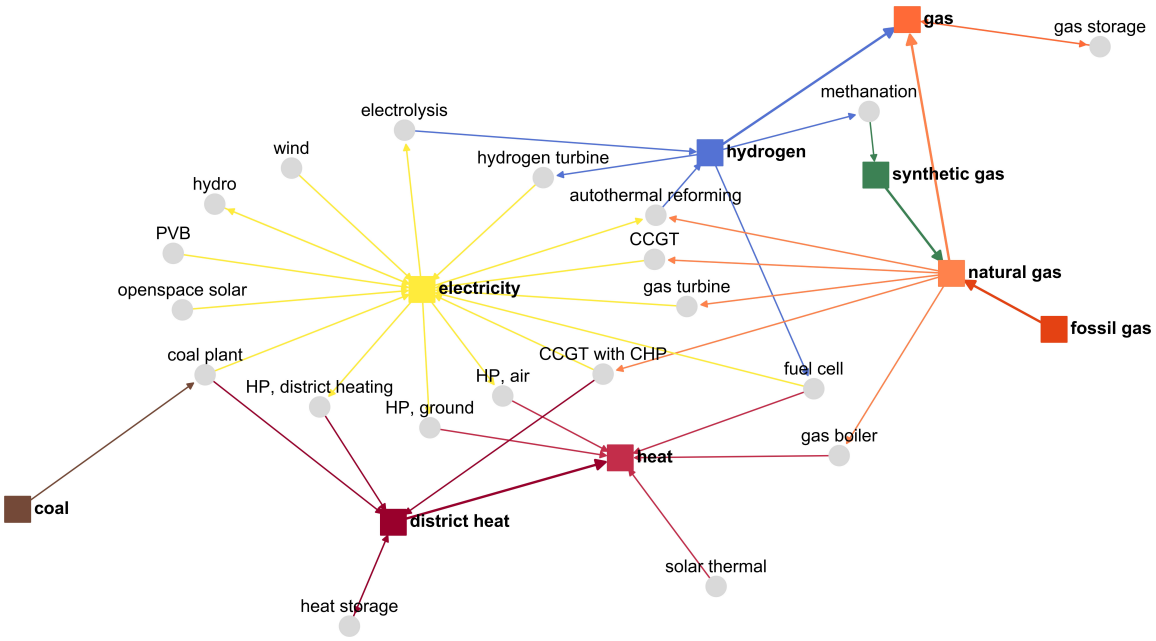

Figure 3.5: Qualitative energy flow graph for example model

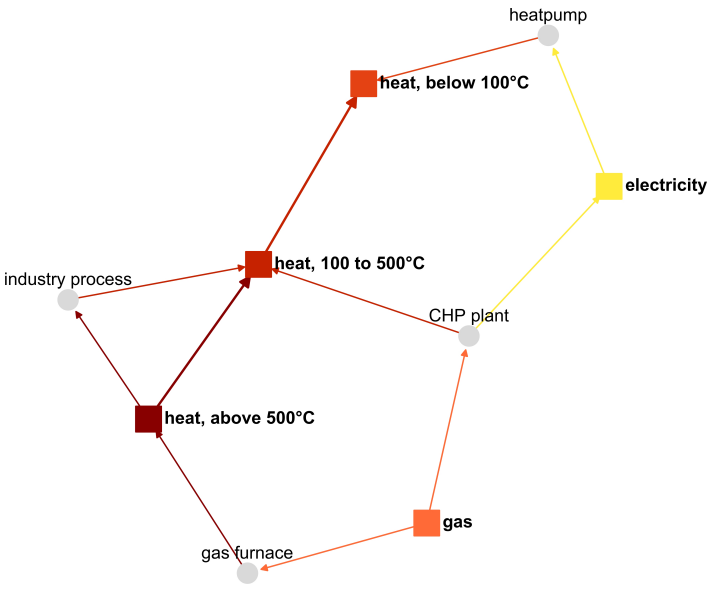

Figure 3.6: Qualitative energy flow graph for alternative application

3.3.1.5 Modes

The rooted tree M organizes the different operational modes m defined within the framework. In contrast to the other graphs, the rooted tree of modes is trivial, meaning it only consists out of the root and its direct descendants. The set μ_e maps its operational modes to each technology or, if only one mode exists, just assigns the root rt_M. In the example model, distinct modes termed *more heat* and *more electricity* are only defined for CCGT plants with CHP. The *more Heat* mode operates at a higher fuel utilization rate, but a smaller CHP coefficient.

3.3.2 Equations of optimization problem

Building on these sets and mappings, the constraints of the model's underlying optimization can be formulated. We start with dispatch related constraints, followed by capacity constraints, which connect dispatch and expansion and close with the equations to describe expansion. Since the cost minimizing objective function does not substantially differ to pre-existing formulations, it is provided in the appendix B.4. The same applies for constraints that impose exogenous limits on variables.

3.3.2.1 Energy balance

The energy balance ensures demand for each carrier c equals or does not exceed its supply at any time t or place r. To model this, all dispatch time-steps τ_c and regions ρ_c of a carrier c are defined as follows:

$$\tau_c \coloneqq \{V(T) \,|\, d(t) = dep_c^{dis,tp}\} \tag{3.10a}$$

$$\rho_c \coloneqq \{V(R) \,|\, d(r) = dep_c^{dis,sp}\} \tag{3.10b}$$

Consequently, the cartesian product of τ_c and ρ_c gives the temporal and spatial granularity φ_c that a carrier c is modeled at.

$$\varphi_c \coloneqq \tau_c \times \rho_c \tag{3.11}$$

Since demand for a carrier c can not only be met by the carrier itself, but also by its descendants $\hat{c}$, these have to be included into the energy balance as well. However, according to Eq. 3.1a and 3.1b, these descendants might be modeled at a granularity more detailed than the carrier itself. Therefore, elements of these descendants must be aggregated to comply with the resolution of the ancestral carrier. When balancing the time-step t, the dispatch time-steps of a descendant carrier $\hat{c}$ that require aggregation, correspond to the intersection of descendant carriers time-steps $\tau_{\hat{c}}$ with the descendants of the balanced time-step δ_t^+. The same reasoning is applied to regions and the set of pairs $\sigma_{\hat{c},r,t}$ can be obtained. As defined by Eq. 3.12, this set contains all time-steps and regions that have to be aggregated to account for dispatch of a carrier $\hat{c}$ at time-step t in region r.

$$\sigma_{\hat{c},r,t} \coloneqq \tau_{\hat{c}} \cap \delta_t^+ \;\times\; \rho_{\hat{c}} \cap \delta_r^+ \tag{3.12}$$

The equation applies as well, if t or r are already at the right granularity, because the set δ_v^+ by definition also includes the vertex v itself.

To enable descendant carriers to satisfy demand, by default the energy balance is not an equality constraint and supply might exceed demand. The carriers *district heat* and *heat* from the example can be used to illustrate this. To let the model endogenously decide whether to use district heating technologies or not, demand was only specified for the ancestral carrier

heat.[5] As a result, formulating the energy balance for *district heat* as an equality constraint, would fix its generation to zero.

Building on this, the energy balance is formulated in eqn. 3.13. To facilitate the understanding, optimization variables have capital initials, while parameters are written in lowercase.

$$\sum_{\hat{c}\in\delta_c^+} \sum_{\langle\hat{t},\hat{r}\rangle\in\sigma_{t,r,\hat{c}}} \underbrace{Te^{cv}_{\hat{t},\hat{r},\hat{c}} + Te^{st}_{\hat{t},\hat{r},\hat{c}}}_{\text{supply}} + \overbrace{Exc^{net}_{\hat{t},\hat{r},\hat{c}}}^{\text{exchange with other regions}} + \underbrace{Trd^{net}_{\hat{t},\hat{r},\hat{c}}}_{\text{and demand by technologies trade with exogenous markets}} - \overbrace{dem_{\hat{t},\hat{r},\hat{c}}}^{\text{exogenous demand}} \geq 0$$

$$\forall c \in V(C),\ \langle t,r\rangle \in \varphi_c \tag{3.13}$$

Conversion related dispatch variables are summarized by Te^{cv} and include Gen for generation and Use for use. Analogously, Te^{st} is composed of StI^{ext} and StO^{ext} to account for external in- and output of storage. Each of these variables is specified for five different dimensions: time-step of dispatch t, region r, carrier c, mode m and lastly time-step of construction $\tilde{t}$. The cartesian product of all dimensions is denoted as Ω.

For stock and mature technologies, which are not differentiated by time-step of construction, $\tilde{t}$ always corresponds to the root of the time-step tree rt_T. In case of an emerging technology, all time-steps of construction that result in a lifespan, which includes the dispatch time-step t, have to be considered separately. To elucidate this, consider the an emerging technology with a constant lifetime $lt_{e,\tilde{t}}$ of 15 years. For any dispatch time-step t within the year 2020, only capacities constructed in 2020 have to be considered. However, if t is within 2050 instead, the construction time-steps 2040 and 2045 have to considered in addition to 2050. In conclusion, Eq. 3.14 defines the set $\theta^{dis}_{e,t}$ that provides the construction time-steps to consider separately for a technology e at dispatch time-step t.

$$\theta^{dis}_{e,\tilde{t}} := \begin{cases} \{r_T\} & \text{,if } g(e) = \text{'mature'} \vee g(e) = \text{'stock'} \\ \{\tilde{t}' \in \Phi \mid \tilde{t}' \in (\alpha^{sup}_t - lt_{e,\tilde{t}'}, \alpha^{sup}_t]\} & \text{,if } g(e) = \text{'emerging'} \end{cases} \tag{3.14}$$

Dispatch variables for all conversion and storage technologies are summed by time-step of construction $\tilde{t}$ and modes m to define Te^{cv} and Te^{st} as denoted in Eqs. 3.15a and 3.15b. Iverson brackets are used to indicate that dispatch variables are only created, if the respective carrier is actually assigned to the technology.

$$Te^{cv}_{t,r,c} = \sum_{e\in\Gamma^{cv}} \sum_{\tilde{t}\in\theta^{dis}_{e,t}} \sum_{m\in\mu_e} Gen_{t,\tilde{t},r,c,e,m}[c \in \gamma^{gen}_e] - Use_{t,\tilde{t},r,c,e,m}[c \in \gamma^{use}_e]$$

$$\forall c \in V(C),\ \langle t,r\rangle \in \varphi_c \tag{3.15a}$$

$$Te^{st}_{t,r,c} = \sum_{e\in\Gamma^{st}} \sum_{\tilde{t}\in\theta^{dis}_{e,t}} \sum_{m\in\mu_e} StO^{ext}_{t,\tilde{t},r,c,e,m}[c \in \gamma^{stEx}_e] - StI^{ext}_{t,\tilde{t},r,c,e,m}[c \in \gamma^{stEx}_e]$$

$$\forall c \in V(C),\ \langle t,r\rangle \in \varphi_c \tag{3.15b}$$

In the energy balance, $Exc^{net}_{\hat{t},\hat{r},\hat{c}}$ refers to net imports of region $\hat{r}$ from other regions. The set $\beta_{c,r}$ includes all regions with that region r can exchange carrier c. Exchange can be considered similar to storage, since both shift energy, one in space and the other in time. Therefore, exchange of carriers is limited to leaves, because otherwise the same effects as described for storage earlier will occur. For instance, to represent the gas network in the example, $\beta_{c,r}$ is

5. In the example, an upper limit on the generation of district heat for each time-step reflects that only a share of consumers can be connected to a district heating network.

defined for *gas*. Consequently, only the carriers *hydrogen*, *synthetic gas* and *fossil gas* are explicitly exchanged.

Applying this, Eq. 3.16 computes the net import based on the exchange variables Exc and the efficiency of exchange eff^{exc} that accounts for exchange losses. The first region in the index always refers to the region energy is being transported to and the second to the region it is being transported from.

$$Exc^{net}_{t,r,\hat{c}} = \sum_{r' \in \beta_{c,r}} \sum_{\hat{r}' \in \rho_{\hat{c}} \cap \delta^{+}_{r'}} \frac{Exc_{t,\hat{r},\hat{r}',c}}{1/eff^{exc}_{t,\hat{r},\hat{r}',\hat{c}}} - Exc_{t,\hat{r}',\hat{r},\hat{c}}$$
$$\forall \langle c, r \rangle \in \{V(C) \times V(R) \,|\, \beta_{c,r}\},\, \hat{c} \in \lambda_c,\, t \in \tau_{\hat{c}},\, \hat{r} \in \rho_{\hat{c}} \cap \delta^{+}_{r} \quad (3.16)$$

Just as explained at the beginning of the section, the region specified in $\beta_{c,r}$ might be less detailed than the regions a descendant carrier $\hat{c}$ is modeled for. Therefore, exchange variables are aggregated by regions using the same formulation introduced earlier.

The net effect of trade is accounted for in the energy balance by Trd^{net} defined in Eq. 3.17. In contrast to exchange, trade refers to buying or selling carriers to an exogenous market at a fixed price. The quantity that can be bought or sold at a given price can be limited, which can be used to create a stepped supply or demand curve. Each of these steps is denoted as ζ^{buy} or ζ^{sell}, respectively.

$$Trd^{net}_{t,r,c} = \sum_{i \in \zeta^{buy}} Trd^{buy}_{t,r,c,i} - \sum_{i \in \zeta^{sell}} Trd^{sell}_{t,r,c,i} \qquad \forall c \in V(C),\, \langle t, r \rangle \in \varphi_c \quad (3.17)$$

Potential applications of this functionality range from a representation of commodity markets to accounting for price-elastic demand in the electricity sector. The last remaining element of the energy balance *dem* is an exogenously set parameter and refers to inelastic demand.

3.3.2.2 Conversion balance

The conversion balance describes how technologies transform energy carriers into one another. For this purpose, the in- and outputs to the conversion process are summarized by carrier as Cv^{in} and Cv^{out}, which are defined in Eqs. 3.18a and 3.18b. As set out in section 3.3.1.4, these in- and outputs are not limited to use and generation variables, but can also include internal storage variables.

$$Cv^{in}_{t,\tilde{t},r,c,e,m} = Use_{t,\tilde{t},r,c,e,m} + StO^{int}_{t,\tilde{t},r,c,e,m}[c \in \gamma^{stO}_e]$$
$$\forall e \in V(E),\, c \in \gamma^{use}_e, \langle t,\, r \rangle \in \varphi_c,\, \tilde{t} \in \theta^{dis}_{e,t},\, m \in \mu_e \quad (3.18a)$$
$$Cv^{out}_{t,\tilde{t},r,c,e,m} = Gen_{t,\tilde{t},r,c,e,m} + StI^{int}_{t,\tilde{t},r,c,e,m}[c \in \gamma^{stI}_e]$$
$$\forall e \in V(E),\, c \in \gamma^{gen}_e,\, \langle t, r \rangle \in \varphi_c,\, \tilde{t} \in \theta^{dis}_{e,t},\, m \in \mu_e \quad (3.18b)$$

Only technologies that are assigned both, used and generated carriers, require a conversion balance. Conversion is balanced at the least detailed granularity of all carriers involved. Otherwise, a carrier with a less detailed granularity could not be accounted for. Applying this, Eq. 3.19 defines the resolution of the energy balance for each technology e.

$$\epsilon_e \coloneqq \{V(T) \,|\, d(t) = \min_{c \in \gamma^{gen}_e \cup \gamma^{use}_e} dep^{dis,tp}_c\} \times \{V(R) \,|\, d(r) = \min_{c \in \gamma^{gen}_e \cup \gamma^{use}_e} dep^{dis,sp}_c\} \quad (3.19)$$

The overall efficiency of a conversion process that determines the ratio between in- and output quantities is denoted as eff^{cv}. If a technology's conversion efficiency differs by operational mode, each of these modes must be considered by a separate equation. Therefore, ω^{cv} provides

all sets of modes that require an individual balance. On this basis, the conversion balance given by Eq. 3.20 can be formed.

$$\sum_{m\in\xi} eff^{cv}_{t,\tilde{t},r,e,m} \sum_{c\in\gamma^{use}_e} \sum_{\langle\hat{t},\hat{r}\rangle\in\sigma_{t,r,c}} Cv^{in}_{\hat{t},\tilde{t},\hat{r},c,e,m} = \sum_{m\in\xi} \sum_{c\in\gamma^{gen}_e} \sum_{\langle\hat{t},\hat{r}\rangle\in\sigma_{t,r,c}} Cv^{out}_{\hat{t},\tilde{t},\hat{r},c,e,m}$$
$$\forall e \in \{V(E) \,|\, \gamma^{use}_e \neq \emptyset \wedge \gamma^{gen}_e \neq \emptyset\},\ \langle t,r\rangle \in \epsilon_e, \tilde{t} \in \theta^{dis}_{e,t},\ \xi \in \omega^{cv}_{t,\tilde{t},r,e} \tag{3.20}$$

For the CCGT plant with CHP from the example, the conversion balance is created daily and for each region of depth one, which corresponds to the granularity of its least detailed carrier *gas*. In addition, separate balances are created for each operational mode, since these differ in terms of efficiency, which means $\omega^{cv} = \{\{$*'more heat'*$\}, \{$*'more electricity'*$\}\}$.

3.3.2.3 Storage balance

The storage balance connects in- and output of a storage system to the storage level. The in- and output to the storage are comprised of external and internal storage variables as defined in Eq. 3.21.

$$St^{in}_{t,\tilde{t},r,c,e,m} = StI^{ext}_{t,\tilde{t},r,c,e,m} + StI^{int}_{t,\tilde{t},r,c,e,m}$$
$$\forall e \in V(E),\ c \in \gamma^{st}_e,\ \langle t,r\rangle \in \varphi_c,\ \tilde{t} \in \theta^{dis}_{e,t},\ m \in \mu_e \tag{3.21a}$$
$$St^{out}_{t,\tilde{t},r,c,e,m} = StO^{ext}_{t,\tilde{t},r,c,e,m} + StO^{int}_{t,\tilde{t},r,c,e,m}$$
$$\forall e \in V(E),\ c \in \gamma^{st}_e,\ \langle t,r\rangle \in \varphi_c,\ \tilde{t} \in \theta^{dis}_{e,t},\ m \in \mu_e \tag{3.21b}$$

In Eq. 3.22 the storage level $StLvl$ at time-step t is computed by summing levels of the previous time-step $t-1$ with storage in- and outputs. To a enforce a cyclic condition, the previous time-step to the first time-step is the last time-step within the same superordinate dispatch time-step (i.e. for *h0001* in *2020* the previous time-step is *h8760* in *2020*).

$$\overbrace{\sum_{m\in\xi} StLvl_{t,\tilde{t},r,c,e,m}}^{\text{current level}} = \overbrace{\sum_{m\in\xi} \frac{StLvl_{t-1,\tilde{t},r,c,e,m}}{1-dis_{t,\tilde{t},r,c,e,m}}}^{\text{loss adjusted previous level}} + \overbrace{in_{t,\tilde{t},r,c,e,m} + \frac{St^{in}_{t,\tilde{t},r,c,e,m}}{1/eff^{stI}_{t,\tilde{t},r,c,e,m}}}^{\text{storage inputs}} - \overbrace{\frac{St^{out}_{t,\tilde{t},r,c,e,m}}{eff^{stO}_{t,\tilde{t},r,c,e,m}}}^{\text{storage outputs}}$$
$$\forall e \in \Gamma^{st},\ c \in \gamma^{st}_e,\ \langle t,r\rangle \in \varphi_c,\ \tilde{t} \in \theta^{dis}_{e,t},\ \xi \in \omega^{st}_{t,\tilde{t},r,e} \tag{3.22}$$

In the storage balance, dis refers to the self-discharge rate, while eff^{stI} and eff^{stO} account for losses associated with charging and discharging. Similar to the conversion balance ω^{st} provides all sets of modes that require an individual balance. Lastly, the parameter in accounts for external inputs into the storage system, for instance inflows into hydro reservoirs.

3.3.2.4 Ratio constraints

Ratios among in- and output carriers can be restricted by an equality, greater-than or less-than constraint. Since all constraints on in- or output ratios are structured the same, only the equality constraint on output carriers is formulated in Eq. 3.23.

$$\underbrace{\sum_{\langle \hat{t},\hat{r}\rangle \in \sigma_{t,r,c}} Cv^{out}_{\hat{t},\tilde{t},\hat{r},c,e,m}}_{\text{output of restricted carrier}} = ratio^{out,eq}_{t,\tilde{t},r,c,e,m} \underbrace{\sum_{c' \in \gamma^{out}_e} \sum_{\langle \hat{t},\hat{r}\rangle \in \sigma_{t,r,c'}} Cv^{out}_{\hat{t},\tilde{t},\hat{r},c',e,m}}_{\text{output of all carriers}}$$

$$\forall \langle t,\tilde{t},r,c,e,m\rangle \in \{\Omega \,|\, ratio^{out,eq}_{t,\tilde{t},r,c,e,m}\} \tag{3.23}$$

The parameter $ratio^{out,eq}$ specifies a carrier's share of the total output. In the example, it is defined for the share of electricity in total outputs of CCGT plants with CHP, coal plants and fuel cells. Accordingly, only in these cases the corresponding constraints are created.

3.3.2.5 Capacity constraints

Dispatch variables are constrained to not exceed the operating capacities Cap^{opr}. To compare dispatch expressed in energy units with capacities, which are expressed in power units, dispatch variables are corrected for the length of the respective dispatch time-step. To this end we define the function s that assigns a correction factor $s(t)$ for each time-step t. As explained in section 3.3.1.3, expansion can be modeled with greater spatial detail than dispatch and as a result comparing expansion with dispatch requires aggregation. For this purpose, expansion regions of technology e are termed η^{sp}_e and by default their resolution corresponds to the most detailed resolution across all carriers assigned, as expressed in Eq. 3.24.

$$\eta^{sp}_e \coloneqq \{V(R) \,|\, d(r) = \max_{c \in \gamma^{in}_e \cup \gamma^{out}_e} (dep^{exp,sp}_c)\} \tag{3.24}$$

Since conversion capacities transform carriers modeled at different granularities, the question arises at which resolution capacity constraints should be enforced. To answer this, part B.3 of the appendix introduces an algorithm that determines the smallest set of constraints required for dispatch variables to comply with the operated capacities $Cap^{opr,cv}$. For each technology e this set is referred to as Ψ_e and can be split into in- and output. The corresponding constraints are provided by Eqs. 3.25a and 3.25b.

$$s(t) \sum_{c \in \kappa} \sum_{\langle \hat{t},\hat{r}\rangle \in \sigma_{t,r,c}} \sum_{m \in \mu_e} \frac{Cv^{in}_{\hat{t},\tilde{t},\hat{r},c,e,m}}{ava^{cv}_{\hat{t},\tilde{t},\hat{r},e,m}} \leq \sum_{\hat{r} \in \eta^{sp}_e \cap \delta^{+}_r} Cap^{opr,cv}_{\alpha^{sup}_t,\tilde{t},\hat{r},e}$$

$$\forall e \in \Gamma^{cv},\ \langle \kappa,t,r\rangle \in \Psi^{in}_e,\ \tilde{t} \in \theta^{dis}_{e,t} \tag{3.25a}$$

$$s(t) \sum_{c \in \kappa} \sum_{\langle \hat{t},\hat{r}\rangle \in \sigma_{t,r,c}} \sum_{m \in \mu_e} \frac{Cv^{out}_{\hat{t},\tilde{t},\hat{r},c,e,m}}{ava^{cv}_{\hat{t},\tilde{t},\hat{r},e,m}\, eff^{cv}_{\hat{t},\tilde{t},\hat{r},e,m}} \leq \sum_{\hat{r} \in \eta^{sp}_e \cap \delta^{+}_r} Cap^{opr,cv}_{\alpha^{sup}_t,\tilde{t},\hat{r},e}$$

$$\forall e \in \Gamma^{cv},\ \langle \kappa,t,r\rangle \in \Psi^{out}_e,\ \tilde{t} \in \theta^{dis}_{e,t} \tag{3.25b}$$

In the introduced formulation capacities of technologies generally refer to input capacities, which is why the constraint on output capacity in Eq. 3.25b must be corrected for the respective efficiency.

For storage, capacity constraints are separately enforced for storage input stI, storage output stO and storage size stS. All storage carriers initially assigned to a technology are denoted as γ^{stCap}_e and each of these carriers has individual storage capacities. Within a constraint, storage capacities for a carrier c are compared with dispatch variables of all the

carriers $\hat{c}$ explicitly stored. The corresponding constraints are given by Eqs. 3.26a to 3.26c.

$$s(t) \sum_{\hat{c} \in \delta_c^+ \cap \gamma_e^{st}} \sum_{\langle \hat{t}, \hat{r} \rangle \in \sigma_{t,r,\hat{c}}} \sum_{m \in \mu_e} \frac{St^{in}_{\hat{t},\tilde{t},\hat{r},\hat{c},e,m}}{ava^{stI}_{\hat{t},\tilde{t},\hat{r},\hat{c},e,m}} \leq \sum_{\hat{r} \in \eta_e^{sp} \cap \delta_r^+} Cap^{opr,stI}_{\alpha_t^{sup},\tilde{t},\hat{r},e,c}$$
$$\forall e \in \Gamma_e^{st},\, c \in \gamma_e^{stCap},\, \langle t, r \rangle \in \varphi_c,\, \tilde{t} \in \theta_{e,t}^{dis} \tag{3.26a}$$

$$s(t) \sum_{\hat{c} \in \delta_c^+ \cap \gamma_e^{st}} \sum_{\langle \hat{t}, \hat{r} \rangle \in \sigma_{t,r,\hat{c}}} \sum_{m \in \mu_e} \frac{St^{out}_{\hat{t},\tilde{t},\hat{r},\hat{c},e,m}}{ava^{stO}_{\hat{t},\tilde{t},\hat{r},\hat{c},e,m}} \leq \sum_{\hat{r} \in \eta_e^{sp} \cap \delta_r^+} Cap^{opr,stO}_{\alpha_t^{sup},\tilde{t},\hat{r},e,c}$$
$$\forall e \in \Gamma_e^{st},\, c \in \gamma_e^{stCap},\, \langle t, r \rangle \in \varphi_c,\, \tilde{t} \in \theta_{e,t}^{dis} \tag{3.26b}$$

$$\sum_{\hat{c} \in \delta_c^+ \cap \gamma_e^{st}} \sum_{\langle \hat{t}, \hat{r} \rangle \in \sigma_{t,r,\hat{c}}} \sum_{m \in \mu_e} \frac{stLvl_{\hat{t},\tilde{t},\hat{r},\hat{c},e,m}}{ava^{stL}_{\hat{t},\tilde{t},\hat{r},\hat{c},e,m}} \leq \sum_{\hat{r} \in \eta_e^{sp} \cap \delta_r^+} Cap^{opr,stS}_{\alpha_t^{sup},\tilde{t},\hat{r},e,c}$$
$$\forall e \in \Gamma_e^{st},\, c \in \gamma_e^{stCap},\, \langle t, r \rangle \in \varphi_c,\, \tilde{t} \in \theta_{e,t}^{dis} \tag{3.26c}$$

Unlike all other capacities, constraints on storage size do not include a scaling factor, because storage size already is provided in energy units.

For exchange, capacities are created for all regions and carriers defined in $\beta_{c,r}$ and capacities are then compared with dispatch variables $\hat{c}$ explicitly exchanged. Exchange capacities can be directed, meaning the energy transportable from r to r' and from r' to r can differ.

$$s(t) \sum_{\hat{c} \in \lambda(c)} \sum_{\langle \hat{t}, \hat{r} \rangle \in \sigma_{t,r,\hat{c}}} \sum_{\hat{r}' \in \rho_{\hat{c}} \cap \delta_{r'}^+} Exc_{\hat{t},\hat{r},\hat{r}',c} \leq Cap^{opr,exc}_{\alpha_t^{sup},r,r',c}$$
$$\forall \langle c,\, r \rangle \in \{V(C) \times V(R) \,|\, \beta_{c,r}\},\, r' \in \beta_{c,r},\, t \in \tau_c \tag{3.27}$$

3.3.2.6 Expansion

The operated capacities $Capa^{opr}$ for conversion, storage and exchange that restrict dispatch variables do not necessarily match installed capacities $Capa^{ist}$. The framework can endogenously decide to decommission installed capacities before the end of their technical lifetime to mitigate operating costs. The following constraints achieve this for conversion capacities and are equally applicable for storage and exchange:

$$Cap^{opr,cv}_{t,\tilde{t},r,e} \leq Cap^{ist,cv}_{t,\tilde{t},r,e} \qquad \forall e \in \Gamma^{cv}, t \in \Phi, \tilde{t} \in \theta_{e,t}^{dis}, r \in \eta_e^{sp} \tag{3.28}$$

$$Cap^{opr,cv}_{t,\tilde{t},r,e} \leq Cap^{opr,cv}_{t-1,\tilde{t},r,e} + Exp^{cv}_{t,r,e} \qquad \forall e \in \Gamma^{cv}, t \in \Phi, \tilde{t} \in \theta_{e,t}^{dis}, r \in \eta_e^{sp} \tag{3.29}$$

Eq. 3.28 simply ensures operated capacities do not exceed installed capacities. To avoid that decommissioned capacities are put into operation again, Eq. 3.29 demands that any rise in operated capacity has to result from capacity expansion, which is denoted as $Exp^{cv}_{t,r,c,e}$.

Installed capacities are a result of pre-existing capacities and capacity expansion. Analogously to expansion regions, time-steps of expansion are termed η_e^{tp} and their resolution corresponds to the most detailed resolution across all carriers assigned as well:

$$\eta_e^{tp} \coloneqq \{V(R) \,|\, d(r) = \max_{c \in \gamma_e^{in} \cup \gamma_e^{out}} (dep_c^{exp,tp})\} \tag{3.30}$$

As explained in section 3.3.1.4, certain technologies are differentiated by time-step of construction, for others the time-step of construction is irrelevant or they cannot be expanded at all. This affects how expansion variables have to be aggregated to obtain installed capacities and is reflected by the set $\theta^{exp}_{e,\tilde{t},t}$ defined in Eq. 3.31. The set provides all expansion time-steps to

be aggregated for obtaining capacities of technology e with construction period $\tilde{t}$ at time-step t. Consequently, this set is empty for technologies that cannot be expanded. For *mature* technologies it contains all time-steps of expansion that result in a lifespan including t. For *emerging* technologies, capacities are not aggregated and accordingly only $\tilde{t}$ itself is assigned.

$$\theta^{exp}_{e,t,\tilde{t}} \coloneqq \begin{cases} \emptyset & \text{,if } g(e) = \textit{'stock'} \\ \{\tilde{t}' \in \eta^{tp}_e \,|\, \tilde{t}' \in (\alpha^{sup}_t - lt_{e,\tilde{t}'}, \alpha^{sup}_t]\} & \text{,if } g(e) = \textit{'mature'} \\ \{\tilde{t}\} & \text{,if } g(e) = \textit{'emerging'} \end{cases} \tag{3.31}$$

Building on this, in 3.32 the installed capacities are defined as the sum of expansion plus pre-existing capacities $capa^{pre}$ set exogenously.

$$Cap^{ist,cv}_{t,\tilde{t},r,e} = cap^{pre,cv}_{t,\tilde{t},r,e} + \sum_{\tilde{t}' \in \theta^{exp}_{e,\tilde{t},t}} Exp^{cv}_{\tilde{t}',r,e} \qquad \forall e \in \Gamma^{cv}, t \in \Phi, \tilde{t} \in \theta^{dis}_{e,t}, r \in \eta^{sp}_e \tag{3.32}$$

3.4 Application of the model formulation

To demonstrate feasibility of the presented formulation, the model its introduction was based on is now created and solved. A particular focus is on how temporal granularity impacts model size, solve time and final results.

For this application, the open-source modelling framework AnyMOD.jl that implements the graph-based formulation is used. Code and documentation of AnyMOD.jl are freely available on Github (Göke 2021a). The corresponding repository and a Zenodo upload with all the other files to run the example model are provided in the Supplementary Material.

As introduced in the previous section, the example models the transformation of the power and heating sector from a fossil and fissile to a renewable system over the course of 20 years in 5 years steps for two stylized regions, but could be freely extended and altered. This includes the addition of energy carriers and technologies to cover more sectors or a different structure of time-steps to achieve different temporal resolutions. Also, the temporal resolution of expansion could be increased for certain technologies to model a constant expansion rate within each decade.

3.4.1 Results of the example model

The example model was parameterized as follows: For location-dependent parameters, like demand or availability of renewables, values were selected such that the regions *East* and *West* resemble Germany and France. Costs and technological properties were based on recent estimates. To actually achieve the levels of renewables and sector integration the framework was developed for, the yearly emission limit linearly decreases from 350 million tons of CO_2 in 2020 to zero in 2040.

The resulting development of operated conversion capacities is displayed in Fig. 3.7. It should be noted that according to the framework's convention, these are input capacities. In the graph, the impact of moving from a small emissions limit in 2035 to no emissions in 2040 is very pronounced. Instead of switching to synthetic gas, gas boilers and OCGT power plants are mostly decommissioned and replaced with solar heating and hydrogen turbines. The resulting energy flow for 2040 is shown in Fig. 3.8, which is the quantitative counterpart to Fig. 3.5 from section 3.3.1.4. Again, colored vertices represent energy carriers and grey vertices correspond to technologies. The graph visualizes several characteristics of the framework's graph-based approach. For example, the flow leaving *district heat* and entering *heat* reflects that according to the energy balance in Eq. 3.13, descendant carriers are included in an ancestors energy balance. As a result, *district heat* can equally satisfy final demand for *heat*

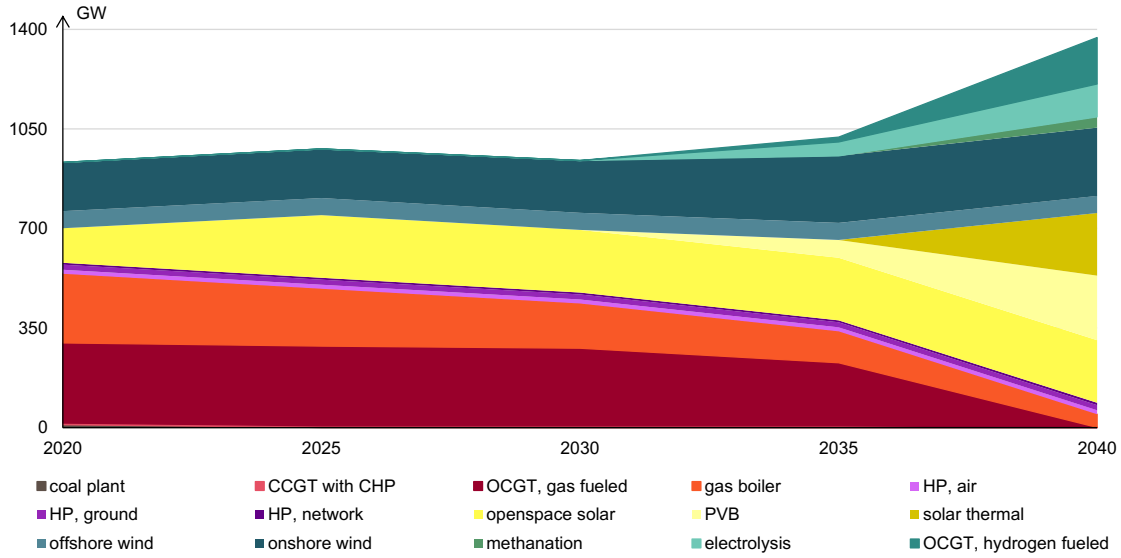

Figure 3.7: Operated conversion capacities for the example model

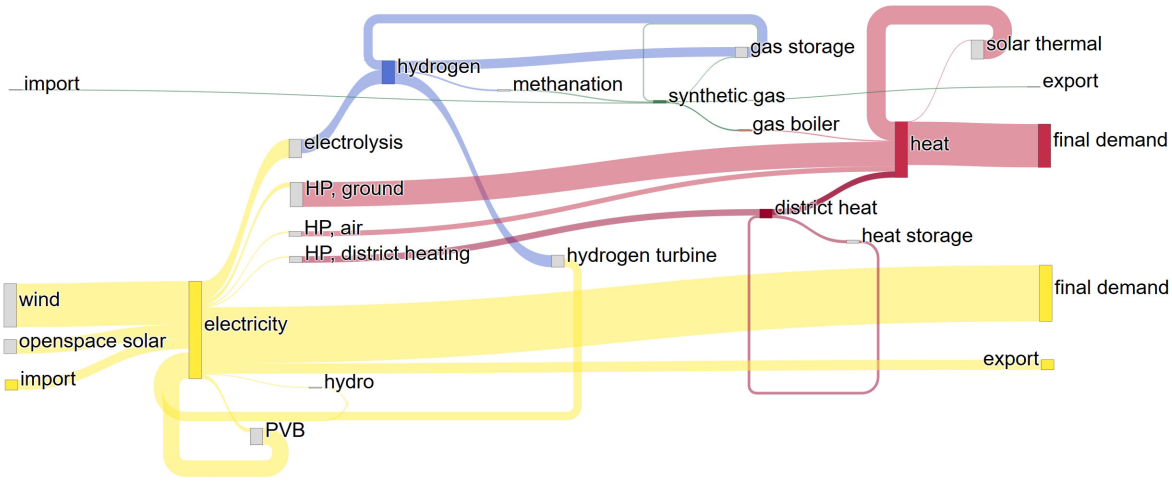

Figure 3.8: Quantitative energy flow in example model for all regions in the year 2040[6]

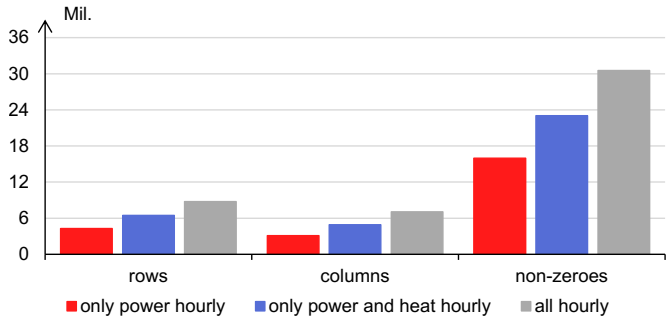

Figure 3.9: Model size across scenarios

despite being produced by different technologies. Also, both *hydrogen* and *synthetic gas* flows enter and leave the *gas storage* technology, which was defined to store their ancestor *gas*. This corresponds to the storage implementation presented in sections 3.3.1.4 and 3.3.2.3.

3.4.2 Impact of temporal resolution

All these results were obtained solving the model with full foresight and the settings outlined in section 3.3.1.3, which proposed an hourly resolution for electricity, four-hour steps for heat and daily balancing of all gaseous carriers. To study the impact of impact temporal granularity, two more detailed scenarios are considered in addition. One extends hourly granularity to *heat* and *district heat*, while all other resolutions remain unchanged. In the other, all carriers are modeled with hourly resolution.

In Fig. 3.9 the size and number of non-zero elements for the model's underlying optimization matrix are shown across all three scenarios. Even though three-quarters of technologies in the model either use or generate electricity, reducing temporal granularity for all carriers but electricity achieves a reduction of about 50% in matrix size and number of non-zero elements. If resolution for heat and electricity is kept hourly and detail is only decreased for gaseous carriers, the reduction still amounts to 25%. A reduced model size will decrease working memory requirements and makes it possible to solve models that previously did not fit into memory, but it does not necessarily reduce computation time. The time to solve a problem also depends on the inner structure of the matrix and the applied solution algorithm.

To assess the scenarios in terms of computation time, they were solved using different algorithms of the Gurobi solver. Using the simplex method did not provide any results in less than a day; solve times when applying the Barrier algorithm with 'Approximate Minimum Degree' or 'Nested Dissection' ordering are displayed in Fig. 3.10.[7] Results indicate that solve time decreases disproportionately to model size. When going from an hourly granularity for all carriers to only modeling electricity hourly, model size was reduced by 50%, but solve time decreased by 64% to 75% depending on the ordering method. The corresponding computations were run on a high-performance computing cluster. If reproduced on a desktop computer with less working memory and parallel processors, the model creation might take longer, because the framework heavily utilizes multi-threading. Also, for 'Nested Dissection' ordering, memory limits are likely to be exceeded.

Lastly, final model results are compared for the three scenarios. To this end, Fig. 3.11 shows the difference in operated capacities for the two more detailed scenarios compared to the reference case for 2040. Positive values indicate that capacities for the more detailed scenario exceed results from the reference case. Only technologies where results differ are included. If heat is modeled with hourly resolution, generation from CHP plants and solar heating is partly replaced by more flexible gas boilers fueled by synthetic gas. To generate this gas, additional

6. Import and export flows are aggregated across all regions, and thus have the same value.

7. Reported times only refer to the barrier algorithm itself and omit crossover. In no case crossover improved results by more than 0.000 007 percent, but typically increased computation time by a factor of four.

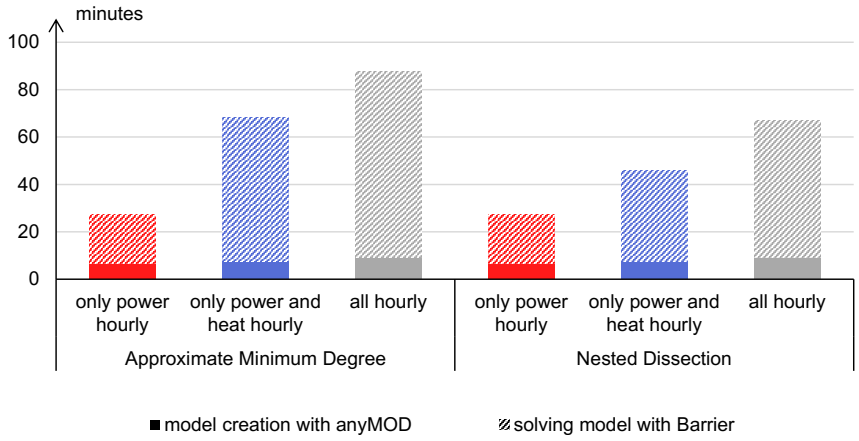

Figure 3.10: Solve time with Barrier algorithm across scenarios

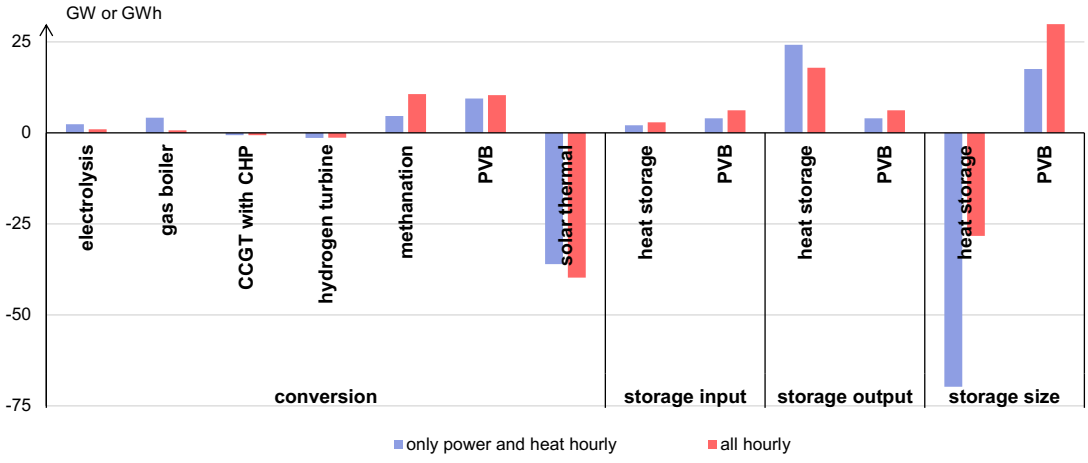

Figure 3.11: Operated capacities compared to reference case in 2040

capacities for electrolysis and methanation are required. CHP plants generating less leads to smaller sized heat storage. Also, reduced solar thermal capacity allow the installation of additional PVB systems, since both technologies compete for rooftop area. If the resolution of gas is changed from daily to hourly as well, shifting gas within the day requires gas storage and thus becomes subject to losses. Consequently, storing gas is avoided and instead methanation capacities are increased to produce gas when required. For the reference case system costs amount to 397.4 € billion and increase to 399.6 € billion when heat is additionally modeled at an hourly resolution. Modeling all carriers hourly further increases costs to 400.1 € billion.

Deviations between the reference case and more detailed scenarios should not necessarily be interpreted as inaccuracies. If a less detailed resolution can be justified from an engineering perspective, it does not only reduce model size, but also allows the consideration of the system's inherent flexibility. Consequently, the decrease in system costs when reducing a carrier's granularity can be interpreted as the economic value of this flexibility. The effects that changing the granularity of a single carrier has across the entire system also emphasizes what was stated at the very beginning of the introduction: Analyzing energy systems characterized by high shares of intermittent renewables requires a cross-sectoral perspective.

3.5 Conclusion and outlook

This paper introduced a novel formulation for modelling macro-energy systems. In contrast to existing formulation, it pursues a novel approach based on graph theory. Organizing sets in rooted trees enables two features that facilitate modeling systems with high shares of renewables and sector integration. First, the method allows the level of temporal and spatial detail to be varied by energy carrier. As a result, model size can be reduced without reducing the level of detail applied to fluctuating renewables. In addition, flexibility inherent to the system, for example in the gas network, can be accounted for. Second, substitution of energy carriers can be modeled in dependence of the respective context: conversion, storage, transport, or demand. This achieves a more comprehensive representation of how technologies and energy carriers can interact in an integrated energy system. In addition, smaller features not found in previous frameworks, namely an accurate representation of technological advancement, endogenous decommissioning and internal storage of generated carriers, have been implemented.

To demonstrate its capabilities, the graph-based formulation was applied to a stylized example that models the transformation of the power and heating sector from a fossil to a renewable system over the course of 20 years in two regions loosely based on Germany and France. The example shows in particular how varying the temporal resolution by carrier reduces solve time by 64% to 75% without imposing a major bias on results.

So far, the introduced formulation cannot account for weather related uncertainties of renewable generation, although this has been identified as a key requirement for modeling high shares of renewables (Ringkjøb, Haugan, and Solbrekke 2018). Therefore, the focus of further development is to enable stochastic capacity expansion to account for a range of weather years. Since this implies a substantial increase in model size, a particular challenge lies in solving such models. One approach could be to implement a distributed solution algorithm based on Benders decomposition that can fully exploit the capabilities of high-performance computing (Conejo et al. 2006).

4

AnyMOD.jl: A Julia package for creating energy system models

This chapter is based on a revised submission of Göke, L. 2021b. "AnyMOD.jl: A Julia package for creating energy system models." *SoftwareX* 16:100871. doi: 10.1016/j.softx.2021.100871.

4.1 Current code version

Nr.	Code metadata description	Please fill in this column
C1	Current code version	v0.1.6
C2	Permanent link to code/repository used for this code version	https://github.com/leonardgoeke/AnyMOD.jl/releases/tag/v0.1.6
C3	Code Ocean compute capsule	
C4	Legal Code License	MIT license (MIT)
C5	Code versioning system used	git
C6	Software code languages, tools, and services used	Julia
C7	Compilation requirements, operating environments & dependencies	Julia 1.3.1
C8	If available Link to developer documentation/manual	https://leonardgoeke.github.io/AnyMOD.jl/stable/
C9	Support email for questions	lqo@wip.tu-berlin.de

Table 4.1: Code metadata

4.2 Motivation and significance

Since the production of energy accounts for three-quarters of global emissions, mitigating climate change requires the decarbonization of the energy system (Edenhofer et al. 2014). Cutting emissions requires to shift supply of primary energy to electricity from wind and solar and extend its use to other sectors. As a result, the energy system has to undergo fundamental change and evolve from largely independent sectors with little supply from renewables into an integrated system characterized by fluctuating renewables.

Capacity expansion models investigate the long-term developments of macro-energy systems, but existing methods were developed for systems still characterized by fossil fuels and struggle to describe the transformation towards a renewable system (Levi et al. 2019). Models like ReEDS, Message, or Switch, pursue a time-slice approach, that reduces the entire year to a small number of independent periods (Cohen et al. 2019; Howells et al. 2011; Johnston et al. 2019). This reduction limits the detail applied to fluctuating renewables and more importantly prohibits to consider long-term storage, a key component of renewable energy systems (Schill 2020). Other models, like PyPSA or Calliope, diverge from this approach and consider a continuous and hourly time-series instead, which enables a detailed representation of renewables and long-term storage (Pfenniger and Pickering 2018; Brown, Hörsch, and Schlachtberger 2018). But in return these models are limited to a single year and, opposed to models using time-slices, cannot analyze development pathways for today's system.

Against this background, AnyMOD.jl provides a framework for modeling the long-term transformation of the energy system with the level of detail necessary to represent fluctuating renewables and long-term storage. The framework implements a novel graph-based method introduced in Göke (2021a) that varies the level of temporal and spatial detail by energy carrier to keep models with high resolution computationally tractable. The approach also enables to model the substitution of energy carriers and, on the practical side, facilitates the read-in of input data.

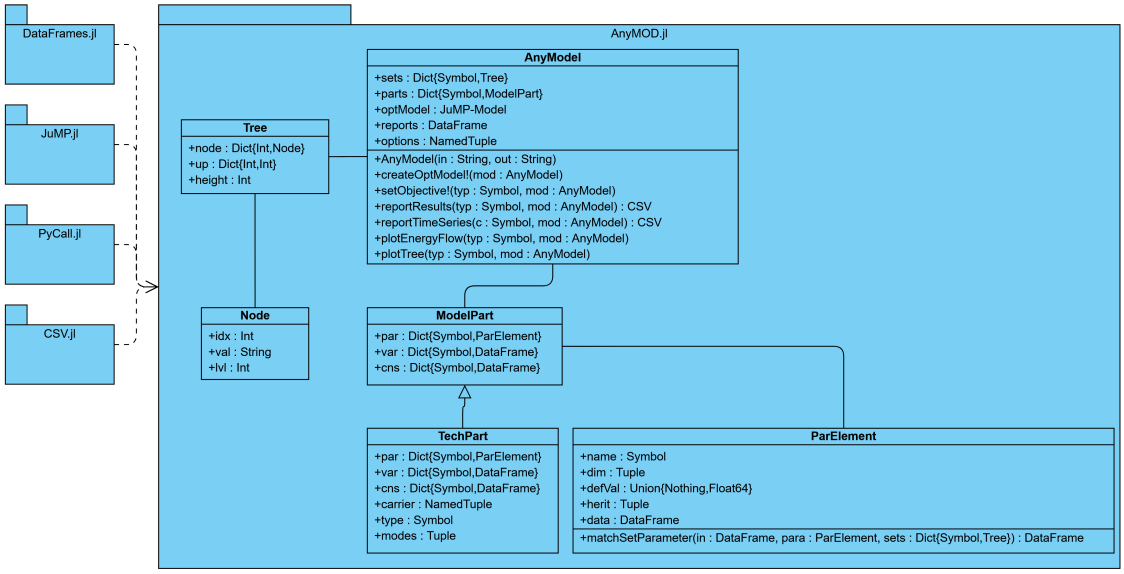

Figure 4.1: UML class diagram of package components

AnyMOD.jl follows an easy to use, but difficult to master principle. Since individual models are solely defined by CSV files and can be run with a few lines of standard code, running an existing model, and performing sensitivity analysis requires little experience. More advanced applications, like creating new models and individually modifying their formulation, requires some programming skills and a deeper understanding of the framework's structure. Since models are defined from CSV files and short code scripts, the framework supports version-controlled model development to promote collaboration and transparency.

The following section gives an overview of the framework's structure and presents two functionalities with greater detail, the read-in of parameter data (section 4.3.2.1) and the re-scaling algorithm (section 4.3.2.2). The subsequent section describes an application that models the transformation of the European power and gas sector. The final section paper highlights the framework's impact and concludes.

4.3 Software description

The package is implemented in Julia. Its key dependencies are JuMP.jl as a backend for linear optimization and DataFrames.jl for data processing (Dunning, Huchette, and Lubin 2017; Bezanson et al. 2017). The framework uses PyCall.jl to create an internal Python environment and apply the Python packages NetworkX and Plotly for plotting. Gurobi is added as an optional dependency, because its function to compute irreducible inconsistent subsystems is utilized to debug infeasible models. Apart from that, the framework is compatible with any open or commercial solver implemented in Julia. To increase performance the package heavily utilizes Julia's multi-threading capabilities. Since not supported by JuMP.jl, the mere creation of constraints uses only one thread, but the computationally more intensive composition of constraints from variables and parameters is multi-threaded.

4.3.1 Software Architecture

The class diagram in Figure 4.1 illustrates the architecture of AnyMOD.jl and how it revolves around the *AnyModel* object. For the sake of clarity, the diagram is not exhaustive and only covers the most relevant dependencies, objects and attributes. Listing 4.3.1 provides the corresponding code to initialize, populate, solve and analyze the model object.

time-step	region	carrier	technology	variable
1	1	1	1	$gen(1,1,1,1)$
2	1	1	1	$gen(2,1,1,1)$
3	1	1	1	$gen(3,1,1,1)$

Table 4.2: Exemplary data frame of generation variables

After loading AnyMOD.jl, the constructor initializes the *AnyModel* object based on two mandatory arguments: an input directory and an output directory. The CSV files defining a model consist of set and parameter files that have to be placed in the input directory. The set files define all time-steps, regions, energy carriers and technologies considered in a model and map how these are related, for example which carriers a technology can generate. Following the graph-based approach, the elements of each set are organized as nodes of hierarchical trees.

```
using AnyMOD # loading packages
model_object = anyModel("../demo","results") # construct model object

# create optimization problem and set an objective
createOptModel!(model_object)
setObjective!(:costs, model_object)

# solve model and report results
using Cbc
set_optimizer(model_object.optModel, Cbc.Optimizer)
optimize!(model_object.optModel)
reportResults(:summary, model_object)
```

Listing 4.1: Script to initialize, create and run a model

Qualitative inputs on sets are complemented with quantitative data from the parameter files, that for instance provide demand time-series or technology properties like investment costs or efficiency. While the naming and format of set files is strictly defined, parameter data can be freely structured and distributed across files. As a result, models can be composed modularly, since different models can share the same input files. After reading in all parameter data, the constructor creates a *ParElement* object for each parameter with data and meta information and assigns it to a *ModelPart* object. The *ModelPart* objects partition the model into different parts, for instance, the *ParElement* for demand time-series will be assigned to a model part dedicated to the energy balance. Each technology got its own part object of the subclass *TechPart*, that also stores technology specific attributes like assigned carriers.

After construction, the *AnyModel* object is passed to the *createModel!* function, which creates all the variables and constraints of the underlying optimization problem *optModel*. These variables and constraints are again assigned to model parts and stored as data frames. For instance, Table 4.2 depicts a data frame of generation variables. The column on the right stores the JuMP variable objects and the four other columns give the time-step, region, carrier, and technology of each variable, which are provided as indexes of the *Node* objects created during initialization. Such data frames for variables are combined with parameter data using database operations to construct constraints. For instance, generation variables are aggregated by technology and than joined with the demand parameter to create the energy balance in Table 4.3.

After the optimization problem is created, its objective is set with the *setObjective* function. At this point the user can also freely modify and extend the automatically generated problem by

time-step	region	carrier	constraint
1	1	1	$dem(1,1,1) = \sum_t gen(1,1,1,t)$
2	1	1	$dem(2,1,1) = \sum_t gen(2,1,1,t)$
3	1	1	$dem(3,1,1) = \sum_t gen(3,1,1,t)$

Table 4.3: Exemplary data frame of energy balance constraints

accessing the JuMP attributes of the *AnyModel* object and its parts. Finally, the optimization problem *optModel* is passed to a solver and analyzed afterwards. All results are written to the output directory, which was passed to the constructor in the beginning. A reporting file with error messages and warnings is written to this directory as well.

4.3.2 Software Functionalities

As outlined above, AnyMOD.jl is a package for the creation of energy system models. Additional features are aimed either at simplifying its application or enhancing the performance of creating and solving models. In the following, two of these features are presented in greater detail.

4.3.2.1 Inheritance Algorithm

As explained above, model constraints are constructed from variables and parameters, which are again defined by input data. Usually, models use a single parameter value in many constraints. For example, the efficiency of a newly build gas power plant does typically not vary by time-step or region and all constraints describing these plants will use the same value. Consequently, it would be inefficient, if AnyMOD.jl required users to provide efficiency data at a temporal and spatial resolution. On the other hand, efficiencies of heat-pumps are highly dependant on region and time-step, because they depend on ambient temperature. So, not permitting efficiencies to depend on time-step and region, would prevent to model these technologies accurately. A similar problem occurs, if investment costs of emerging technologies, like PV, are expected to decrease within the model horizon, but costs for other technologies remain constant. Here, providing all costs at a yearly resolution leads to redundant inputs for most technologies, but if costs cannot be varied by year at all, cost degression of PV cannot be modelled. In conclusion a predefined resolution of input data either results in an highly inefficient read-in of input data or restricts modelling capabilities.

To resolve this problem, AnyMOD.jl does not predefine the resolution of input data and instead automatically infers how data should be used from the way it is specified. For example, providing different efficiencies in dependence of time-step and region will result in temporally and spatially resolved efficiencies in the model, but if instead a parameter is provided without time-steps or regions, the model uses a uniform value. This concept is not limited to certain parameters or dimensions, but applies comprehensively. The implementing algorithm builds on the idea to "inherit" missing data for a specific node from its relatives in the hierarchical tree.[1]

Figure 4.2 illustrates the basic mechanism of the algorithm based on an exemplary hierarchical tree organizing time-steps. The first level of the tree organizes different years with days, 4-hours steps and hours following on the subsequent levels. Green numbers indicate input data provided for a specific node. If input data is not specified in dependence of the time-step, it is assigned to the root of the tree. The algorithm can obtain missing data at the circled node in three different ways: either move up the tree and use '8.3', move down the tree and sum the hourly values, or move down the tree and average the hourly values. How the algorithm deploys these three methods for each dimension depends on the inheritance rules of

1. This idea of "inheritance" is not be confused with inheritance in the context of object orientated programming.

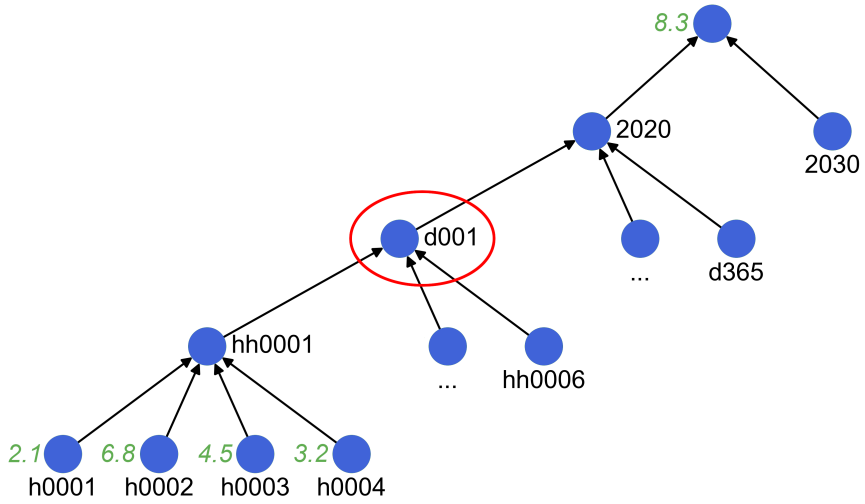

Figure 4.2: Basic mechanism of inheritance within hierarchical trees

the parameter. A detailed overview for each parameter is provided in the parameter list of the documentation.

Figure 4.3 outlines how these rules then are deployed to obtain parameter data. The described algorithm corresponds to the *matchSetParameter* function of *ParElement* in Figure 4.1 and takes the following inputs: a data frame to be filled with parameter data, a respective parameter object and the hierarchical trees. First, the algorithm checks for direct matches between the input data frame and the parameter data. Afterwards, it loops over the inheritance rules to inherit new data for missing nodes as described above. If new data is obtained, the algorithm checks again for matches with the input data frame. The loops ends when either all rows are matched with data, or all inheritance rules have been applied. In the latter case, unassigned rows are either dropped or assigned a default value, if one is defined for the respective parameter.

```
Input: data frame requiring data, parameter object, hierarchical trees
Output: data frame with parameters assigned
find matches of data frame with parameter data;
for I do
    try to inherit new data for missing nodes;
    if new data obtained then
        add newly obtained data to parameter object;
        find new matches of data frame and parameter data;
        if no unmatched rows in data frame anymore then
            exit loop;
        end
    end
end

if parameter has default value then
    use default for unmatched rows;
else
    drop unmatched rows;
end
```

Figure 4.3: Inheritance algorithm

4.3.2.2 Scaling

The formulation of an optimization problem can have a major impact on solver performance. The barrier algorithm, the fastest method for solving large linear problems, is particularly sensitive to a model's numerical properties, and poor formulations will thus greatly increase computation time. For this reason, AnyMOD.jl automatically applies a two-step scaling process when creating optimization problems. The process aims to narrow the range of coefficients and constants in a problem between 10^{-3} and 10^{6}, as recommended.[2]

As a demonstration of how this range is achieved, Eq. 4.1 constitutes the constraints of an exemplary linear model. In the first and second row, the coefficients for x_1 are currently outside of the targeted interval. In addition, the maximum range of coefficients in the second row amounts to 10^{11} ($= \frac{10^2}{10^{-9}}$), which exceeds the maximum range of the targeted interval of 10^{9} ($= \frac{10^6}{10^{-3}}$) and means the equation cannot be multiplied with a constant factor to shift coefficients into the desired interval.

$$\begin{aligned} 10^{-8}\ x_1 &+ 10^{3}\ x_2 + x_3 \leq b_1 \\ 10^{-9}\ x_1 &+ 10^{2}\ x_2 + x_3 \leq b_2 \\ x_1 &+ x_2 + x_3 \leq b_2 \end{aligned} \tag{4.1}$$

Therefore, in the first step the maximum range of coefficients is decreased by substituting variables. In the example, x_1 is substituted with $10^3\, x_1'$, which results in the system displayed in Eq. 4.2.

$$\begin{aligned} 10^{-5}\ x_1' &+ 10^{3}\ x_2 + x_3 \leq b_1 \\ 10^{-6}\ x_1' &+ 10^{2}\ x_2 + x_3 \leq b_2 \\ 10^{3}\ x_1' &+ x_2 + x_3 \leq b_2 \end{aligned} \tag{4.2}$$

Since the first step decreased the maximum range, in the second step coefficients can be shifted into the interval between 10^{-3} and 10^{6}. For this purpose, each constraint (or row) is scaled with a constant factor. In the example, the first row is multiplied by 10^2 and the second row by 10^3 resulting in the system displayed in Eq. 4.3 that finally complies with the recommended range.

$$\begin{aligned} 10^{-3}\ x_1' &+ 10^{5}\ x_2 + 10^{2}\ x_3 \leq 10^{2}\ b_1 \\ 10^{-3}\ x_1' &+ 10^{5}\ x_2 + 10^{3}\ x_3 \leq 10^{3}\ b_2 \\ 10^{3}\ x_1' &+ x_2 + x_3 \leq b_2 \end{aligned} \tag{4.3}$$

AnyMOD.jl uses default factors for substitution that depend on the variable type and can be adjusted if they fail to achieve the desired result. Factors for scaling can be automatically computed based on the current coefficients in a constraint.

Figure 4.4 demonstrates the impact of automated scaling by comparing the solve times of Gurobi's barrier implementation for a test model.[3] To ensure robustness of the results, Barrier was run with both available ordering algorithms, "approximate minimum degree" and "nested dissection." With automated scaling disabled, a *NumericFocus* parameter of three is necessary to avoid early termination or extremely long solve times due to numerical difficulties. In conclusion, automated scaling decreases solve time of the test model roughly by a factor of three.

2. See the Gurobi Guidelines for Numerical Issues for details.

3. The corresponding model files can be found in the following repository: https://github.com/leonardgoeke/AnyMOD_example_model/tree/May2020

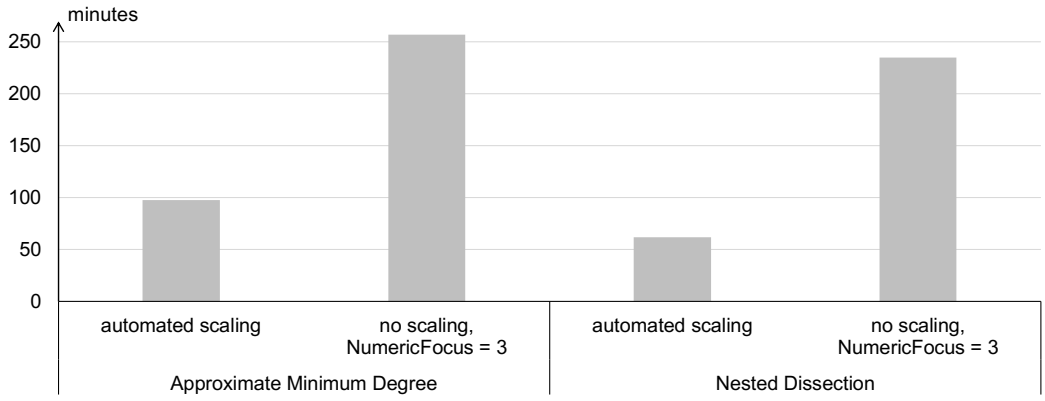

Figure 4.4: Impact of scaling algorithm on solver run-time

4.4 Illustrative Example

Hainsch et al. (2020) applied AnyMOD.jl to the decarbonization of the European power and gas sector on a pathway from 2030 to 2040 instead of a single year. The analysis with AnyMOD.jl complements results from another energy system model with less spatiotemporal detail. The application subdivides Europe on a country level and includes an aggregated representation of transmission infrastructure to enable the exchange of energy carriers between countries.

Figure 4.5 was plotted with the *plotEnergyFlow* function and provides an overview of the technologies and energy carriers considered. In the graph, carriers are symbolized by colored vertices and technologies by gray vertices. Entering edges of technologies point towards their input carriers; outgoing edges refer to outputs. Since the model includes both the power and gas sector, it is not limited to short-term storage of power, like batteries, but also considers creation and utilization of synthetic fuels for long-term storage. Since fluctuating renewables are the main source of supply by 2040, power is modelled at an hourly resolution. To reduce model size and account for the inherent flexibility of gaseous energy carriers, fossil gas, hydrogen, and synthetic gas are balanced daily instead. All other energy carriers are modelled yearly.

The energy flows for France in 2040 when solving the model are displayed in Figure 4.6. The sankey diagram does not only show how hydrogen is used for long-term storage of power, but also how final demand for hydrogen and synthetic gases, for example from the industry sector, is covered. In addition, the substantial amount of imports and exports for all carriers highlights the importance of large models that can account for several regions at once.

4.5 Impact and conclusions

AnyMOD.jl provides a framework for modeling the transformation towards a decarbonized energy system at a high spatiotemporal resolution. For this purpose, it implements a graph-based method introduced that enables to vary the level of detail by energy carrier. In addition, the framework introduces a more flexible method to read-in input data and automatically scales created optimization problems to increase solver performance. Lastly, the tool provides advanced plotting features, like Sankey diagrams.

To facilitate access for users, AnyMOD.jl can be used without any proprietary software. Using the framework does not require extensive programming skills but supports version-controlled model development, since models are created from CSV files. To extend and modify a created model, advanced users can easily access and manipulate its underlying JuMP objects. The organization of input files is highly flexible and eases the creation of new models from existing files.

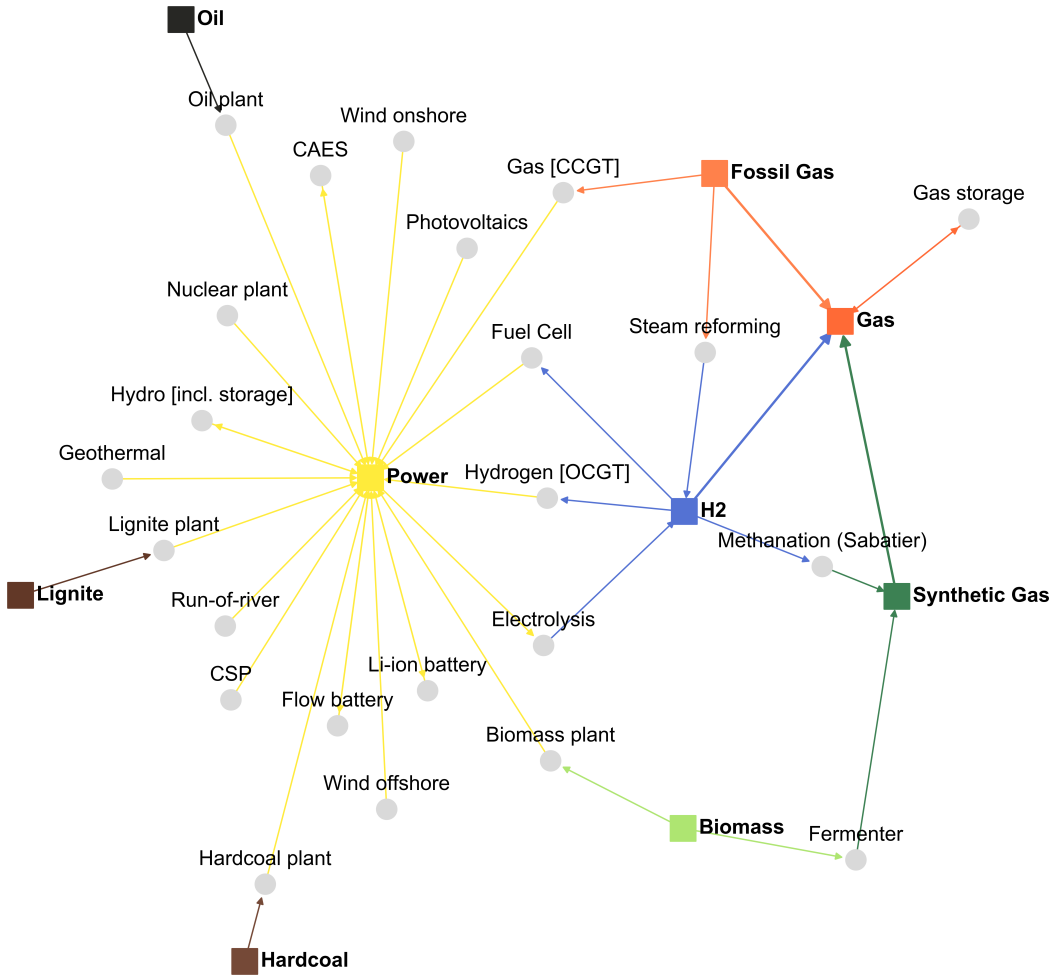

Figure 4.5: Graph of technologies and energy in example

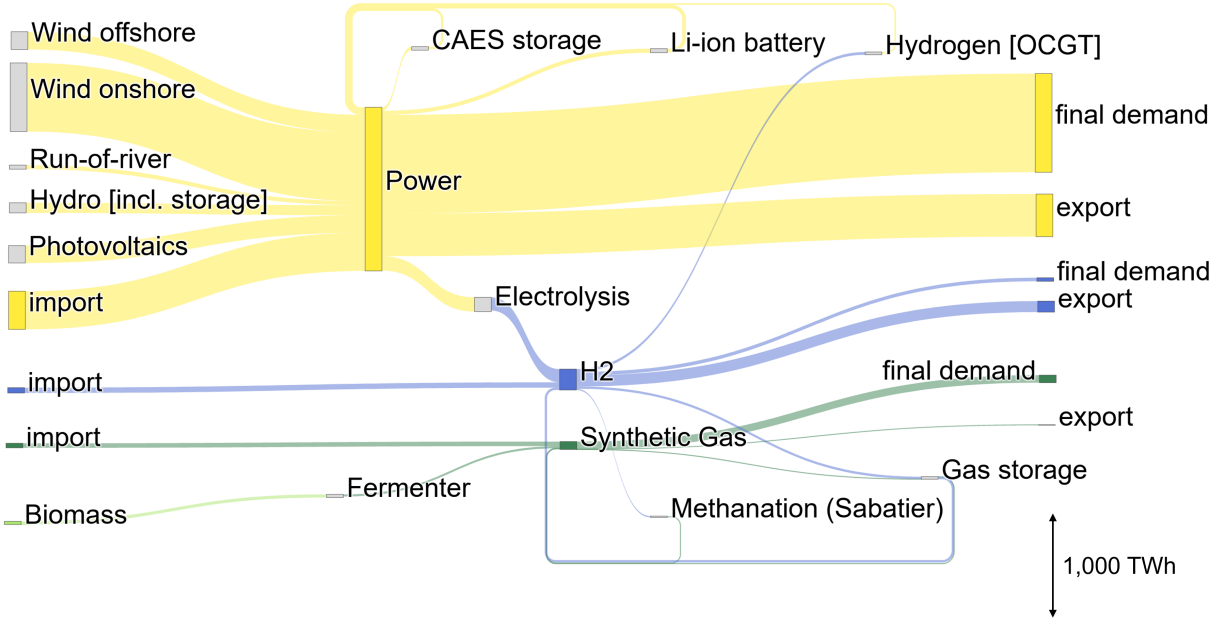

Figure 4.6: Sankey diagram for France in 2040 in example

In conclusion, AnyMOD.jl enables research to spend less time on coding and data management and more time focusing on the scientific part of their work. Its high level of accessibility also makes AnyMOD.jl suitable for use by companies, regulators, or non-governmental organizations. Finally, AnyMOD.jl promotes openness and transparency in various ways. Due to the relevance of these qualities for public policy, this is of particular importance with energy system models (Pfenniger et al. 2017).

Additional features currently developed include a more detailed representation of transmission infrastructure and the inclusion of more than one weather year in a single model. The later also includes the development of a distributed solution algorithm to keep the resulting increase in model size manageable.

5

Accounting for spatiality of renewables and storage in transmission planning

This chapter is based on joint work with Mario Kendziorski, Claudia Kemfert, and Christian von Hirschhausen currently under review in *Energy Economics* under the title: "Accounting for spatiality of renewables and storage in transmission planning".

5.1 Introduction

To decarbonize the energy system, the primary supply of energy has to shift towards renewables like wind and solar. As a result, also the topology of power generation shifts and new options for grid planning arise.

First, cost and potential of wind or solar greatly depend on location and, compared to fossil sources, capacities of individual plants are an order of magnitude smaller (Pfenninger, Hawkes, and Keirstead 2014). This imposes a trade-off on their deployment: either place plants where site conditions are best and rely on the grid to bring electricity to consumers or – to reduce the need for transmission infrastructure – place plants close to demand.

Second, with increasing shares of wind and solar, matching intermittent generation with demand increasingly requires storage systems (Schill 2020). If placed the right way, storage systems can be charged while the grid is underutilized and discharged when the grid is under stress to relieve congestion, making storage a substitute for grid expansion.

In Germany, planning transmission infrastructure is the responsibility of TSOs. In a continuous process the four TSOs, under regulation of the Federal Network Agency, develop scenarios for the next 15 years of power supply and use these scenarios to identify impending congestion and outages. Since Germany, a single zonal market, pursues a "copper-plate", meaning free flow of electricity within the country, it is the TSOs' task to prevent any congestion and enable market-based dispatch of all generators plus commercial exchanges with neighboring markets. Therefore, planning is focused on optimizing operation or expanding the transmission grid. Only in extreme situations or as a temporary measures to manage congestion until other projects are completed, TSOs adjust the market-based dispatch ex-post, referred to as redispatch (Weber 2017).

In addition, the outlined process does not account for the two options to substitute grid infrastructure in renewable systems: placing renewables closer to demand and storage systems. Investment into generation capacities is private and driven by a single zonal market and a support scheme for renewables that is largely independent of location. Consequently, sites selected for renewables do not reflect the spatiality of demand or bottlenecks of the transmission grid. In the past this lead to a concentration of investment in the north contributing to congestion within the German market zone. For storage systems the situation is similar, the market design provides no incentive for regional investments and TSOs do not include them in the planning process. Regulation in other European countries is similar, although smaller market zones often provide better incentives for regional investments (Weber et al. 2013).

Grimm et al. (2016) and Kemfert, Kunz, and Rosellón (2016) investigate how including redispatch in the planning framework and not just as a temporary measure impacts grid expansion. Both papers base their analysis on the same TSO projections for 2035, but apply different models (50Hertz and Amprion and TenneT and TransnetBW 2015). The multi-stage equilibrium model in Grimm et al. relies on a stylized grid representation, but accounts for the different objectives of TSOs, private investors and the central planner. The optimization model in Kemfert, Kunz, and Rosellón on the other hand is limited to the central planner, but represents the power grid with greater detail instead. Both papers find that deviating from the zonal market dispatch increases social welfare and is able to substitute 57 percent of planned transmission lines according to Grimm et al., or 48 percent according to Kemfert, Kunz, and Rosellón, respectively. In addition, Grimm et al. point out that in a first-best case where investment into generation considers grid constraints as well, the required transmission lines are reduced by two thirds. Using a very disaggregated model, Drechsler et al. (2017) also find that the location of renewable energies has a clear impact on transmission requirements.

Following up on these findings, this paper investigates how including redispatch and the placement of generation and storage systems impacts system planning. In contrast to the sources above, we do not base our analysis on current energy scenarios by the TSOs, but on an own scenario that models a fully renewable energy system in Germany and Europe. This

system is characterized by intermittent renewables, a consequent dependence on storage, and new demands for electricity outside the power sector. Thus, it fundamentally differs from the system analyzed in previous research.

The applied model is introduced in section 5.2, followed by comparative scenarios and the underlying data assumptions in section 5.3. The results obtained on this basis are discussed in section 5.4, before the a summary of key findings, policy implications and an outlook on future work follows in section 5.5.

5.2 Applied modeling framework

Quantification of different planning processes follows a two-step procedure based on a techno-economic optimization model of the German energy system using the AnyMOD framework (Göke 2021b, 2021a). The model chooses from a range of technologies that generate, convert, or store energy carriers to efficiently satisfy an exogenous demand.

Eqs. 5.1a to 5.1h provide a highly stylized version of the model formulation. To differentiate them, variables are written in capital and parameters in lower-case letters. According to the energy balance in Eq. 5.1b, the sum of generation $Gen_{t,i,c}$, storage input $St^{in}_{t,i,c}$ and storage output $St^{out}_{t,i,c}$ over all technologies i has to match demand given by the parameter $dem_{t,i,c}$ at each time-step t and for each energy carrier c. The following storage balance connects storage in- and output with the storage level $St^{size}_{t,i}$ at each time-step t for each storage technology. Eqs. 5.1d to 5.1f enforce capacity constraints on storage in- and output, storage levels and generation ensuring production does not exceed the capacity $Capa_i$. For generation, capacity constraints include a capacity factor $cf_{t,i}$ that specifies the share of capacity available for generation at time-step t. Finally, the objective function Eq. 5.1a is composed of total investment costs $InvCost$ computed from capacities and specific investment costs $invCost_i$ in Eq. 5.1g and total variable costs $VarCost$ computed from generation Gen_t and specific variable costs $varCost$ in Eq. 5.1h. For a full description of the underlying optimization model, that also includes the representation of different regions and how they can exchange energy carriers, see Göke (2021b).

$$\min \quad InvCost + \sum_{c \in C} VarCost_c \tag{5.1a}$$

$$\text{s.t.} \quad \sum_{i \in I} Gen_{t,i,c} + St^{out}_{t,i,c} - St^{in}_{t,i,c} = dem_{t,i,c} \qquad \forall t \in T, c \in C \tag{5.1b}$$

$$St^{size}_{t-1,i} + \sum_{c \in C} St^{in}_{t,i,c} - St^{out}_{t,i,c} = St^{size}_{t,i} \qquad \forall t \in T, i \in I_{st} \tag{5.1c}$$

$$\sum_{c \in C} Gen_{t,i,c} \leq cf_{t,i} \cdot Capa^{gen}_i \qquad \forall t \in T, i \in I \tag{5.1d}$$

$$\sum_{c \in C} St^{out}_{t,i,c} + St^{in}_{t,i,c} \leq Capa^{st}_i \qquad \forall t \in T, i \in I \tag{5.1e}$$

$$St^{size}_{t,i} \leq Capa^{size}_i \qquad \forall t \in T \tag{5.1f}$$

$$\sum_{\forall i \in I} Capa_i \cdot invCost_i = InvCost \tag{5.1g}$$

$$\sum_{\forall t \in T,\, i \in I} Gen_{t,i,c} \cdot varCost = VarCost \tag{5.1h}$$

In Figure 5.1 all considered technologies, depicted as gray circles, and their interaction with energy carriers, depicted as colored squares, are visualized. Entering edges of technologies refer to their input carriers; outgoing edges relate to outputs. For example, the biomass plant

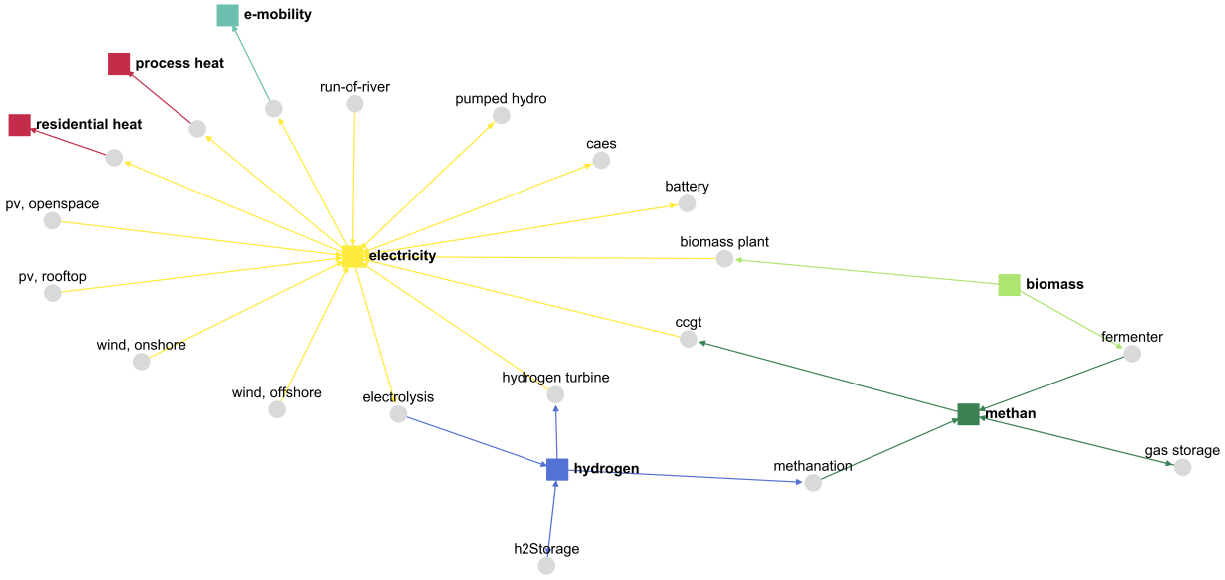

Figure 5.1: Graph of model elements

uses biomass as an input to generate electricity. Storage technologies, like pumped hydro or CAES, have an entering and an outgoing edge to represent charging and discharging.

Due to its pivotal role for renewable systems, the model's focus is on electricity. For long-term storage of electricity, the analysis includes hydrogen and synthetic methane. Setting an exogenous demand for these carriers also captures the demand for synthetic fuels outside of the power sector, for example in aviation. Beyond that, representation of other sectors is limited to their electricity demand induced by sector integration. These demands are treated separately using the carriers "residential heat" for hot water and space heat, "process heat" for industrial heating, and "e-mobility" for electric vehicles. Demand from these sectors is exogenous since the model does not include deployment of technologies outside the power sector.

The demand for each carrier has to be met by the various technologies for each considered time-step and region whereby time-steps and regions can vary by energy carrier.[1] For electricity, the model applies an hourly temporal resolution to capture the fluctuating nature of intermittent renewables. Hydrogen and synthetic gas are balanced daily since they are less sensitive to short-term imbalances. Electric mobility uses a daily resolution, too, assuming vehicle charging is flexible. Lastly, residential and process heat apply a 4-hour resolution to account for the thermal inertia of buildings and load shifting potentials in the industry.

The spatial resolution is uniform for all energy carriers but varies by scenario for reasons that will be elaborated on in the following section. Figure 5.2 provides an overview of all regions. These include 29 regions for European countries and 38 NUTS2 regions for Germany, which are modelled separately since our research question focuses on spatial effects and requires great regional detail.

Furthermore, the model allows for regular trading: Electricity, hydrogen and synthetic gases can be exchanged between regions, given the required grid infrastructure. Investment and dispatch for this infrastructure is, analogously to technologies, calculated by the model. Since the paper focuses on Germany, other European countries are only included to account for cross-border trade of energy. Therefore, technology and grid capacities for these countries are exogenous and the model only decides on their dispatch.

The high-spatio temporal detail for Germany paired with a representation of the European energy system and impact of sector integration on the system, is a unique feature of the model enabled by the AnyMOD framework. For deciding on investment and dispatch of technology

1. For a detailed description of how this feature is achieved see Göke (2021b).

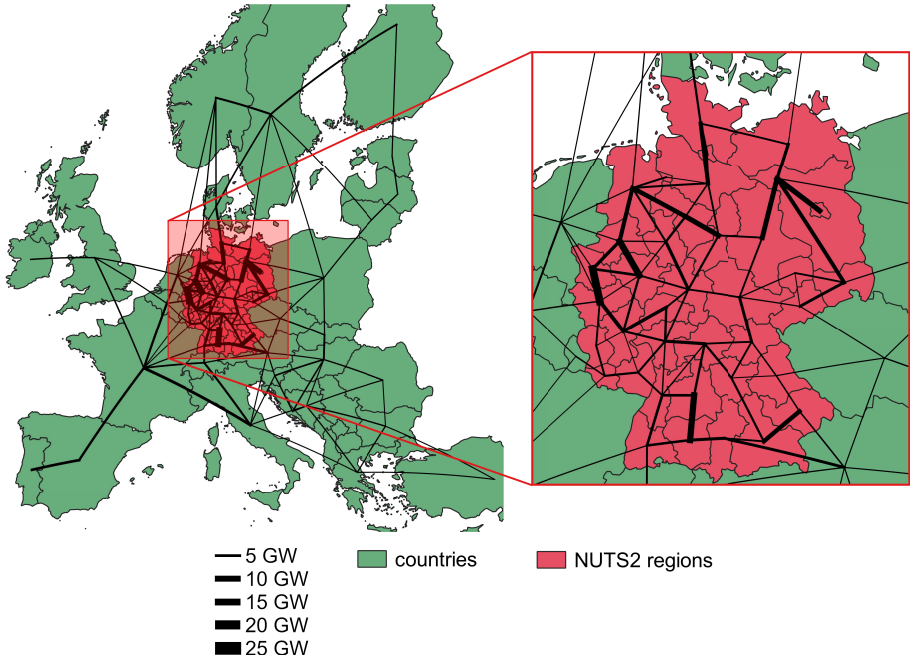

Figure 5.2: Overview of regions including pre-existing electricity grid, Sources: Kunz et al. (2017) and ENTSO-E (2020)

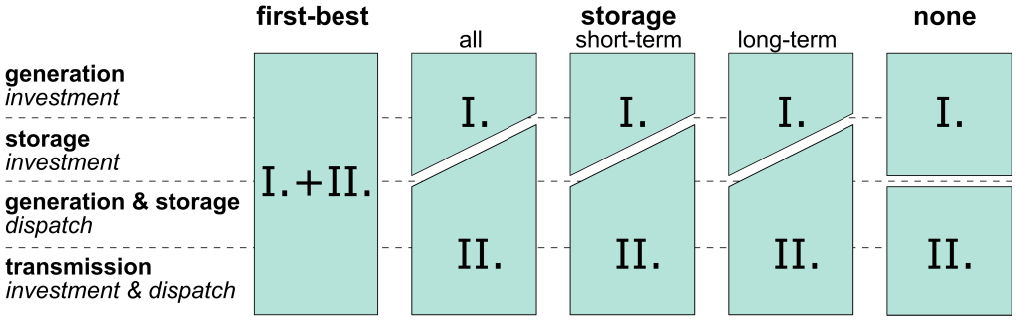

Figure 5.3: Overview of considered scenarios

and grid capacities, the model considers investment, operating, and dispatch costs to find the least-cost solution to satisfy the given demand. So, mathematically our approach is a linear minimization of system costs, which, since demand is exogenous and therefore assumed to be inelastic, is equivalent to welfare maximization. The model is limited to a single year and omits the transformation from today to a renewable system. Also, exchange of electricity neglects loop flows and how line expansion affects transmission losses. These simplifying assumptions are necessary to keep the computational complexity manageable.

5.3 Scenarios and data

5.3.1 Considered scenarios

Analysis of the different planning processes builds on several scenarios summarized by Figure 5.3. These scenarios differ regarding the sequence in which investment and dispatch decisions are determined.

The first-best case on the very left only deploys the model once. Investment and dispatch of generation, storage, and transmission are all determined simultaneously for each of the 38 German NUTS2 regions. As a result, the trade-offs between grid expansion and placing generation differently, using storage systems, or deviating from a market-based dispatch are

all internalized by the model. The scenario thus corresponds to a social welfare optimum. Note that this setting is currently not practiced, as it would require a major change to current regulation. A policy frequently proposed in the dedicated literature to achieve this optimum is nodal pricing (Harvey and Hogan 2000). To gain insight on the general importance of transmission, analysis also includes a sensitivity of the first-best without any transmission expansion at all.

In all other scenarios, investment and dispatch of generation, storage, and transmission is not determined simultaneously but sequential. The first step computes investment in generation and storage technologies, ignoring all grid constraints and assuming a free flow of electricity within Germany. Accordingly, results correspond to a market-based dispatch with a single German zone. The second step introduces the grid to determine investment into transmission, but fixes technology investment depending on the scenario. Since in the absence of grid constraints the model is indifferent where to place storage systems, these are distributed proportionally to renewable generation across the 38 regions. This is plausible given the assumed absence of regional prices, because investors have an incentive to place renewables and storage at the same sights to decrease costs for construction and grid access. If transmission losses incurred in the second step render the problem unsolvable, because demand cannot be fully met, the entire process is repeated with a correspondingly increased demand in the first step.

Since the sequential scenarios separate investment into generation and transmission, they contrast from the first-best and represent today's planning approach. In that case, the implementation of corresponding policies likely requires less regulatory change.

The following lists all sequential scenarios detailing how they fix results from the first in the second step and what kind of planning policy is simulated this way. The list follows the order from left to right in Figure 5.3.

- **All storage**: In this scenario, dispatch decisions in the second step can deviate from the market-based dispatch determined in the first. In addition, storage investment in the first step is not binding, but serves as a lower limit instead. This means storage is considered for grid relieve in the planning process, resulting in additional storage capacities on top of market driven investments.
- **Short-term storage**: This scenario is equivalent to "All storage", but additional storage investment is limited to short-term storage, namely battery and CAES.
- **Long-term storage**: The scenario is again equivalent to "All storage", but now additional investment is limited to technologies for long-term storage of electricity, which are electrolysis, methanation, hydrogen plants, and gas plants.
- **None**: In this scenario all technology investment, even storage is fixed in the second step. However, dispatch in the second step can still deviate from the market-dispatch computed in the first step.

In conclusion, only in the first-best scenario system planning considers all three substitutes for grid expansion: placement of generation, storage systems, and deviating from the zonal market dispatch. The following three scenarios consider storage and a deviating dispatch, but do not consider a different placement of generation. The last scenario only considers dispatching capacities differently.

5.3.2 Data

The following section summarizes the most important quantitative assumptions used in the model. To ensure consistency, as much data as possible was based on the same underlying scenario of a renewable European energy system, the "Societal Commitment" scenario developed in the openENTRANCE project (Auer et al. 2020). For comprehensive information on all inputs see the link in the supplementary material.

5.3.2.1 Supply

For the German NUTS regions, generation and storage capacities are determined according to the outlined scenarios based on investment and operating costs (Göke, Poli, and Weibezahn 2019; Auer et al. 2020; Kost et al. 2018). To account for cross-border trade, the other European countries are included in these scenarios as well, but their generation and storage capacities are fixed to not distort results. These capacities are instead computed in a preceding step using the same input data, but reducing Germany to a single node. For the sensitivity of the first-best case without grid expansion, this preceding step is carried out without any expansion of the European transmission grid.

Capacity limits and factors of renewables for the other European countries are based on Auer et al. Capacity factors from the German NUTS regions are extracted from renewables.ninja (Pfenninger and Staffell 2016; Staffell and Pfenninger 2016). An input not provided anywhere in the literature are capacity limits of wind and PV) broken down by German NUTS2 regions. Therefore, these assumptions were derived based on publicly available sources specifically for this study. To ensure consistency with the rest of input data, summed limits for Germany corresponds to Auer et al. (2020).

First, highly resolved satellite data for land use provides the urban, sub-urban, agricultural, and forested area in each NUTS2 region (Copernicus Programme 2020). Other literature gives the share for those areas that are typically suited for wind an solar (Nahmmacher, Schmid, and Knopf 2014; Bódisa et al. 2019). According to the product of area size and share suited for renewables, the total limit is distributed across all urban, sub-urban, agricultural, and forested areas.

Next, site quality for each of these area is extracted from geodata on average full-load hours for wind and PV (Solargis 2020; Technical University of Denmark 2020). To derive renewable limits graded by quality in each NUTS2 region, areas are clustered into different groups based on site quality. Capacity factors for each group are derived by scaling the original time-series according to site quality, but keeping the total energy potential of each NUTS region unchanged.

Fig. 5.4 shows the resulting energy potential per area for onshore wind, openspace PV and rooftop PV. Potential for onshore wind and openspace PV is based on agricultural and forested areas and, thus, potential is highest in the least populated regions. Potential for roofop PV on the contrary relates to urban and sub-urban areas, which means potential concentration in densely populated NUTS regions, in particular cities.

To provide some context Fig. 5.5 compares potentials used in this paper to other literature. The derived capacity limits are sorted by full-load hours, aggregated, and plotted against energy quantities. Accordingly, the decreasing slope of these lines represents the declining site quality when the share of exploited potential increases. Other sources are represented as points. Wherever these only specified a capacity limit, plotting assumed the same full-load hours as in our data. For onshore wind the assumed potential is at the lower end of values found in the literature, whereas assumptions for PV are largely in the middle of the observed range (Sterchele et al. 2020; Robinius et al. 2020; Bódisa et al. 2019; Mainzer et al. 2014; Lödl et al. 2010; Bundesministerium für Verkehr und digitale Infrastruktur 2015; Masurowski 2016).

The set potential for offshore wind amounts to 70 GW with 5,100 full-load hours that strongly decrease due to wake effects as soon as installed capacities exceed 50 GW (Agora Energiewende, Agora Verkehrswende, Technical University of Denmark and Max-Planck-Institute for Biogeochemistry 2020). The potential is distributed across NUTS regions currently connected to offshore wind parks.

5.3.2.2 Demand

Given the importance of sector integration, analysis of renewable systems must consider all sectors, but our model only covers synthetic fuels and electricity explicitly. Therefore, heating

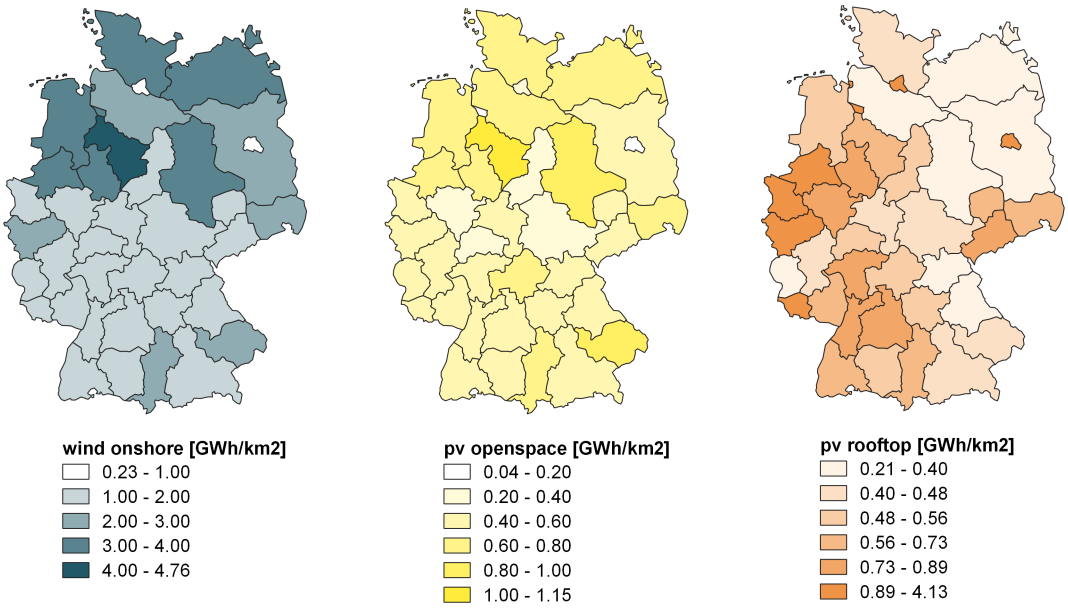

Figure 5.4: Comparison of energy potential per area by technology, Source: own calculations

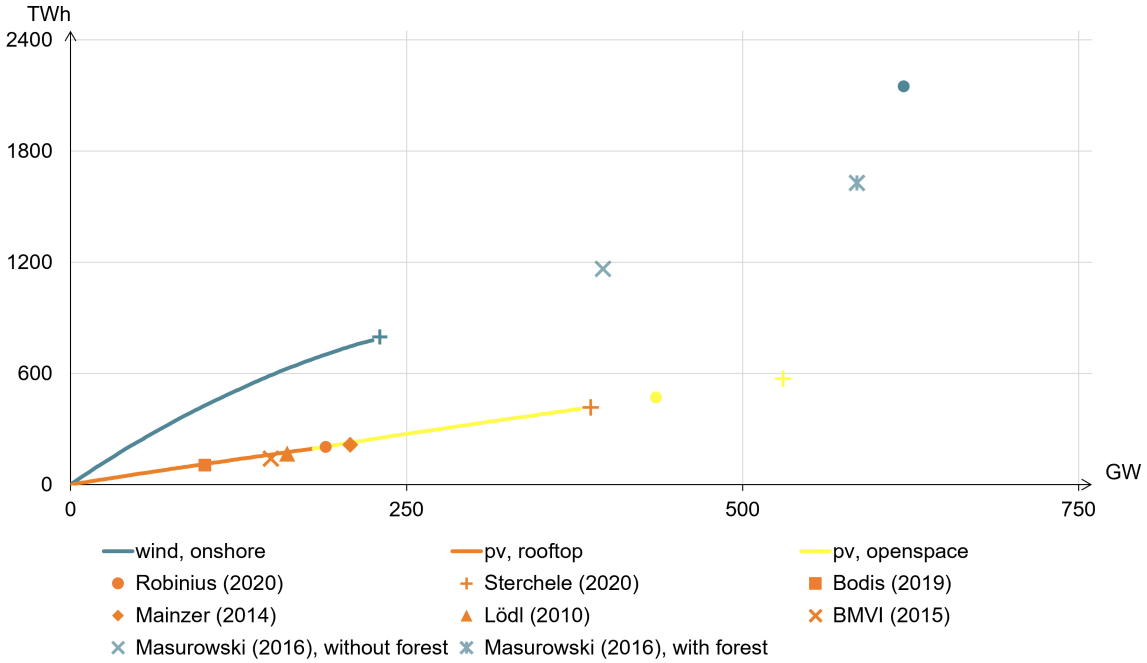

Figure 5.5: Renewable potentials for Germany compared to other sources (openspace cumulative to rooftop)

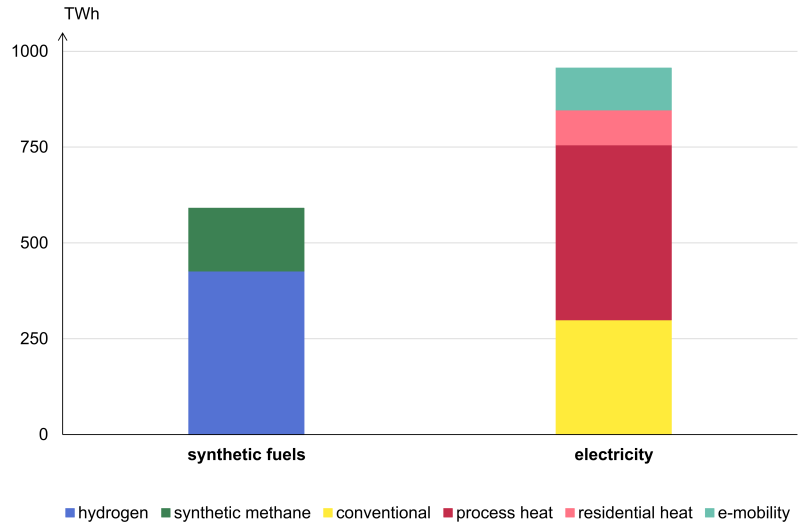

Figure 5.6: Demand for synthetic fuels and electricity in Germany, Source: Auer et al. (2020)

and transport are implicitly included by adding the demand for synthetic fuels and electricity that decarbonization of these sectors requires (Auer et al. 2020). Fig. 5.6 provides the resulting demand for Germany; magnitude and structure are similar for other countries.

The data distinguishes between two different synthetic fuels: synthetic methane and hydrogen. According to Auer et al., synthetic methane is exclusively used to provide process heat for industrial processes. Hydrogen is also used for industrial processes, but to a small extent also for residential heating. The majority of hydrogen demand, namely 60 percent, stems from freight transport. Also, a small share is used in aviation.

As has been explained in section 5.2, the model treats electricity demand from process heat, residential heat, and electric mobility separately. Process heat, in particular steam generation, constitutes the largest share of electricity demand. Shares for residential heat, mostly heat-pumps, and electric mobility are considerably smaller. Finally, demand that does not fit into any of these categories, for example household appliances, is labelled "conventional".

For Germany, national demand from Auer et al. has to be distributed across the 38 NUTS2 regions modelled. For this purpose, electricity demand from process heat is distributed according to gross domestic product, residential heat according to reported heating demand, and mobility according to population (eurostat 2020a, 2020b; Fleiter et al. 2017).

5.3.2.3 Transmission

For representation in the model, the physical transmission infrastructure is aggregated according to the covered regions. Due to the long lifetime of transmission infrastructure, the current electricity grid displayed in Fig. 5.2, is available in the model without additional investments. For Europe, these pre-existing capacities built on TSO data on net transfer capacities and include all projects to be completed by 2025 (ENTSO-E 2020). Capacities between German NUTS2 regions are aggregated from a nodal dataset. Apart from electricity, the model also includes a representation of today's gas grid assuming future utilization for hydrogen (Kunz et al. 2017). However, today's capacities were found to already exceed future needs. For this reason, transport restrictions for hydrogen are neglected within Germany.

The model represents transmission infrastructure as net transfer capacities and consequently simplifies their dispatch to a transport problem neglecting technical constraints. Investment costs and losses of transmission depend on the length of the aggregated lines as displayed in Fig. 5.2 and amount to 2.29 million Euro per GWkm and 5 percent per 1000 km, respectively

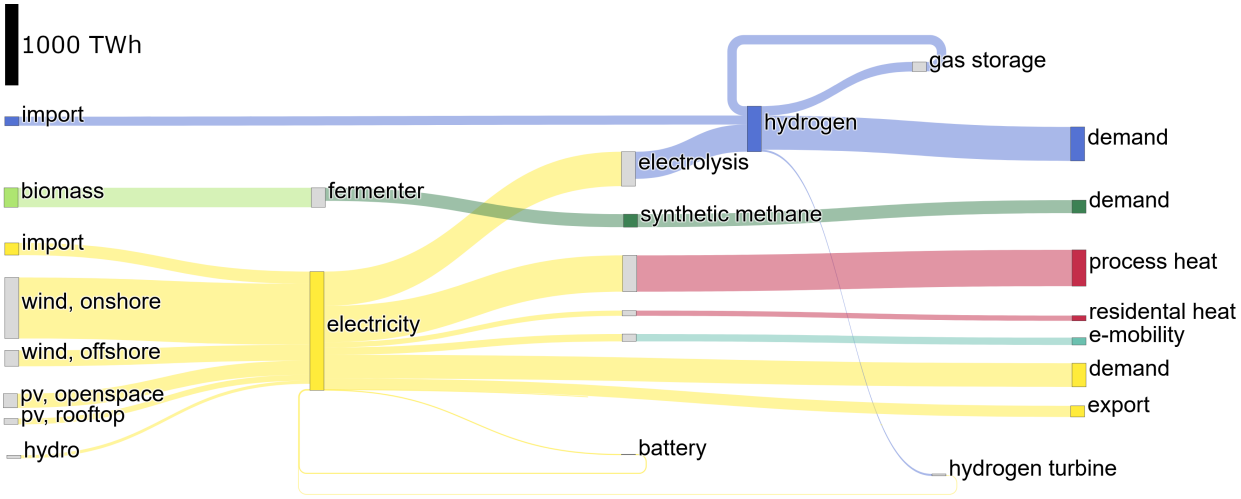

Figure 5.7: Energy flows in first-best scenario

(Joint Research Centre of the European Commission 2014; Neumann, Hagenmeyer, and Brown 2020).

5.4 Results

The results first focus on the first-best scenario and its sensitivity to create an understanding for the modelled system in general and for the role of the transmission infrastructure in that system in particular. This understanding is then necessary to comprehend the comparison of the first-best to the sequential planning scenarios in the second part.

5.4.1 First-best scenario

Fig. 5.7, the quantitative counterpart to Fig. 5.1, shows the energy flows for Germany that result from solving the model for the first-best scenario. Energy flows for the other scenarios differ of course but show no fundamental differences. Total electricity demand amounts to 1350 TWh and is covered by 766 TWh of generation from wind onshore, 200 TWh from wind offshore, 178 TWh from openspace PV, 74 TWh from rooftop PV and lastly 39 TWh from hydro, which includes run-of-river and reservoirs. With regard to Fig. 5.7, this means all renewables technologies except rooftop PV fully exploit their energy potential. Since sector integration makes up most of the demand and is assumed to be flexible within certain limits, storage systems only play a relatively minor role. Batteries provide 18 TWh of electricity and 16 TWh of electricity are generated from stored hydrogen, while the larger share of hydrogen satisfies the exogenous hydrogen demand. In addition, 114 TWh of hydrogen are imported from other European countries. Electricity is both imported and exported leading to an import surplus of 13 TWh. The demand for synthetic methane is entirely met through biomass, independent from the rest of the energy system.

If the first-best is solved without grid expansion, generation from rooftop PV increases by 50 TWh, but plant capacities do not shift and just increase in regions with unexploited potential. Instead, long- and short-term storage substitute for grid expansion; generation from hydrogen turbines increases to 55 TWh, output from batteries to 27 TWh. This substitution can also be observed when mapping grid and storage capacities as done in Fig. 5.8.[2] If grid expansion is disabled, less capacity is available to transport electricity from regions in the

2. For better illustration the figure shows technology capacities aggregated by NUTS1 regions. Small NUTS1 regions, like city states, were assigned to their nearest neighbor.

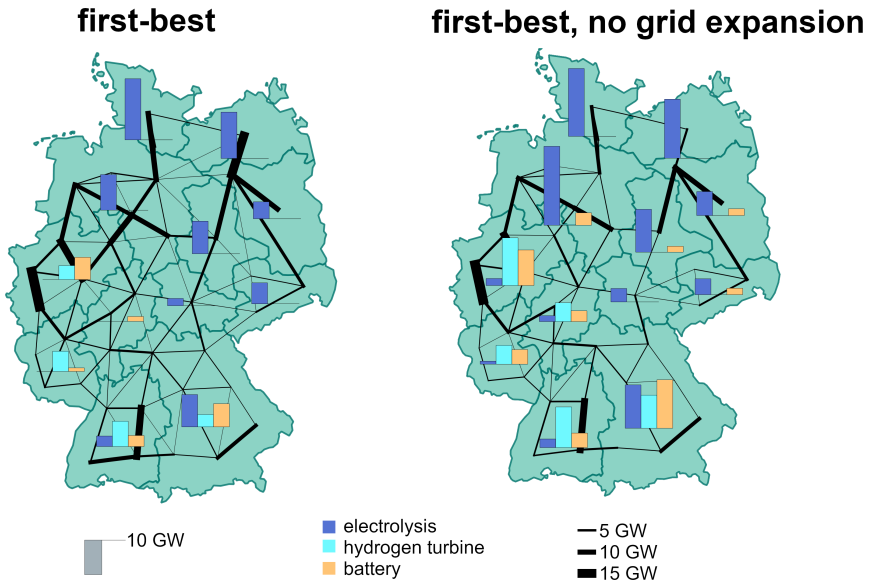

Figure 5.8: Storage capacities and grid expansion for first-best

north with large potential to regions in the south and southwest with highest demand. In return, capacities of hydrogen turbines and batteries increase substantially in these regions.

Since grid expansion occurs in the first-best solution, disabling it will rise system costs, with higher investment costs for generation and storage overcompensating the decrease of transmission costs. For Germany system costs for Germany rise by 2.5 percent, but the more meaningful comparison of European system costs shows an increase of 4.5 percent. This seems plausible given Neumann and Brown (2021) observe a 10 percent increase of system costs when limiting capacities to today's grid when modeling a renewable European power system, but note that consideration of sector integration is likely to reduce this difference. Such reduction could be explained by the added flexibility and high utilization of renewables potential from sector integration.

5.4.2 Sequential scenarios compared to first-best

To compare the first-best with today's planning framework, grid expansion and system costs in Germany are compared for different scenarios in Table 5.1. For a sensible benchmark of grid investment, expansion of each line is multiplied with its length and totalled. In comparison, the pre-existing grid that is available without additional investments amounts to 39,653 GWkm.

As expected, system costs and grid expansion are smallest for the first-best scenario. If grid expansion is determined after generation and storage, but considers all storage technologies as a substitute, results only show a slight increase in grid expansion. However, in the scenarios that only consider short-term storage or no storage at all, expansion increases substantially doubling the capacity of the pre-existing grid. If the second planning step only allows for additional long-term storage, viz. electrolyzers and hydrogen turbines, grid capacities increase by 50 percent. Long-term storage presumably has a more pronounced effect than short-term storage because strictly speaking it does not only allow for additional storage, but also to shift demand to some extent since electrolyzers also have to satisfy an exogenous hydrogen demand and hydrogen can be freely transported within Germany.

Difference in system costs are closely correlated with grid expansion. Overall, the largest proportion of costs, about 77 percent in the first-best scenario, is incurred by generation. The next factor is transmission costs, accounting for 12 percent of costs, followed by long- and short-storage with 9 and 2 percent, respectively. Since transmission only makes up a relatively small proportion of system costs, they are affected less severely by the different scenarios. Still,

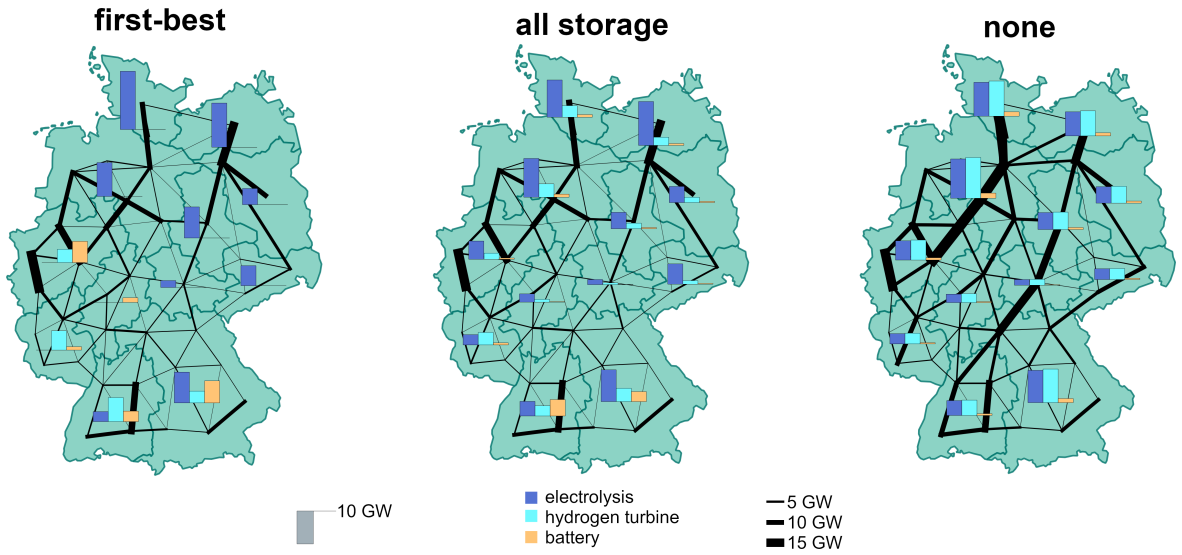

Figure 5.9: Storage capacities and grid expansion compared to first-best

system costs increase by up to 8 percent if grid expansion does not consider long-term storage, which is higher than in the first-best case without grid expansion.

	grid expansion *[GWkm]*	system costs *[Bil. €]*
first-best	8,734	51.69
all storage	9,781	51.94
short-term storage	40,640	55.58
long-term storage	17,274	52.75
none	40,654	55.59

Table 5.1: Key benchmarks of scenarios compared

Again, the scenarios show little difference with regard to the placement of generation, because capacity limits are almost fully exploited to satisfy demand. Difference are most significant when comparing the first-best to the "none" scenario. To compensate for lower capacity factors from placing renewables closer to demand, the first-best installs 13 GW more rooftop PV and 5 GW more onshore wind.

The trade-off between grid and storage is again visualized in Fig. 5.9. Between the first-best and the scenario with storage as a substitute ("all storage"), no differences are visible with regard to transmission capacities. For storage investment on the other hand, there are significant differences. In the first-best, hydrogen turbines and batteries are exclusively located in importing regions with high demand. In the storage scenario, capacities are concentrated in these regions too, but since here only the second step of investment considers the grid, all regions have some capacity. The map on the right shows capacities, if no substitute for grid expansion is considered. Here, storage capacities are evenly distributed and grid capacities, especially from exporting regions in the North to importing regions in the South, are considerably higher. Also, average utilization of transmission capacities decreases to 909 full-load hours, compared to 1,300 in the first-best.

5.5 Conclusions

In this paper we applied a capacity expansion model to investigate substitutes for transmission infrastructure in renewable energy systems and how use of these substitutes depends on the

underlying planning approach. The model is applied to the German power sector but takes detailed account of sector integration and cross-border exchange.

Results show that consideration of storage, in particular long-term storage, for congestion management greatly decreases grid investment and thus also system costs. If this option is enabled by a first-best setting that optimizes investment and dispatch of generation, storage, and transmission simultaneously, or, more similar to today's planning process, independent from generation investment in a subsequent step together with transmission investment, does not make significant difference. Findings also suggest that grid expansion can be substituted largely by storage placed in high-demand regions, causing a 4.5 percent increase in system costs.

On the other hand, very small effects on welfare and grid expansion were observed from considering grid constraints when placing renewables. These results are partly driven by the characteristics of the underlying scenario for the entire energy system used in this study. As section 5.3.2.1 shows, the assumed capacity limits for renewables, in particular for wind, are at the lower end of literature values. Therefore, the available potential for renewables is almost fully exploited to satisfy demand leaving little room to optimize their placement.

Similar to findings on redispatch in Grimm et al. (2016), results indicate that transmission planning can substantially benefit from modifications to the current policy framework. The first-best solution requiring invasive changes, like the introduction of nodal pricing, can be well approximated, if planning considers storage as a substitute for grid expansion. Conceivable instruments to this end are an obligation for TSOs to consider storage investments or a split of the Germany market into a north-east and south-west price zone to create incentives for private storage investment. In both cases, consumers in exporting regions benefit at the expense of importing regions, either in the form of lower grid charges or smaller market prices. Apart from that, the relatively small sensitivity of grid expansion on system costs suggests that an exclusive focus on costs is too narrow. Given the public opposition transmission faced in the past, a bearable increase in system costs might be preferable to high levels of grid expansion.

The applied capacity expansion framework AnyMOD captures all important features of renewable energy systems: intermittent renewables, importance of storage, increased demand and added flexibility from sector integration, as well as cross-border trade of electricity. In return, some economic and technical aspects relevant for transmission planning had to be neglected, which may limit the significance of our results. On the economic side, the approach omits path dependencies by focusing on a single year and abstracts from the different agents involved in the planning process, which hinders the recommendation of more specific policy instruments. On the technical side, restrictions of operating power grids, like physical power flows or n-1 security, were omitted. Also, although dividing Germany into 38 different regions is comparatively detailed, it does not compare to the 500 nodes of the actual transmission grid represented in power system models. To cover these aspects, future research needs to adapt economic and technical models to the characteristics of renewable energy systems.

Bibliography

50Hertz and Amprion and TenneT and TransnetBW. 2015. *Szenariorahmen für die Netzentwicklungspläne Strom 2015: Entwurf der Übertragungsnetzbetreiber.* https://www.netzentwicklungsplan.de/de/netzentwicklungsplaene/netzentwicklungsplaene-2025.

Abelshauser, W. 2014. "Der Traum von der umweltverträglichen Energie und seine schwierige Verwirklichung." *Vierteljahrschrift für Sozial- und Wirtschaftsgeschichte : VSWG,* Vierteljahrschrift für Sozial- und Wirtschaftsgeschichte, 101 (1): 49–61.

Agora Energiewende, Agora Verkehrswende, Technical University of Denmark and Max-Planck-Institute for Biogeochemistry. 2020. *Making the Most of Offshore Wind: Re-Evaluating the Potential of Offshore Wind in the German North Sea.* Technical report. Agora Energiewende.

Agora Energiewende, Wattsight. 2020. *Die Ökostromlücke, ihre Strommarkteffekte und wie sie gestopft werden kann. Effekte der Windenergiekrise auf Strompreise und CO2-Emissionen sowie Optionen, um das 65-Prozent-Erneuerbare-Ziel 2030 noch zu erreichen.* Technical report. Agora Energiewende. https://www.agora-energiewende.de/veroeffentlichungen/die-oekostromluecke-ihre-strommarkteffekte-und-wie-die-luecke-gestopft-werden-kann/.

Almaimouni, A., A. Ademola-Idowu, J.N. Kutz, A. Negash, and D. Kirschen. 2018. "Selecting and Evaluating Representative Days for Generation Expansion Planning." *2018 Power Systems Computation Conference,* doi: 10.23919/PSCC.2018.8442580.

Antenucci, A., P.C. del Granado, B. Gjorgiev, and G. Sansavini. 2019. "Can models for long-term decarbonization policies guarantee security of power supply? A perspective from gas and power sector coupling." *Energy Strategy Reviews* 26:100410. doi: 10.1016/j.esr.2019.100410.

Armytage, W. H. G. 1956. "J. A. Etzler, an American Utopist." *The American Journal of Economics and Sociology* 16 (1): 83–88. doi: 10.2307/3484798.

Auer, H., P. Crespo del Granado, P.-Y. Oei, K. Hainsch, K. Löffler, T. Burandt, D. Huppmann, and I. Grabaak. 2020. "Development and modelling of different decarbonization scenarios of the European energy system until 2050 as a contribution to achieving the ambitious 1.5°C climate target—establishment of open source/data modelling in the European H2020 project openENTRANCE." *Elektrotechnik und Informationstechnik* 137(7):346–358. doi: 10.1007/s00502-020-00832-7.

Bahl, B., J. Lützow, D. Shu, D. E. Hollermann, M. Lampe, M. Hennen, and A. Bardow. 2018. "Rigorous synthesis of energy systems by decomposition via time-series aggregation." *Computers & Chemical Engineering* 112:70–81. doi: 10.1016/j.compchemeng.2018.01.023.

Bataille, C., M. Åhman, K. Neuhoff, L.J. Nilsson, M. Fischedick, S. Lechtenböhmer, B. Solano-Rodriquez, A. Denis-Ryan, S. Stiebert, H. Waisman, O. Sartor, and S. Rahbar. 2018. "A review of technology and policy deep decarbonization pathway options for making energy-intensive industry production consistent with the Paris Agreement." *Journal of Cleaner Production* 187:960–973. doi: 10.1016/j.jclepro.2018.03.107.

Bauknecht, D., S. Funcke, and M. Vogel. 2020. "Is small beautiful? A framework for assessing decentralised electricity systems." *Renewable and Sustainable Energy Reviews* 118:109543. doi: 10.1016/j.rser.2019.109543.

Baumgärtner, N., D. Shu, B. Bahl, M. Hennen, D. E. Hollermann, and A. Bardow. 2020. "DeLoop: Decomposition-based Long-term operational optimization of energy systems with time-coupling constraints." *Energy* 198:117272. doi: 10.1016/j.energy.2020.117272.

Bebel, A. 1900. *Women and Socialism.* 2nd ed. Frankfurt a.M.

Beckert, J. 2013. "Imagined futures: fictional expectations in the economy." *Theory and Society* 42:219–240. doi: 10.1007/s11186-013-9191-2.

Beckert, J. 2016. *Imagined Futures: Fictional Expectations and Capitalist Dynamics.* Harvard University Press.

Bezanson, J., A. Edelman, S. Karpinski, and V.B. Shah. 2017. "Julia: A Fresh Approach to Numerical Computing." *SIAM Review* 59(1):65–98. doi: 10.1137/141000671.

Blaumann, A. Z., C. Rodriguez del Angel, J. Winkler, E. Zozmann, L. Göke, M. Kendziorski, and C. v. Hirschhausen. Forthcoming. *The potential of sufficiency measures to achieve a fully renewable energy system - A case study for Germany.*

Bloess, A. 2019. "Impacts of heat sector transformation on Germany's power system through increased use of power-to-heat." *Applied Energy* 239:560–580. doi: 10.1016/j.apenergy.2019.01.101.

Bloomfield, H.C., D.J. Brayshaw, L.C. Shaffrey, P.J. Coker, and H.E. Thornton. 2016. "Quantifying the increasing sensitivity of power systems to climate variability." *Environmental Research Letters* 11(12):124025. doi: 10.1088/1748-9326/11/12/124025.

Bockris, J. O.M. 2013. "The hydrogen economy: Its history." *International Journal of Hydrogen Energy* 38 (6): 2579–2588. doi: 10.1016/j.ijhydene.2012.12.026.

Bódisa, K., I. Kougiasa, A. Jäger-Waldaua, N. Taylora, and S. Szabób. 2019. "A high-resolution geospatial assessment of the rooftop solar photovoltaic potential in the European Union." *Renewable and Sustainable Energy Reviews* 114:109309. doi: 10.1016/j.rser.2019.109309.

Bogdanov, D., M. Child, and C. Breyer. 2019. "Reply to 'Bias in energy system models with uniform cost of capital assumption'." *Nature Communications* 10 (1). doi: 10.1038/s41467-019-12469-y.

Bondy, J.A., and U.S.R Murty. 2008. *Graph Theory: Graduate Texts in Mathematics.* Springer.

Braunger, I, and C. Hauenstein. 2020. "How Incumbent Cultural and Cognitive Path Dependencies Constrain the 'Scenario Cone': Reliance on Carbon Dioxide Removal due to Techno-bias." *Economics of Energy & Environmental Policy* 9 (1). doi: 10.5547/2160-5890.9.1.ibra.

Braunreiter, L., and Y. B. Blumer. 2018. "Of sailors and divers: How researchers use energy scenarios." *Energy Research & Social Science* 40:118–126. doi: 10.1016/j.erss.2017.12.003.

Braunreiter, L., M. Stauffacher, and Y. B. Blumer. 2020. "How the public imagines the energy future: Exploring and clustering non-experts' techno-economic expectations towards the future energy system." *PLOS ONE* 15 (3): 1–20. doi: 10.1371/journal.pone.0227369.

Brown, T., J. Hörsch, and D. Schlachtberger. 2018. "PyPSA: Python for Power System Analysis." *Journal of Open Research Software* 6, no. 4 (1). doi: 10.5334/jors.188. eprint: 1707.09913. 10.5334/jors.188.

Brown, T., D. Schlachtberger, A. Kies, S. Schramm, and M. Greiner. 2018. "Synergies of sector coupling and transmission extension in a cost-optimised, highly renewable European energy system." *Renewable and Sustainable Energy Reviews* 160:720–739. doi: 10.1016/j.energy.2018.06.222.

Brown, T.W., T. Bischof-Niemz, K. Blok, C. Breyer, H. Lund, and B.V. Mathiesen. 2018. "Response to 'Burden of proof: A comprehensive review of the feasibility of 100% renewable-electricity systems'." *Renewable and Sustainable Energy Reviews* 92:834–847. doi: 10.1016/j.rser.2018.04.113.

Buchholz, S., M. Gamst, and D. Pisinger. 2019. "A comparative study of time aggregation techniques in relation to power capacity expansion modeling." *TOP* 27:353–405. doi: 10.1007/s11750-019-00519-z.

———. 2020. "Finding a Portfolio of Near-Optimal Aggregated Solutions to Capacity Expansion Energy System Models." *SN Operations Research Forum* 1 (1): 1–40.

Bundesministerium für Verkehr und digitale Infrastruktur. 2015. "Räumlich differenzierte Flächenpotentiale für erneuerbare Energien in Deutschland." *BMVI-Online-Publikation* 8. https://www.bbsr.bund.de/BBSR/DE/veroeffentlichungen/ministerien/bmvi/bmvi-online/2015/BMVI_Online_08_15.html.

Burre, J., D. Bongartz, L. Brée, K. Roh, and A. Mitsos. 2020. "Power-to-X: Between Electricity Storage, e-Production, and Demand Side Management." *Chemie Ingenieur Technik* 92:74–84. doi: 10.1002/cite.201900102.

Carbon Brief. 2020. *Coronavirus: Tracking how the world's 'green recovery' plans aim to cut emissions.* https://www.carbonbrief.org/coronavirus-tracking-how-the-worlds-green-recovery-plans-aim-to-cut-emissions.

Carbon Brief. 2021. *Exceptional new normal: IEA raises growth forecast for wind and solar by another 25%.* https://www.carbonbrief.org/exceptional-new-normal-iea-raises-growth-forecast-for-wind-and-solar-by-another-25.

Carrington, G., and J. Stephenson. 2018. "The politics of energy scenarios: Are International Energy Agency and other conservative projections hampering the renewable energy transition?" *Energy Research & Social Science* 46:103–113. doi: 10.1016/j.erss.2018.07.011.

Clark II, W. W., and X. Li. 2013. "The Political-Economics of the Green Industrial Revolution: Renewable Energy as the Key to National Sustainable Communities." Chap. 21 in *Renewable Energy Governance Complexities and Challenges,* edited by E. Michalena and J. M. Hills, 363–385. Springer London.

Clarke, L. 2014. "The Origins of Nuclear Power: A Case of Institutional Conflict." *Social Problems* 32 (5): 474–487. doi: 10.2307/800776.

Cohen, Stuart M., Jonathon Becker, David A. Bielen, Maxwell Brown, Wesley J. Cole, Kelly P. Eurek, Allister Frazier, Bethany A. Frew, Pieter J. Gagnon, Jonathan L. Ho, Paige Jadun, Trieu T. Mai, Matthew Mowers, Caitlin Murphy, Andrew Reimers, James Richards, Nicole Ryan, Evangelia Spyrou, Daniel C. Steinberg, Yinong Sun, Nina M. Vincent, and Matthew Zwerling. 2019. *Regional Energy Deployment System (ReEDS) Model Documentation: Version 2018.* doi: 10.2172/1505935. https://www.osti.gov/biblio/1505935.

Collins, S., J.P. Deane, K. Poncelet, E. Panos, R.C. Pietzcker, E. Delarue, and B.P. Ó Gallachóir. 2017. "Integrating short term variations of the power system into integrated energy system models: A methodological review." *Renewable and Sustainable Energy Reviews* 76:839–856. doi: 10.1016/j.rser.2017.03.090.

Conejo, A.J., E. Castillo, R. Minguez, and R. Garcia-Bertrand. 2006. *Decomposition Techniques in Mathematical Programming: Engineering and Science Applications.* Springer.

Copernicus Programme. 2020. *CORINE Land Cover data 2012-2018.* https://land.copernicus.eu/.

Craig, P. P., A. Gadgil, and J. G. Koomey. 2002. "What Can History Teach Us? A Retrospective Examination of Long-Term Energy Forecasts for the United States." *Annual Review of Energy and the Environment* 27 (1): 83–118. doi: 10.1146/annurev.energy.27.122001.083425.

Deane, J.P., G. Drayton, and B.P. Ó Gallachóir. 2014. "The impact of sub-hourly modelling in power systems with significant levels of renewable generation." *Applied Energy* 113:152–158. doi: 10.1016/j.apenergy.2013.07.027.

DeCarolis, J., P. Jaramillo, J. Johnson, D. McCollum, E. Trutnevyte, D. Daniels, G. Akın-Olçum, J. Bergerson, S. Cho, J.-H. Choi, M. Craig, A. de Queiroz, H. Eshraghi, C. Galik, T. Gutowski, K. Haapala, B.-M. Hodge, S. Hoque, J. Jenkins, A. Jenn, D. Johansson, N. Kaufman, J. Kiviluoma, Z. Lin, H. MacLean, E. Masanet, M. Masnadi, C. McMillan, D. Nock, N. Patankar, D. Patino-Echeverri, G. Schively, S. Siddiqui, A. Smith, A. Venkatesh, G. Wagner, S. Yeh, and Y. Yuyu Zhou. 2020. "Macro-Energy Systems: Toward a New Discipline." *Joule* 4:1–4. doi: 10.1016/j.joule.2020.11.002.

Diestel, R. 2000. *Graph Theory: Graduate Texts in Mathematics.* Springer.

Doucette, R.T., and M.D. McCulloch. 2011. "Modeling the CO_2 emissions from battery electric vehicles given the power generation mixes of different countries." *Energy Policy* 39:803–811. doi: 10.1016/j.enpol.2010.10.054.

Drechsler, Martin, Jonas Egerer, Martin Lange, Frank Masurowski, Jürgen Meyerhoff, and Malte Oehlmann. 2017. "Efficient and equitable spatial allocation of renewable power plants at the country scale." *Nature Energy* 2:17124. doi: 10.1038/nenergy.2017.124.

Dunning, I., J. Huchette, and M. Lubin. 2017. "JuMP: A Modeling Language for Mathematical Optimization." *SIAM Review* 59(2):295–320. doi: 10.1137/15M1020575.

E4SMA. 2021. *The JRC-EU-TIMES model now open source!* https://www.e4sma.com/en/jrc-eu-times_opening/.

Edenhofer, O., R. Pichs-Madruga, Y. Sokona, E. Farahani, S. Kadner, K. Seyboth, A. Adler, I. Baum, S. Brunner, P. Eickemeier, B. Kriemann, J. Savolainen, S. Schlömer, C. von Stechow, T. Zwickel, and J.C. Minx. 2014. *Climate Change 2014: Mitigation of Climate Change. Contribution of Working Group III to the Fifth Assessment Report of the Intergovernmental Panel on Climate Change.* Cambridge, United Kingdom and New York, NY, USA: Cambridge University Press.

Elsner, P., and D.U. Sauer. 2015. "Energiespeicher, Technologiesteckbrief zur Analyse „Flexibilitätskonzepte für die Stromversorgung 2050"." *Energiesysteme der Zukunft.*

ENTSO-E. 2020. *Completing the map - Power system needs in 2030 and 2040.* Technical report. https://www.entsoe.eu/Documents/TYNDP%5C%20documents/TYNDP2018/european_power_system_2040.pdf.

ENTSO-E. 2020. *TYNDP 2020 - Main Report.* Technical report. European Network of Transmission System Operators for Electricity. https://consultations.entsoe.eu/system-development/tyndp2020/.

Ergen, T. 2015. "Große Hoffnungen und brüchige Koalitionen: Industrie, Politik und die schwierige Durchsetzung der Photovoltaik." *Schriften aus dem Max-Planck-Institut für Gesellschaftsforschung Köln* 83.

eurostat. 2020a. *Population on 1 January by NUTS 2 region.* https://ec.europa.eu/eurostat/web/products-datasets/-/tgs00096.

eurostat. 2020b. *Regional gross domestic product (million PPS) by NUTS 2 regions.* https://ec.europa.eu/eurostat/web/products-datasets/-/tgs00004.

Fahy, K., M. Stadler, Z.K. Pecenak, and J. Kleissl. 2019. "Input data reduction for microgrid sizing and energy cost modeling: Representative days and demand charges." *Journal of Renewable and Sustainable Energy* 11:065301. doi: 10.1063/1.5121319.

Fattahi, A., M. Sánchez Diéguez, J. Sijm, G. Morales España, and A. Faaij. 2021. "Measuring accuracy and computational capacity trade-offs in an hourly integrated energy system model." *Advances in Applied Energy* 1:100009. doi: 10.1016/j.adapen.2021.100009.

Febles, E. A. 2008. "The Anarchic Commune as World's Fair in Émile Zola's "Travail"." *Nineteenth-Century French Studies* 36 (3/4): 286–304.

Fleiter, T., R. Elsland, M. Rehfeldt, J. Steinbach, U. Reiter, G. Catenazzi, M. Jakob, C. Rutten, R. Harmsen, F. Dittmann, P. Rivière, and P. Stabat. 2017. "Profile of heating and cooling demand in 2015." *Heat Roadmap Europe.*

Frysztacki, M.M., J. Hörsch, V. Hagenmeyer, and T. Brown. 2021. "The strong effect of network resolution on electricity system models with high shares of wind and solar." *Applied Energy* 291:116726. doi: 10.1016/j.apenergy.2021.116726.

Galvin, R., and N. Healy. 2020. "The Green New Deal in the United States: What it is and how to pay for it." *Energy Research & Social Science* 67:101529. doi: 10.1016/j.erss.2020.101529.

Gerbaulet, C., C. v. Hirschhausen, C. Kemfert, C. Lorenz, and P.Y. Oei. 2019. "European electricity sector decarbonization under different levels of foresight." *Renewable Energy* 141:973–987. doi: 10.1016/j.renene.2019.02.099.

Gerbaulet, C., and C. Lorenz. 2017. "dynELMOD: A Dynamic Investment and Dispatch Model for the Future European Electricity Market." *DIW Data Documentation 88.*

Gierkink, M., and T. Sprenger. 2020. *Die Auswirkungen des Klimaschutzprogramms 2030 auf den Anteil erneuerbarer Energien an der Stromnachfrage.* Technical report. Energiewirtschaftliches Institut an der Universität zu Köln. https://www.ewi.uni-koeln.de/de/aktuelles/ee-ziel-2030/.

Göke, L. 2021a. "A graph-based formulation for modeling macro-energy systems." *Applied Energy* 301:117377. doi: 10.1016/j.apenergy.2021.117377.

———. 2021b. "AnyMOD.jl: A Julia package for creating energy system models." *SoftwareX* 16:100871. doi: 10.1016/j.softx.2021.100871.

Göke, L., and M. Kendziorski. 2021. "The adequacy of time-series reduction for renewable energy systems." *Energy* 238:121701. doi: 10.1016/j.energy.2021.121701.

Göke, L., D. Poli, and J. Weibezahn. 2019. "Current and Perspective Technology and Cost Data of Flexibility Options." *OSMOSE Project EU Horizon 2020.*

GOV.UK. 2020. *PM outlines his Ten Point Plan for a Green Industrial Revolution for 250,000 jobs.* https://www.gov.uk/government/news/pm-outlines-his-ten-point-plan-for-a-green-industrial-revolution-for-250000-jobs.

Govorukha, K., P. Mayer, D. Rübbelke, and S. Vögele. 2020. "Economic disruptions in long-term energy scenarios – Implications for designing energy policy." *Energy* 212:118737. doi: 10.1016/j.energy.2020.118737.

Grimm, V., B. Rückel, C. Sölch, and G. Zöttl. 2016. "Zur Reduktion des Netzausbaubedarfs durch Redispatch und effizientes Einspeisemanagement: Eine modellbasierte Abschätzung." *List Forum* 41:465–498. doi: 10.1007/s41025-016-0027-5.

Groissböck, M. 2019. "Are open source energy system optimization tools mature enough for serious use?" *Renewable and Sustainable Energy Reviews* 102:234–248. doi: 10.1016/j.rser.2018.11.020.

Growitsch, C., R. Malischek, S. Nick, and H. Wetzel. 2013. "The Costs of Power Interruptions in Germany - an Assessment in the Light of the Energiewende." *EWI working paper* 13(7).

Grunwald, A. 2011. "Energy futures: Diversity and the need for assessment." *Futures* 43 (8): 820–830. doi: 10.1016/j.futures.2011.05.024.

Häfele, W., J. Anderer, A. McDonald, and N. Nakicenovic. 1981. *Energy in a Finite World: Paths to a Sustainable Future (Volume 1).* Vol. 1. Cambridge, MA: Ballinger.

Häfele, W., and H. H. Rogner. 1986. "A technical appraisal of the IIASA energy scenarios? A rebuttal." *Policy Sciences* 17:341–365. doi: 10.1007/BF00138400.

Hainsch, K., L. Göke, C. Kemfert, P.-Y. Oei, and C. v. Hirschhausen. 2020. "European Green Deal: Using Ambitious Climate Targets and Renewable Energy to Climb Out of the Economic Crisis." *DIW Weekly Report* 28+29. doi: 10.18723/diw_dwr:2020-28-1.

Hammond, A. L. 1977. ""Soft Technology" Energy Debate: Limits to Growth Revisited?" *Science* 196 (4293): 959–961. doi: 10.1126/science.196.4293.959.

Hansen, K., C. Breyer, and H. Lund. 2019. "Status and perspectives on 100% renewable energy systems." *Energy* 175:471–480. doi: 10.1016/j.energy.2019.03.092.

Harvey, S. M., and W. Hogan. 2000. "Nodal and zonal congestion management and the exercise of market power." *Harvard University,* 21.

Hauser, P. 2019. "A modelling approach for the German gas grid using highly resolved spatial, temporal and sectoral data (GAMAMOD-DE)." *EconStor Preprints,* https://ideas.repec.org/p/zbw/esprep/197000.html.

Haydt, G., V. Leal, A. Pina, and C.A. Silva. 2011. "The relevance of the energy resource dynamics in the mid/long-term energy planning models." *Renewable Energy* 36:3068–3074. doi: 10.1016/j.renene.2011.03.028.

Heggarty, T., J.-Y. Bourmaud, R. Girard, and G. Kariniotakis. 2019. "Multi-temporal assessment of power system flexibility requirement." *Applied Energy* 238:1327–1336. doi: 10.1016/j.apenergy.2019.01.198.

Hilbers, A. P., D. J. Brayshaw, and A Gandy. 2021. "Efficient quantification of the impact of demand and weather uncertainty in power system models." *IEEE Transactions on Power Systems* 36 (3): 1771–1779. doi: 10.1109/TPWRS.2020.3031187.

Hilbers, A.P., D.J. Brayshaw, and A. Gandy. 2019. "Importance subsampling: improving power system planning under climate-based uncertainty." *Applied Energy* 251:113114. doi: 10.1016/j.apenergy.2019.04.110.

Hirschhausen, C. v., C. Gerbaulet, C. Kemfert, C. Lorenz, and P.-Y. Oei, eds. 2018. *Energiewende "Made in Germany": low carbon electricity sector reform in the European context.* Cham, Switzerland: Springer. doi: 10.1007/978-3-319-95126-3.

Hoffmann, M., L. Kotzur, D. Stolten, and M. Robinius. 2020. "A Review on Time Series Aggregation Methods for Energy System Models." *energies* 13(3):641. doi: 10.3390/en13030641.

Hohmeyer, O. H., and S. Bohm. 2015. "Trends toward 100% renewable electricity supply in Germany and Europe: a paradigm shift in energy policies." *Wiley Interdisciplinary Reviews: Energy and Environment* 4:74–97. doi: 10.1002/wene.128.

Howells, M., H. Rogner, N. Strachan, C. Heaps, H. Huntington, S. Kypreos, A. Hughes, S. Silveira, J. DeCarolis, M. Bazillian, and A. Roehrl. 2011. "OSeMOSYS: The Open Source Energy Modeling System: An introduction to its ethos, structure and development." *Energy Policy* 39(10):5850–5870. doi: 10.1016/j.enpol.2011.06.033.

Hughes, L., and P. Y. Lipscy. 2013. "The Politics of Energy." *Annual Review of Political Science* 16:449–469. doi: 10.1146/annurev-polisci-072211-143240.

Hughes, T. P. 1993. *Networks of Power: Electrification in Western Society, 1880-1930.* Johns Hopkins University Press.

International Energy Agency. 2021. *World Energy Outlook - The gold standard of energy analysis.* Paris, OECD. https://www.iea.org/topics/world-energy-outlook.

Jackson, G. 2017. "A Future for Capitalism - Jens Beckert, Imagined Futures. Fictional Expectations and Capitalist Dynamics (Cambridge, MA, Harvard University Press, 2016)." *European Journal of Sociology* 58 (3): 460–467. doi: 10.1017/S0003975617000236.

Jacobson, M. Z., M. A. Delucchi, Z.A.F. Bauer, S.C. Goodman, W.E. Chapman, M.A. Cameron, C. Bozonnat, L. Chobadi, H.A. Clonts, P. Enevoldsen, J.R. Erwin, S.N. Fobi, O.K. Goldstrom, E.M. Hennessy, J. Liu, J. Lo, C.B. Meyer, S.B. Morris, K.R. Moy, P.L. O'Neill, P.I. Petkov, S. Redfern, R. Schucker, M.A. Sontag, J. Wang, E. Weiner, and A.S. Yachanin. 2017. "100 % Clean and Renewable Wind, Water, and Sunlight All-Sector Energy Roadmaps for 139 Countries of the World." *Joule* 1:108–121. doi: 10.1016/j.joule.2017.07.005.

Janda, K. B., and M. Topouzi. 2015. "Telling tales: using stories to remake energy policy." *Building Research & Information* 43 (4): 516–533. doi: 10.1080/09613218.2015.1020217.

Jänicke, M., and K. Jacob. 2009. "A Third Industrial Revolution? Solutions to the Crisis of Resource-Intensive Growth." *FFU-Report* 2.

Jenkins, J.D., M. Luke, and S. Thernstrom. 2018. "Getting to Zero Carbon Emissions in the Electric Power Sector." *Joule* 2:2487–2510. doi: 10.1016/j.joule.2018.11.013.

Jevons, W. S. 1865. *The Coal Question.* London.

Johnston, J., R. Henriquez-Auba, B. Maluenda, and M. Fripp. 2019. "Switch 2.0: A modern platform for planning high-renewable power systems." *Software X* 10:100251. doi: 10.1016/j.softx.2019.100251.

Joint Research Centre of the European Commission. 2014. "Energy Technology Reference Indicator projections for 2010-2050." *JRC Science and Policy Reports,* https://setis.ec.europa.eu/publications/relevant-reports/etri-2014.

Junne, T., M. Xiao, L. Xu, Z. Wang, P. Jochem, and T. Pregger. 2019. "How to assess the quality and transparency of energy scenarios: Results of a case study." *Energy Strategy Reviews* 26:100380. doi: 10.1016/j.esr.2019.100380.

Kainiemi, L., K. Karhunmaa, and S. Eloneva. 2020. "Renovation realities: Actors, institutional work and the struggle to transform Finnish energy policy." *Energy Research & Social Science* 70:101778. doi: 10.1016/j.erss.2020.101778.

Kannan, R. 2011. "The development and application of a temporal MARKAL energy system model using flexible time slicing." *Applied Energy* 88(6):2261–2272. doi: 10.1016/j.apenergy.2010.12.066.

Kapoor, N. 2019. ""Who Has Seen the Wind": Imagining Wind Power for the Generation of Electricity in Victorian Britain." *Technology and Culture* 60:467–493.

Keepin, B., and B. Wynne. 1984. "Technical analysis of IIASA energy scenarios." *Nature* 312 (5996): 691. doi: 10.1038/312691a0.

Kemfert, K., F. Kunz, and J. Rosellón. 2016. "A welfare analysis of electricity transmission planning in Germany." *Energy Policy* 94:446–452. doi: 10.1016/j.enpol.2016.04.011.

Kendziorski, M., L. Göke, C. Kemfert, and C. v. Hirschhausen. 2021. "100% Renewable Energy for Germany: Coordinated Expansion Planning Needed." *DIW Weekly Report* 29+30. doi: 10.18723/diw_wb:2021-29-1.

Knosala, K., L. Kotzur, F. T.C Röben, P. Stenzel, L. Blum, M. Robinius, and D. Stolten. 2021. "Hybrid Hydrogen Home Storage for Decentralized Energy Autonomy." *International Journal of Hydrogen Energy* 46 (42): 21748–21763. doi: 10.1016/j.ijhydene.2021.04.036.

Kondziella, H., and T. Bruckner. 2016. "Flexibility requirements of renewable energy based electricity systems – a review of research results and methodologies." *Renewable and Sustainable Energy Reviews* 53:10–22. doi: 10.1016/j.rser.2015.07.199.

Kost, C., S. Shammugam, V. Jüluch, H.-T. Nguyen, and T. Schlegl. 2018. "Stromgestehungskosten Erneuerbare Energien." *Fraunhofer-Institut für Solare Energiesysteme ISE, Freiburg.*

Kotzur, L., P. Markewitz, M. Robinius, and D. Stolten. 2018a. "Impact of different time series aggregation methods on optimal energy system design." *Renewable Energy* 117:474–487. doi: 10.1016/j.renene.2017.10.017.

Kotzur, L., P. Markewitz, M. Robinius, and D. Stolten. 2018b. "Time series aggregation for energy system design: Modeling seasonal storage." *Applied Energy* 213:123–135. doi: 10.1016/j.apenergy.2018.01.023.

Krause, F., H. Bossel, and K.-F. Müller-Reissmann. 1980. *Energie-Wende: Wachstum und Wohlstand ohne Erdöl und Uran.* Frankfurt am Main, Germany: S. Fischer.

Kunz, F., M. Kendziorski, W.-P. Schill, J. Weibezahn, J. Zepter, C. Hirschhausen, P. Hauser, M. Zech, D. Möst, S. Heidari, B. Felten, and C. Weber. 2017. "Electricity, Heat and Gas Sector Data for Modelling the German System." *DIW Data Documentation* 92. doi: 10.5281/zenodo.1044463.

Laes, E., L. Gorissen, and F. Nevens. 2014. "A Comparison of Energy Transition Governance in Germany, The Netherlands and the United Kingdom." *Sustainability* 6 (3): 1129–1152. doi: 10.3390/su6031129.

Landis, F., A. Marcucci, S. Rausch, R. Kannan, and L. Bretschger. 2019. "Multi-model comparison of Swiss decarbonization scenarios." *Swiss Journal of Economics and Statistics* 155 (12). doi: 10.1186/s41937-019-0040-8.

Leahy, E., and R. S.J. Tol. 2011. "An estimate of the value of lost load for Ireland." *Energy Policy* 39(3):1514–1520. doi: 10.1016/j.enpol.2010.12.025.

Leuthold, F., H. Weigt, and C. v. Hirschhausen. 2012. "A Large-Scale Spatial Optimization Model of the European Electricity Market." *Networks and Spatial Economics* 12 (1): 75–107. doi: 10.1007/s11067-010-9148-1.

Levi, P.J., S.D. Kurland, M. Carbajales-Dale, J.P. Weyant, A.-R. Brandt, and S.M. Benson. 2019. "Macro-Energy Systems: Toward a New Discipline." *Joule* 3:2282–2286. doi: 10.1016/j.joule.2019.07.017.

Lödl, M., G. Kerber, R. Witzmann, C. Hoffmann, and M. Metzger. 2010. "Abschätzung des Photovoltaik-Potentials auf Dachflächen in Deutschland." *Symposium Energieinnovation, 10.-12.2.2010, Graz/Austria.*

Löffler, K., T. Burandt, K. Hainsch, and P.Y. Oei. 2019. "Modeling the low-carbon transition of the European energy system - A quantitative assessment of the stranded assets problem." *Energy Strategy Reviews* 26:100422. doi: 10.1016/j.esr.2019.100422.

Lopion, P., P. Markewitz, M. Robinius, and D. Stolten. 2018. "A review of current challenges and trends in energy systems modeling." *Renewable and Sustainable Energy Reviews* 96:156–166. doi: 10.1016/j.rser.2018.07.045.

Lopion, P., P. Markewitz, D. Stolten, and M. Robinius. 2019. "Cost Uncertainties in Energy System Optimization Models: A Quadratic Programming Approach for Avoiding Penny Switching Effects." *Energies* 12 (20). doi: 10.3390/en12204006.

Loulou, R., A. Lehtilä, A. Kanudia, U. Remme, and G. Goldstein. 2016. "Documentation for the TIMES Model, Part 2." *Energy Technology Systems Analysis Programme,* http://www.iea-etsap.org/web/Documentation.asp.

Lovins, A. B. 1976. "Energy Strategy: The Road Not Taken?" *Foreign Affairs* 6 (20): 9–19.

Lund, H., N. Duić, G. Krajacic, and M. da Graca Carvalho. 2007. "Two energy system analysis models: A comparison of methodologies and results." *Energy* 32 (6): 948–954. doi: 10.1016/j.energy.2006.10.014.

Lund, P.D., J. Lindgren, J. Mikkola, and J. Salpakari. 2015. "Review of energy system flexibility measures to enable high levels of variable renewable electricity." *Renewable and Sustainable Energy Reviews* 45:785–807. doi: 10.1016/j.rser.2015.01.057.

Mainzer, K., K. Fath, R. McKenna, J. Stengel, W. Fichtner, and F. Schultmann. 2014. "A high-resolution determination of the technical potential for residential-roof-mounted photovoltaic systems in Germany." *Solar Energy* 105:715–731. doi: 10.1016/j.solener.2014.04.015.

Mallapragada, D.S., D.J. Papageorgiou, A. Venkatesh, C.L. Lara, and I.E. Grossmann. 2018. "Impact of model resolution on scenario outcomes for electricity sector system expansion." *Energy* 163(15):1231–1244. doi: 10.1016/j.energy.2018.08.015..

Martínez-Gordón, R., G. Morales-España, J. Sijm, and A.P.C. Faaij. 2021. "A review of the role of spatial resolution in energy systems modelling: Lessons learned and applicability to the North Sea region." *Renewable and Sustainable Energy Reviews* 141:110857. doi: 10.1016/j.rser.2021.110857.

Martinot, E., C. Dienst, L. Weiliang, and C. Qimin. 2007. "Renewable Energy Futures: Targets, Scenarios, and Pathways." *Annual Review of Environment and Resources* 32 (1): 205–239. doi: 10.1146/annurev.energy.32.080106.133554.

Masurowski, F. 2016. "Eine deutschlandweite Potenzialanalyse für die Onshore-Windenergie mittels GIS einschließlich der Bewertung von Siedlungsdistanzenänderungen." PhD diss., Universität Osnabrück, Fachbereich Mathematik/Informatik. https://repositorium.ub.uni-osnabrueck.de/handle/urn:nbn:de:gbv:700-2016071114613.

Merrick, J.H. 2016. "On Representation of Temporal Variability in Electricity Capacity Planning Models." *Energy Economics* 59:261–274. doi: 10.1016/j.eneco.2016.08.001.

Metayer, M., C. Breyer, and H.-J. Fell. 2015. "The projections for the future and quality in the past of the World Energy Outlook for solar PV and other renewable energy technologies." In *31st European PV Solar Energy Conference and Exhibition.*

Midttun, A., and T. Baumgartner. 1986. "Negotiating Energy Futures: The Politics of Energy Forecasting." *Energy Policy* 14 (3): 219–241. doi: 10.1016/0301-4215(86)90145-X.

Miller, C. A., J. O'Leary, E. Graffy, E. B. Stechel, and G. Dirks. 2015. "Narrative futures and the governance of energy transitions." *Futures* 70:65–74. doi: 10.1016/j.futures.2014.12.001.

Moezzi, M., K. B. Janda, and S. Rotmann. 2017. "Using stories, narratives, and storytelling in energy and climate change research." *Energy Research & Social Science* 31:1–10. doi: 10.1016/j.erss.2017.06.034.

Morrison, R. 2018. "Energy system modeling: Public transparency, scientific reproducibility, and open development." *Energy Strategy Reviews* 20:49–63. doi: 10.1016/j.esr.2017.12.010.

Nahmmacher, P., E. Schmid, L. Hirth, and B. Knopf. 2016. "Carpe diem: A novel approach to select representative days for longterm power system modeling." *Energy* 112:430–442. doi: 10.1016/j.energy.2016.06.081.

Nahmmacher, P., E. Schmid, and B. Knopf. 2014. "Documentation of LIMES-EU - A long-term electricity system model for Europe." *Working Paper,* https://www.pik-potsdam.de/en/institute/departments/transformation-pathways/models/limes/Documentation LIMESEU_2014.pdf.

Neumann, F., V. Hagenmeyer, and T. Brown. 2020. "Approximating Power Flow and Transmission Losses in Coordinated Capacity Expansion Problems." *Working Paper,* https://arxiv.org/abs/2008.11510.

Neumann, T., and T. Brown. 2021. "The Near-Optimal Feasible Space of a Renewable Power System Model." *Electric Power Systems Research* 190:106690. doi: 10.1016/j.epsr.2020.106690.

"Vast Power of the Sun Is Tapped by Battery Using Sand Ingredient." 1954. *New York Times.*

Nielsen, S. K., and K. B. Karlsson. 2007. "Energy scenarios: A review of methods, uses and suggestions for improvement." *International Journal of Global Energy Issues* 27:302–322. doi: 10.1504/IJGEI.2007.014350.

Nikas, A., J. Lieu, A. Sorman, A. Gambhir, E. Turhan, B. V. Baptista, and H. Doukas. 2020. "The desirability of transitions in demand: Incorporating behavioural and societal transformations into energy modelling." *Energy Research & Social Science* 70:101780. doi: 10.1016/j.erss.2020.101780.

Nørgård, J. S. 2000. "Models of energy saving systems: the battlefield of environmental planning." *International Journal of Global Energy Issues* 13 (1/2/3): 102–122. doi: 10.1504/IJGEI.2000.000867.

Oberle, S., and R. Elsland. 2019. "Are open access models able to assess today's energy scenarios?" *Energy Strategy Reviews* 26:100396. doi: 10.1016/j.esr.2019.100396.

Oei, P.-Y., T. Burandt, K. Hainsch, K. Löffler, and C. Kemfert. 2020. "Lessons from Modeling 100% Renewable Scenarios Using GENeSYS-MOD." *Economics of Energy & Environmental Policy* 9 (1). doi: 10.5547/2160-5890.9.1.poei.

Oei, P.-Y., L. Göke, C. Kemfert, M. Kendziorski, and C. von Hirschhausen. 2019. "Erneuerbare Energien als Schlüssel für das Erreichen der Klimaschutzziele im Stromsektor." *Politikberatung Kompakt* 133. https://www.diw.de/de/diw_01.c.616185.de/publikationen/politikberatung_kompakt/2019_0133/erneuerbare_energien_als_schluessel_fuer_das_erreichen_der_k____ie_im_auftrag_der_bundestagsfraktion_buendnis_90/die_gruenen.html.

Ohlendorf, N., and W.-P. Schill. 2020. "Frequency and duration of low-wind-power events in Germany." *Environmental Research Letters* 15:084045.

Orths, A., C.L. Anderson, T. Brown, J. Mulhern, D. Pudjianto, B. Ernst, M. O'Malley, J. McCalley, and G. Strbac. 2019. "Flexibility From Energy Systems Integration: Supporting Synergies Among Sectors." *IEEE Power and Energy Magazine* 17(6):67–87. doi: 10.1109/MPE.2019.2931054.

Paltsev, S. 2017. "Energy scenarios: the value and limits of scenario analysis." *Wiley Interdisciplinary Reviews: Energy and Environment* 6. doi: 10.1002/wene.242.

Pavičevića, M., A. Mangipinto, W. Nijs, F. Lombardi, K. Kavvadias, J.P.J Navarro, E. Colombo, and S. Quoilin. 2020. "The potential of sector coupling in future European energy systems: Soft linking between the Dispa-SET and JRC-EU-TIMES models." *Applied Energy* 267:9115100. doi: 10.1016/j.apenergy.2020.115100.

Pedersen, T. T., M. Victoria, M. G. Rasmussen, and G. B. Andresen. 2021. "Modeling all alternative solutions for highly renewable energy systems." *Energy* 234:121294. doi: 10.1016/j.energy.2021.121294.

Petrovic, B., H. Rogers, H. Hecking, S. Schulte, and F. Weiser. 2017. "Future European Gas Transmission Bottlenecks in Differing Supply and Demand Scenarios." *Oxford Institute for Energy Studies* 119. https://ora.ox.ac.uk/objects/uuid:9486b8a3-2c4c-4991-a4ef-c4cd27cf928f.

Pfenniger, S., J. DeCarolis, L. Hirth, S. Quoilin, and I. Staffel. 2017. "The importance of open data and software: Is energy research lagging behind?" *Energy Policy* 101:211–215. doi: 10.1016/j.enpol.2016.11.046.

Pfenniger, S., and B. Pickering. 2018. "Calliope: a multi-scale energy systems modelling." *The Journal of Open Source Software* 3(29):825. doi: 10.21105/joss.00825.

Pfenninger, S. 2017. "Dealing with multiple decades of hourly wind and PV time series in energy models: A comparison of methods to reduce time resolution and the planning implications of inter-annual variability." *Applied Energy* 197:1–13. doi: 10.1016/j.apenergy.2017.03.051.

Pfenninger, S., A. Hawkes, and J. Keirstead. 2014. "Energy systems modeling for twenty-first century energy challenges." *Renewable and Sustainable Energy Reviews* 33:74–86. doi: 10.1016/j.rser.2014.02.003.

Pfenninger, S., B. Pickering, T. Tröndle, M. Garchery, G. Hawker, and F. Lombardi. 2020. *Calliope Documentation Release 0.6.5.* https://readthedocs.org/projects/calliope/.

Pfenninger, S., and I. Staffell. 2016. "Long-term patterns of European PV output using 30 years of validated hourly reanalysis and satellite data." *Energy* 114:1251–1265. doi: 10.1016/j.energy.2016.08.060.

Poncelet, K., E. Delarue, D. Six, J. Duerinck, and W. D'haeseleer. 2016a. "Impact of the level of temporal and operational detail in energy-system planning models." *Applied Energy* 162:631–643. doi: 10.1016/j.apenergy.2015.10.100.

Poncelet, K., H. Höschle, E. Delarue, A. Virag, and D'haeseleer. W. 2016b. "Selecting Representative Days for Capturing the Implications of Integrating Intermittent Renewables in Generation Expansion Planning Problems." *IEEE Transactions on Power Systems* 32(3):1936–1948. doi: 10.1109/TPWRS.2016.2596803.

Praktiknjo, A.J., A. Hähnel, and G. Erdmann. 2011. "Assessing energy supply security: Outage costs in private households." *Energy Policy* 39(12):7825–7833. doi: 10.1016/j.enpol.2011.09.028.

Raventós, O., and J. Bartels. 2020. "Evaluation of Temporal Complexity Reduction Techniques Applied to Storage Expansion Planning in Power System Models." *energies* 13:988. doi: 10.3390/en13040988.

Rehfeldt, D., H. Hobbie, D. Schönheit, T. Koch, D. Möst, and A. Gleixner. 2021. "A massively parallel interior-point solver for LPs with generalized arrowhead structure, and applications to energy system models." *European Journal of Operational Research,* doi: 10.1016/j.ejor.2021.06.063.

Reichenberg, L., A.S. Siddiqui, and S. Wogrin. 2018. "Policy implications of downscaling the time dimension in power system planning models to represent variability in renewable output." *Energy* 159:870–877. doi: 10.1016/j.energy.2018.06.160.

Renaldi, R., and D. Friedrich. 2017. "Multiple time grids in operational optimisation of energy systems with short- and long-term thermal energy storage." *Energy* 133:784–795. doi: 10.1016/j.energy.2017.05.120.

Ringkjøb, H.K., P.M. Haugan, and I.M. Solbrekke. 2018. "A review of modelling tools for energy and electricity systems with large shares of variable renewables." *Renewable and Sustainable Energy Reviews* 96:440–459. doi: 10.1016/j.rser.2018.08.002.

Ritchie, H., and M. Roser. 2020. *Energy.* https://ourworldindata.org/energy.

Robinius, M., P. Markewitz, P. Lopion, F. Kullmann, P.-M. Heuser, K. Syranidis, S. Cerniauskas, T. Schöb, M. Reuß, S. Ryberg, L. Kotzur, D. Caglayan, L. Welder, J. Linßen, T. Grube, H. Heinrichs, P. Stenzel, and D. Stolten. 2020. "Wege für die Energiewende - Kosteneffiziente und klimagerechte Transformationsstrategien für das deutsche Energiesystem bis zum Jahr 2050." *Energy & Environment* 499.

Roser, M. 2020. *Why did renewables become so cheap so fast? And what can we do to use this global opportunity for green growth?* https://ourworldindata.org/cheap-renewables-growth.

Schill, W.P. 2020. "Electricity Storage and the Renewable Energy Transition." *Joule* 4:2047–2064. doi: 10.1016/j.joule.2020.07.022.

Schmidt-Scheele, R. 2020. "'Plausible' energy scenarios?! How users of scenarios assess uncertain futures." *Energy Strategy Reviews* 32:100571. doi: 10.1016/j.esr.2020.100571.

Schmitz, K., and A. Voß. 1980. "Energiewende? : Analysen, Fragen und Anmerkungen zu dem vom ÖKO-Institut vorgelegten "Alternativ-Bericht"." *Aktuelle Beiträge zur Energiediskussion* 2. doi: 10.18419/opus-8916.

Schopfer, S., V. Tiefenbeck, and T. Staake. 2018. "Economic assessment of photovoltaic battery systems based on household load profiles." *Applied Energy* 223:229–248. doi: 10.1016/j.apenergy.2018.03.185.

Schubert, D. K. J., S. Thuß, and D. Möst. 2015. "Does political and social feasibility matter in energy scenarios?" *Energy Research & Social Science* 7:43–54. doi: 10.1016/j.erss.2015.03.003.

Schütz, T., M.H. Schraven, M. Fuchs, P. Remmen, and D. Müller. 2018. "Comparison of clustering algorithms for the selection of typical demand days for energy system synthesis." *Renewable Energy* 129:570–582. doi: 10.1016/j.renene.2018.06.028.

Scott, I.J., P.M.S Carvalho, A. Botterud, and C.A. Silva. 2019. "Clustering representative days for power systems generation expansion planning: Capturing the effects of variable renewables and energy storage." *Applied Energy* 253:113603. doi: 10.1016/j.apenergy.2019.113603.

Seljom, P., and A. Tomasgarda. 2015. "Short-term uncertainty in long-term energy system models — A case study of wind power in Denmark." *Energy Economics* 49:157–167. doi: 10.1016/j.eneco.2015.02.004.

Senkpiel, C., A. Dobbins, C. Kockel, J. Steinbach, Fahl. U, F. Wille, J. Globisch, S. Wassermann, B. Droste-Franke, W. Hauser, C. Hofer, L. Nolting, and C. Bernath. 2020. "Integrating Methods and Empirical Findings from Social and Behavioural Sciences into Energy System Models—Motivation and Possible Approaches." *Energies* 13 (18). doi: 10.3390/en13184951.

Sepulveda, N.A. 2020. "Decarbonization of Power Systems, Multi-Stage Decision-Making with Policy and Technology Uncertainty." PhD diss., Massachusetts Institute of Technology. Department of Nuclear Science and Engineering. https://hdl.handle.net/1721.1/127311.

Shiller, R.J. 2019. *Narrative Economics: How Stories Go Viral and Drive Major Economic Events.* Princeton University Press.

Sica, C. E., and M. Huber. 2017. ""We Can't Be Dependent on Anybody": The rhetoric of "Energy Independence" and the legitimation of fracking in Pennsylvania." *The Extractive Industries and Society* 4 (2): 337–343. doi: 10.1016/j.exis.2017.02.003.

Silvast, A., E. Laes, S. Abram, and G. Bombaerts. 2020. "What do energy modellers know? An ethnography of epistemic values and knowledge models." *Energy Research & Social Science* 66:101495. doi: 10.1016/j.erss.2020.101495.

Solargis. 2020. *Global Solar Atlas.* https://globalsolaratlas.info.

Sørensen, B. 1975. "Energy and Resources." *Science* 189 (4199): 255–260. doi: 10.1126/science.189.4199.255.

Staffell, I., and S. Pfenninger. 2016. "Using Bias-Corrected Reanalysis to Simulate Current and Future Wind Power Output." *Energy* 114:1224–1239. doi: 10.1016/j.energy.2016.08.068.

Stephens, J. C. 2019. "Energy Democracy: Redistributing Power to the People Through Renewable Transformation." *Environment: Science and Policy for Sustainable Development* 61 (2): 4–13. doi: 10.1080/00139157.2019.1564212.

Sterchele, P., J. Brandes, J. Heilig, D. Wrede, C. Kost, T. Schlegl, A. Bett, and H.-M. Henning. 2020. "Wege zu einem klimaneutralen Energiesystem - Die deutsche Energiewende im Kontext gesellschaftlicher Verhaltensweisen." *Fraunhofer-Institut für Solare Energiesysteme ISE, Freiburg.*

Stern, D. I. 2017. "How accurate are energy intensity projections?" *Climatic Change* 143 (3): 537–545. doi: 10.1007/s10584-017-2003-3.

Stirling, A. 1997. "Limits to the value of external costs." *Energy Policy* 25 (5): 517–540. doi: 10.1016/S0301-4215(97)00041-4.

Taylor, P. G., P. Upham, W. McDowall, and D. Christopherson. 2014. "Energy model, boundary object and societal lens: 35 years of the MARKAL model in the UK." *Energy Research & Social Science* 4:32–41. doi: 10.1016/j.erss.2014.08.007.

Technical University of Denmark. 2020. *Global Wind Atlas.* https://globalwindatlas.info.

Teichgraeber, H., and A.R. Brandt. 2019. "Clustering methods to find representative periods for the optimization of energy systems: An initial framework and comparison." *Applied Energy* 239:1283–1293. doi: 10.1016/j.apenergy.2019.02.012.

Teichgraeber, H., L.E. Kuepper, and A.R. Brandt. 2019. "TimeSeriesClustering: An extensible framework in Julia." *Journal of Open Source Software* 4(41):1573. doi: 10.21105/joss.01573.

Teichgraeber, H., C.P. Lindenmeyer, N. Baumgärtner, L. Kotzur, D. Stolten, M. Robinius, A. Bardow, and A.R. Brandt. 2020. "Extreme events in time series aggregation: A case study for optimal residential energy supply systems." *Applied Energy* 275:115223. doi: 10.1016/j.apenergy.2020.115223.

Tejada-Arango, D.A., M. Domeshek, S. Wogrin, and E. Centeno. 2018. "Enhanced Representative Days and System States Modeling for Energy Storage Investment Analysis." *IEEE Transactions on Power Systems* 33(6):6534–6544. doi: 10.1109/TPWRS.2018.2819578.

The White House. 2021. *President Biden Sets 2030 Greenhouse Gas Pollution Reduction Target Aimed at Creating Good-Paying Union Jobs and Securing U.S. Leadership on Clean Energy Technologies.* https://www.whitehouse.gov/briefing-room/statements-releases/2021/04/22.

Thellufsen, J.Z., and H. Lund. 2017. "Cross-border versus cross-sector interconnectivity in renewable energy systems." *Energy* 124:492–501. doi: 10.1016/j.energy.2017.02.112.

Tröndle, T., J. Lilliestam, S. Marelli, and S. Pfenninger. 2020. "Trade-Offs between Geographic Scale, Cost, and Infrastructure Requirements for Fully Renewable Electricity in Europe." *Applied Energy* 4(9):1929–1948. doi: 10.1016/j.joule.2020.07.018.

Trutnevyte, E. 2016. "Does cost optimization approximate the real-world energy transition?" *Energy* 106:182–193. doi: 10.1016/j.energy.2016.03.038.

Upham, P., R. Klapper, and S. Carney. 2016. "Participatory energy scenario development as dramatic scripting: A structural narrative analysis." *Technological Forecasting and Social Change* 103:47–56. doi: 10.1016/j.techfore.2015.10.003.

Verne, J. 1901. *The Mysterious Island.* Paris: Charpentier.

Weber, A. 2017. "Eine institutionenökonomische Analyse der Bedarfsplanung der Stromübertragungsnetze unter Berücksichtigung der Interdependenzen zur Erzeugungsplanung." PhD diss., Technical University of Berlin.

Weber, A., T. Beckers, P. Behr, N. Bieschke, S. Fehner, and C. v. Hirschhausen. 2013. *Long-term Power System Planning in the Context of Changing Policy Objectives.*

Weibezahn, J., and M. Kendziorski. 2019. "Illustrating the Benefits of Openness: A Large-Scale Spatial Economic Dispatch Model Using the Julia Language." *Energies* 12:1153. doi: 10.3390/en12061153.

Welsch, M., M. Howells, M. Bazilian, J.F. DeCarolis, S. Hermann, and H.H. Rogner. 2012. "Modelling elements of Smart Grids e Enhancing the OSeMOSYS (Open SourceEnergy Modelling System) code." *Energy* 46:337–350. doi: 10.1016/j.energy.2012.08.017.

Wiese, F., S. Hilpert, C. Kaldemeyer, and G. Pleßmann. 2018. "A qualitative evaluation approach for energy system modelling frameworks." *Energy, Sustainability and Society* 8:13. doi: 10.1186/s13705-018-0154-3.

Williams, Archibald. 1910. *The Romance of Modern Invention.*

Wynne, B. 1984. "The Institutional Context of Science, Models, and Policy: The IIASA Energy Study." *Policy Sciences* 17 (3): 277–320.

Yokoyama, R., Y. Shinano, S. Taniguchi, M. Ohkura, and T. Wakui. 2015. "Optimization of energy supply systems by MILP branch and bound method in consideration of hierarchical relationship between design and operation." *Energy Conversion and Management* 92:92–104. doi: 10.1016/j.enconman.2014.12.020.

Zerrahn, A., and W.-P. Schill. 2015. "On the representation of demand-side management in power system models." *Energy* 84:840–845. doi: 10.1016/j.energy.2015.03.037.

———. 2017. "Long-run power storage requirements for high shares of renewables: review and a new model." *Renewable and Sustainable Energy Reviews* 79:1518–1534. doi: 10.1016/j.rser.2016.11.098.

Zola, E. 1901. *Travail.* Hetzel.

Zozmann, E., L. Göke, M. Kendziorski, D. Rodriguez del Angel, C. v. Hirschhausen, and J. Winkler. 2021. "100% Renewable Energy Scenarios for North America—Spatial Distribution and Network Constraints." *Energies* 14 (3). doi: 10.3390/en14030658.

A

Appendix to Chapter 2

A.1 Supplementary material

Three different open-source tools were applied for the research in this paper. These include version 0.1.6 of the modeling framework AnyMOD.jl (https://github.com/leonardgoeke/AnyMOD.jl), version 0.6.5 of of the modeling framework Calliope (https://github.com/calliope-project/calliope) and an extension to version 0.5.3 of TimeSeriesClustering.jl (https://github.com/leonardgoeke/TimeSeriesClustering.jl/tree/dev) specifically created for this paper.

All scripts and data files for creating the reduced time-series and evaluating them with a capacity expansion model are available on Zenodo (https://doi.org/10.5281/zenodo.4992922). The upload also includes additional information on the input parameters used.

B

Appendix to Chapter 3

B.1 Supplementary material

Code and documentation of the AnyMOD.jl framework can found in the following GitHub repository: https://github.com/leonardgoeke/AnyMOD.jl. All other scripts and data files to run the example are available on Zenodo (https://doi.org/10.5281/zenodo.4699276). The upload also includes additional information on the input parameters used. The example uses version 0.1.0 of AnyMOD.jl.

B.2 Nomenclature

B.2.1 Basic definitions

rt_G	root of tree G
α_v, α_v^+	ancestors of vertex v, + includes v
α_v^z	ancestors of vertex v at depth z
δ_v, δ_v^+	descendants of vertex v, + includes v
δ_v^z	descendants of vertex v at depth z
λ_v	leaves descendant to v

B.2.2 Variables

$Te^{cv/st}_{\hat{t},\hat{r},\hat{c}}$	net-output of conversion/storage
$Exc^{net}_{\hat{t},\hat{r},\hat{c}}$	net-exchange
$Trd^{net}_{\hat{t},\hat{r},\hat{c}}$	net-trade
$Cv^{in/out}_{t,\tilde{t},r,c,e,m}$	aggregated conversion input/output
$St^{in/out}_{t,\tilde{t},r,c,e,m}$	aggregated storage input/output
$Gen_{t,\tilde{t},r,c,e,m}$	generated energy
$Use_{t,\tilde{t},r,c,e,m}$	used energy
$StO^{ext/int}_{t,\tilde{t},r,c,e,m}$	externally/internally discharged energy
$StI^{ext/int}_{t,\tilde{t},r,c,e,m}$	externally/internally charged energy
$StLvl_{t,\tilde{t},r,c,e,m}$	storage level
$Exc_{t,r,r',c}$	energy exchange from region r to region r'
$Trd^{buy/sell}_{t,r,c,i}$	bought/sold energy
$Cap^{opr/ist,cv}_{t,\tilde{t},r,e}$	operated/installed conversion capacity
$Cap^{opr/ist,stI}_{t,\tilde{t},r,e,c}$	operated/installed storage input capacity
$Cap^{opr/ist,stO}_{t,\tilde{t},r,e,c}$	operated/installed output storage capacity
$Cap^{opr/ist,stS}_{t,\tilde{t},r,e,c}$	operated/installed storage size
$Cap^{opr/ist,exc}_{t,r,r',c}$	operated/installed exchange capacity
$Exp^{cv}_{t,r,e}$	expansion of conversion capacity
$Exp^{stI}_{t,r,c,e}$	expansion of storage input capacity
$Exp^{stO}_{t,r,c,e}$	expansion of storage output capacity
$Exp^{stS}_{t,r,c,e}$	expansion of storage size
$Exp^{exc}_{t,r,r',c}$	expansion of exchange capacity

B.2.3 Parameter

$ava^{cv}_{t,\tilde{t},r,e,m}$	availability of conversion capacity
$ava^{stI/stO/stL}_{t,\tilde{t},r,c,e,m}$	availability of storage capacity
$eff^{cv}_{t,\tilde{t},r,e,m}$	efficiency of conversion process
$eff^{stI/stO}_{t,\tilde{t},r,c,e,m}$	efficiency of charging/discharging
$eff^{exc}_{t,r,r',c}$	efficiency of energy exchange
$ratio^{out,eq}_{t,\tilde{t},r,c,e,m}$	fixed share of carrier c on total output
$in_{t,\tilde{t},r,c,e,m}$	inflows into storage system
$dis_{t,\tilde{t},r,c,e,m}$	self-discharge rate of storage
$dem_{\hat{t},\hat{r},\hat{c}}$	energy demanded
$cap^{buy/sell}_{t,r,c,i}$	capacity for buying/selling

B.2.4 Sets

Ω	all possible indices for dispatch variables of technologies
$\Gamma^{cv/st}$	technologies converting/storing carriers
$\Psi^{in/out}_{e}$	pairs defining capacity constraints on conversion input/output
$\gamma^{use/gen}_{e}$	carriers used/generated by technology e
γ^{stEx}_{e}	carriers stored explicitly and externally
γ^{stCap}_{e}	carriers assigned to storage capacity
γ^{st}_{e}	all carriers stored explicitly
$\gamma^{in/out}_{e}$	external input/output carriers
μ_e	modes assigned to technology e
τ_c	dispatch time-steps
ρ_c	dispatch regions
φ_c	pairs of dispatch time-steps and regions
$\sigma_{\hat{c},r,t}$	pairs of dispatch time-steps and regions aggregated to determine dispatch of $\hat{c}$ at time-step t in region r
ϵ_e	pair of dispatch time-steps and regions the conversion balance is created for
$\theta^{dis}_{e,\tilde{t}}$	time-steps of construction considered dispatched separately
$\theta^{exp}_{e,t,\tilde{t}}$	time-steps of construction aggregated to obtain capacity
$\beta_{c,r}$	regions with that region r can exchange carrier c
$\zeta^{buy/sell}_{t,r,c,i}$	steps in supply/demand curve for trade
$\omega^{cv/st}_{t,\tilde{t},r,e}$	set of modes, each set requires an individual conversion/storage balance
$\eta^{tp/sp}_{e}$	time-steps/regions of capacity expansion

B.2.5 Functions and mappings

$d(v)$	depth of vertex v
dep_c	depth assigned to carrier c
dep_{sup}	depth of superordinate dispatch time-steps
$s(t)$	scaling factor for capacities at time-step t
$g(e)$	type assigned to technology e

B.3 Set of required capacity constraints

The algorithm to obtain the smallest set of constraints required to correctly restrict the use of conversion capacities is displayed below. The key part is of the algorithm is carried out separately for input and output carriers and for the temporal and spatial domain. In the first step, the respective input and output carriers are obtained and sorted according to their temporal or spatial depth. In case the respective technology requires a conversion balance, carriers that are inputs and have the same granularity as the conversion balance can be omitted from further analysis. In these cases, the conversion balance itself already ensures correct use of the installed capacities. The algorithm then iterates over the remaining carriers. Within this iteration, κ is used to collect the current carrier c and all carriers of previous iterations. For each iteration, the spatial or temporal depth of the current carrier c, the smallest depth among all carriers in κ, and κ itself are written to the set ψ_e. When this has been done for the temporal and spatial dimension, redundant entries are removed from ψ_e. An entry is redundant, if it includes the same or less carriers then another entry, but is not more detailed, neither in the temporal nor spatial domain.

For the output of CCGT plants with CHP for example, the resulting temporal and spatial sets of ψ are provided by Eqs. B.1 and B.2.

$$\begin{aligned}\psi_e^{out,tp} =&\{\{\{'electricity'\},5,1\},\\ &\{\{'electricity','districtheat'\},4,1\}\}\end{aligned} \tag{B.1}$$

$$\begin{aligned}\psi_e^{out,sp} =&\{\{\{'districtheat'\},4,2\},\\ &\{\{'districtheat','electricity'\},4,1\}\}\end{aligned} \tag{B.2}$$

The second set of $\psi_e^{out,sp}$ or $\psi_e^{out,tp}$ is redundant and can be removed. The remaining entries of ψ_e^{out} are then used to create the set Ψ_e^{out} replacing depths with actual time-steps and regions. The only input carrier of CCGT plants is *gas* which is modeled at the same resolution as the conversion balance. Therefore, it is removed within the algorithm, Ψ_e^{in} is empty and no

capacity constraint on input variables must be enforced in this case.

for *'input'/'output'* **do**
  for *'temporal'/'spatial'* **do**
    if *'input'* **then**
      $\upsilon = \gamma_e^{use}$;
    else if *'output'* **then**
      $\upsilon = \gamma_e^{gen}$;
    end
    sort υ ascending by $dep_c^{dis,tp/sp}$;
    if *'input'* **and** $\gamma_e^{use} \neq \emptyset$ **and** $\gamma_e^{gen} \neq \emptyset$ **then**
      filter c with $dep_c^{dis,tp/sp} = \min_{c \in \gamma_e^{gen} \cup \gamma_e^{use}} dep_c^{dis,tp/sp}$ from υ;
    end
    $\kappa = \emptyset$;
    for $c \in \upsilon$ **do**
      $\kappa = \kappa \cup \{c\}$;
      if *'temporal'* **then**
        add $\langle \kappa, dep_c^{dis,tp}, \min_{c' \in \kappa} (dep_c^{dis,sp}) \rangle$ to ψ_e;
      else if *'spatial'* **then**
        add $\langle \kappa, \min_{c' \in \kappa} (dep_c^{dis,tp}), dep_c^{dis,tp} \rangle$ to ψ_e;
      end
    end
  end
  filter redundant entries of ψ_e;
  $\Psi_e^{in/out} = \{\langle \kappa, z^{tp}, z^{sp} \rangle \in \psi \,|\, \{\kappa\} \times \{V(T) \,|\, d(t) = z^{tp}\} \times \{V(R) \,|\, d(r) = z^{sp}\}\}$;
end

Algorithm 1: Determine constraints on conversion capacity for technology e

B.4 Objective function and limiting constraints

The frameworks objective function given in Eq. B.3 minimizes costs. These are compromised of expansion costs $Cost^{exp}$, operating costs $Cost^{opr}$, variable costs $Cost^{var}$ and trade costs $Cost^{trd}$.

$$\min Cost^{trd} + \sum_{t \in \Phi} Cost_t^{exp} + Cost_t^{opr} + Cost_t^{var} \tag{B.3}$$

Expansion costs includes costs for expanding conversion, exchange, storage-input and storage-output capacities as well as costs related to storage size:

$$Cost_t^{exp} = Cost_t^{exp,cv} + Cost_t^{exp,stI} + Cost_t^{exp,stO} + Cost_t^{exp,stS} + Cost_t^{exp,exc} \quad \forall t \in \Phi \tag{B.4}$$

Each of these cost components is computed by summing the product of the discount factor $disc$, the annuity ann, and the expansion variable Exp for each time-step in a technologies lifetime. Operating costs are obtained analogously, but instead of the annuity and expansion variable, operating costs opr are multiplied with the installed capacities $Capa^{opr}$. In Eqs. B.5

and B.6 both equations are exemplary provided for conversion capacities.

$$Cost_t^{exp,cv} = \sum_{e \in \Gamma^{cv}} \sum_{r \in \eta_e^{sp}} \sum_{\tilde{t} \in [t, t+lt_{e,\tilde{t}})} disc_{t,r}\ ann_{\tilde{t},r,e}^{cv}\ Exp_{\tilde{t},r,e}^{cv} \qquad \forall t \in \Phi \tag{B.5}$$

$$Cost_t^{opr,cv} = \sum_{e \in \Gamma^{cv}} \sum_{r \in \eta_e^{sp}} \sum_{\tilde{t} \in [t, t+lt_{e,\tilde{t}})} disc_{t,r}\ opr_{\tilde{t},r,e}^{cv}\ Capa_{t,\tilde{t},r,e}^{opr,cv} \qquad \forall t \in \Phi \tag{B.6}$$

Variable cost can be imposed on all used, generated, charged, discharged or exchanged quantities:

$$Cost_t^{var} = Cost_t^{var,use} + Cost_t^{var,gen} + Cost_t^{var,stI} + Cost_t^{var,stO} + Cost_t^{var,exc} \quad \forall t \in \Phi \tag{B.7}$$

The corresponding constraints are only created where a corresponding cost parameter *var* is defined. In Eq. B.8 this is expressed for used quantities. In the example model, this is only the case for quantities used by the methanation technology to account for the carbon the process requires.

$$Cost_t^{var,use} = \sum_{\langle t,\tilde{t},r,c,e,m \rangle \in \{\Omega \,|\, var_{t,\tilde{t},r,c,e,m}^{use}\}} disc_{t,r}\ var_{t,\tilde{t},r,c,e,m}^{use}\ Use_{t,\tilde{t},r,c,e,m} \qquad \forall t \in \Phi \tag{B.8}$$

Trade costs reflect the costs or revenues from trading energy with exogenous markets. Prices on these markets are reflected by the parameter *prc* and the entire costs can be defined by equation B.9.

$$Cost^{trd} = \sum_{c \in V(C)} \sum_{r \in \rho_c} \sum_{t \in \tau_c} disc_{t,r}\ \Big(\sum_{i \in \zeta^{buy}} prc_{t,r,c,i}^{buy}\ Trd_{t,r,c,i}^{buy} - \sum_{i \in \zeta^{sell}} prc_{t,r,c,i}^{sell}\ Trd_{t,r,c,i}^{sell} \Big) \tag{B.9}$$

Similar to constraints on input or output ratios in section 3.3.2.4, the creation of limiting constraints depends on the dimension of the provided parameters. If limits are defined at a resolution less detailed then the corresponding variables, constraints apply to the sum of all descendant variables. For example, the limit on installed capacities in Eq. B.10 can be defined for the vertex *rooftop* in the rooted trees of technology. As a result, an upper limit will be enforced on the installed capacities of the descendant technologies *PVB* and *solar thermal*.

$$capaL_{t,r,e}^{inst,cv} = \sum_{\hat{t} \in \delta_t^+} \sum_{\hat{r} \in \delta_r^+} \sum_{\hat{e} \in \delta_e^+} \sum_{\tilde{t}' \in \theta_{e,t,\tilde{t}}^{exp}} Capa_{\hat{t},\tilde{t}',\hat{r},\hat{e}}^{inst,cv} \quad \forall \langle t,r,e \rangle \in \{\langle t,r,e \rangle |\, capaL_{t,r,e}^{inst,cv}\} \tag{B.10}$$

A special case are emission constraints, because they are not applied to variables, but to the product of the emission factor emF and used quantities Use as denoted in Eq. B.11.[1]

$$emL_{t,r} = \sum_{\hat{t} \in \delta_t^+} \sum_{\hat{r} \in \delta_r^+} \sum_{\langle \hat{t},\tilde{t},\hat{r},c,e,m \rangle \in \{\Omega \,|\, emF_{\hat{t},\tilde{t},\hat{r},c,e,m}^{use}\}} emF_{\hat{t},\tilde{t},\hat{r},c,e,m}\ Use_{\hat{t},\tilde{t},\hat{r},c,e,m}$$
$$\forall \langle t,\tilde{t},r,c,e,m \rangle \in \{\Omega |\, emL_{t,\tilde{t},r,c,e,m}^{out,eq}\} \tag{B.11}$$

1. Optionally, the emission constraint can be extended to additionally account for storage and exchange losses.

C

Appendix to Chapter 5

C.1 Supplementary material

All computations in this paper were run with version 0.1.6 of the modelling framework AnyMOD.jl (https://github.com/leonardgoeke/AnyMOD.jl). All scripts and data files to replicate results are available on Zenodo (https://doi.org/10.5281/zenodo.4569880). The upload also includes additional information on the input parameters used.